Winter 1999

Elasto-Plastic Responses of Buried Pipeline Systems Under Wave Propagation

Yuean-Chen Lau
Old Dominion University

ELASTO-PLASTIC RESPONSES OF BURIED PIPELINE SYSTEMS UNDER WAVE PROPAGATION

by

Yuean-Chen Lau
B.S. June 1978, National Taiwan University
Taipei, Taiwan, R. O. C.
M.S. August 1984, University of Oklahoma, Norman, Oklahoma

A Dissertation Submitted to the Faculty of
Old Dominion University in Partial Fulfillment of the
Requirements for the Degree of

DOCTOR OF PHILOSOPHY

CIVIL ENGINEERING

OLD DOMINION UNIVERSITY
December 1989

Approved by:

Dr. Leon R. L. Wang (Director)

Dr. Isao Ishibashi

Dr. Duc T. Nguyen

Dr. John E. Kroll

ABSTRACT

ELASTO-PLASTIC RESPONSES OF BURIED PIPELINE SYSTEMS UNDER WAVE PROPAGATION

Yuean-Chen Lau
Old Dominion University, 1989
Director: Dr. Leon R. L. Wang

The purpose of this research is to study the elastic and inelastic behavior of buried pipeline system under arbitrary seismic wave propagation. Both continuous and segmented pipes with joints and junctions are included. The surrounding soil is simulated by a series of elasto-plastic springs uniformly distributed longitudinally and laterally along the pipes. To the joints, elasto-plastic longitudinal springs and bilinear rotational springs are adopted. It is assumed that the pipes remain linearly elastic. The effects of soil liquefaction and fault movement are not considered.

Since the dynamic effect has been found to be negligible, a quasi-static analysis is adopted in this study. In use of the finite element technique, the equations of static equilibrium at any particular time have been obtained and a rigorous procedure for solving the inelastic responses of buried pipeline considering hysteretic characteristics of soil and joints is developed. The effects of wave forms, pipe sizes, wave velocities and incident angles are investigated with various combinations

of soil and joint properties. The comparison of elastic and inelastic analysis is also done. Recommendations for future seismic design of buried pipeline systems are drawn.

DEDICATION

To my mother, for her love, support, encouragement and belief in me.

ACKNOWLEDGEMENT

I wish to express my sincerest gratitude to my advisor, Dr. Leon R. L. Wang, for his invaluable advice and guidance throughout my doctoral study. I would also like to thank the other members of my dissertation committee, Drs. Isao Ishibashi, Duc T. Nguyen and John E. Kroll for their suggestions and comments on my dissertation.

A special note of appreciation is extended to Miss Grace J. I. Hwang, a dear friend whose love, understanding and encouragement made this work possible.

Finally, I would like to thank my mother, my brothers and sisters, for their support and encouragement throughout my academic career.

TABLE OF CONTENTS

LIST OF TABLES

LIST OF FIGURES

LIST OF SYMBOLS

A : Cross sectional area of pipe

A_{max} : Amplitude of ground displacement

C_p : Primary wave velocity

C_S : Shear wave velocity

D : Outer Diameter of pipeline

$Det[K_S]$: Determinant of elastic system soil stiffness

$Det[K_S]_m$: Determinant of modified system soil stiffness

e^* : Tolerance to determine if the surrounding soil is failure

E : Young's modulus

$\{e\}$: Tolerance vector for checking convergence

f_J : Reaction force of joint spring

$f_{J,y}$: Tensile yielding reaction force of joint spring

$f_{J,-y}$: Compressive yielding reaction force of joint spring

f_S : Resistant force of soil spring

$f_{S,y}$: Tensile yielding resistant force of soil spring

$f_{S,-y}$: Compressive yielding resistant force of soil spring

$f_{SA,y}$: Tensile yielding resistant force of soil spring in longitudinal direction

$f_{SA,-y}$: Compressive yielding resistant force of soil spring in longitudinal direction

$\{F(t)\}$: Equivalent force vector

$\{F(t)\}_p$: Inelastic nodal force vector

$g(t)$: Ground displacement function

H : Burial depth

I : Moment of inertia of pipe

k_{JA} : Longitudinal joint spring constant

k_{JAs} : Longitudinal secant modulus of joint

k_{JR} : Rotational joint spring constant

k_{JRs} : Rotational secant modulus of joint

k_{SA} : Longitudinal soil spring constant

k_{SL} : Lateral soil spring constant

$[K]$: Coefficient matrix

$[K]_m$: Inelastic coefficient matrix

$[K_{BJ}]$: Boundary joint stiffness matrix

$[K_{BJ}]_m$: Inelastic boundary joint stiffness matrix

$[K_J]$: Joint stiffness matrix

$[K_J]_m$: Inelastic joint stiffness matrix

$[K_P]$: Pipe stiffness matrix

$[K_S]$: Soil stiffness matrix

$[k_S]$: Soil stiffness matrix in local coordinates

$[K_S]_m$: Modified soil stiffness matrix

$[K_S]_{Inel}$: Soil stiffness matrix of inelastic portions

$[K_{SYS}]$: System stiffness matrix

$[K_{SYS}]_m$: Modified system stiffness matrix

L_i : Element length

NA : Total number of elements that surrounding soil is inelastic in longitudinal direction

NBJ : Total number of boundary joints

NJ : Total number of joints

NL : Total number of elements that surrounding soil is inelastic in lateral direction

NM : Total number of elements

$[N_A]$: Assumed longitudinal shape function

$[N_L]$: Assumed lateral shape function

OD : Outer diameter of pipe

[T] : Transformation matrix

$u_{JA,y}$: Elastic limit of longitudinal joint spring

$u_{JR,y}$: Elastic limit of rotational joint spring

$u_{J,c}$: Contact space of joint

$u_{J,u}$: Pull-out displacement of joint

$u_{SA,y}$: Elastic limit of longitudinal soil spring

$u_{SL,y}$: Elastic limit of lateral soil spring

$\{u_J\}$: Joint displacement vector in local coordinates

$\{u_P\}$: Pipe displacement vector in local coordinates

$\{u_{PA}\}$: Longitudinal pipe displacement vector in local coordinates

$\{u_{PL}\}$: Lateral pipe displacement vector in local coordinates

$\{u_S\}$: Soil-pipe relative displacement vector in local coordinates

$\{u_{SA}\}$: Longitudinal soil-pipe relative displacement vector in local coordinates

$\{u_{SL}\}$: Lateral soil-pipe relative displacement vector in local coordinates

$\{U_P\}$: Pipe displacement vector in global coordinates

$\{U_S\}$: Soil-pipe relative displacement vector in global coordinates

U^i_{Joint} : Strain energy of the ith joint

U^i_{Pipe} : Strain energy of the ith pipe element

U^i_{Soil} : Strain energy of soil along the ith pipe element

$U^i_{Soil,Long}$: Longitudinal strain energy of soil along the ith pipe element

$U^i_{Soil,Lateral}$: Lateral strain energy of soil along the ith pipe element

U^{Total} : Total potential energy of buried pipeline system

U^{Total}_{Joint} : Total strain energy of joint

U^{Total}_{Pipe} : Total strain energy of pipe

U^{Total}_{Soil} : Total strain energy of soil

$U^{Total}_{Soil,Inel}$: Total strain energy of inelastic portions of soil

$U^{Total}_{Soil,m}$: Total strain energy of soil without inelastic portions

x_{ci} : Compressive inelastic length of soil along the ith pipe element

x_{ti} : Tensile inelastic length of soil along the ith pipe element

$\{x_G\}$: Ground displacement vector in local coordinates

$\{x_{GA}\}$: Longitudinal ground displacement vector in local coordinates

$\{x_{GB}\}$: Ground displacement vector of boundary joint in local coordinates

$\{x_{GL}\}$: Lateral ground displacement vector in local coordinates

$\{X_G\}$: Ground displacement vector in global coordinates

$y_A(x)$: Longitudinal displacement function between soil and pipe

$y_L(x)$: Lateral displacement function between soil and pipe

α : Ratio of rotational joint stiffness after yielding to the elastic rotational joint stiffness

Δt : Delay time of seismic wave

θ : Angle between global and local coordinates

ϕ : Incident angle of ground wave

$\{\Delta u_S\}$: Incremental soil response vector in local coordinates

$\{\Delta U_S\}$: Incremental soil response vector in global coordinates

$\{\Delta X_G\}$: Incremental ground displacement vector in global coordinates

$\{\varepsilon(x)\}$: Strain function of pipe

$\{\chi(x)\}$: Curvature function of pipe

Chapter 1

INTRODUCTION

1.1 Background

Buried pipelines including water, sewage, gas and oil pipelines have been damaged by strong ground motions due to earthquakes. The major causes to the damage of buried pipelines can be classified as: (1) soil liquefaction, which usually occurs in the area of sandy soil with high level of water table. The pipeline might be damaged by dynamic effect on axial tension, buckling or uplift due to loss of soil support and buoyancy possibilities; (2) large ground displacement, which causes large deformation of buried pipeline by surface faulting and soil lateral spreading; (3) seismic ground shaking, which covers the largest area and most buried pipelines are damaged due to the ground motion or wave propagation effects. Researches to study the failure behavior/mechanisms have been carried out by many investigators [8, 11, 19, 21, 39, 40, 41, 42, 44, 50, 51, 52]* in the past decade. The elasto-plastic behavior of

*The numbers in the brackets indicate references.

buried pipelines subjected to seismic ground shaking is of interest in this study.

Not as above-ground structures, the dynamic effects are unimportant to the behavior of buried pipelines subjected to ground movement because of the high restraint and damping of surrounding soil. However, the ground movement is time dependent, therefore a so-called quasi-static approach introduced by Wang et al. [50] is widely accepted by many researchers [28, 29, 30, 38, 42] in this area. The longitudinal behavior of straight buried pipelines subjected to compression waves has been investigated by Wang et al. [50]. However, for a buried pipeline system where junctions are included subjected to seismic shaking, the shear type of waves, which will cause bending to the pipe, should also be considered in addition to compressive type of waves of the ground. In this research both longitudinal and lateral responses of buried pipeline systems under either compression or shear waves are investigated.

1.2 Literature Review

Damage of buried pipelines caused by strong ground motions in the past earthquakes has been reported in a number of papers [13, 15, 16, 18, 19, 20, 22, 37, 49]. In general, damage to the buried pipelines occurred at joints/junctions and transition area of soft soil to stiff

soil by pull-outs, breaks and cracks. Recently, in the Whittier Narrow earthquake, October 1, 1987, some new patterns of damage such as blowout as a hole and longitudinal cracks in the buried pipelines is reported and being investigated by Wang et al. [54].

The fact that the dynamic effects can be ignored for buried pipelines under seismic environment has been studied experimentally and analytically by Sakurai et al. [34] and Shinozuka et al. [38], respectively. It was pointed out that the longitudinal strain predominates for buried straight pipelines in seismic environment [7, 8, 18, 20, 22, 28, 29, 38, 41, 44, 49, 50, 51]. In 1967, Newmark [24] provided a conservative analysis for buried pipeline under wave propagation. Wang et al. [50, 51, 52] have studied the elastic and inelastic behavior of a straight buried pipeline subjected to compressive seismic waves. It was pointed out that the pipe size, wave propagation velocity and soil stiffness will affect the pipe strain and joint responses. Shah [35], Goodling [9] and Igbal and Goodling [14] have derived general formula by considering the critical cases of elbow, bend and T-junction of continuous buried pipelines. Some Japanese researchers [21, 42, 43, 44] have also studied the behavior of buried pipelines (continuous/segmented). Koike [21] furnished the calculation formula presented by Goodling with arbitrary angle other than 90 degree. Takada

et al. [42] studied the behavior of a straight pipe for different numbers of the branch pipes within one wave length. It is found that the maximum pipe strain is increased as the number of the branch pipes increases. Tamura [43, 44] presented general elastic solutions for responses of a submerged tunnel under seismic motion. It should be noted that in the previous studies, there is no general formula for solving inelastic responses of buried pipeline by considering the hysteretic characteristics of soil and joints, which is important for the time-dependent inelastic behavior of buried pipelines and has been considered in this study.

To study the response behavior of buried pipelines under strong ground motions, some important parameters such as soil stiffness (longitudinal and lateral) and pipe joint stiffness (longitudinal and rotational) have to be included. For soil stiffness related to the soil-structure interaction, Brumund and Leonards [5] and Potyondy [32] have determined interface friction between various soils and construction materials experimentally. Colton et al. [6], Novak and Nogami [26], O'Leary et al. [27], Saito et al. [33], Toki et al. [46], Shibata [36], and Wang [53] have studied or recommended the value of longitudinal soil stiffness; Audibert et al. [2, 3], Toki et al. [46], and Trautmann et al. [47, 48] for the lateral soil stiffness.

The data of longitudinal and lateral soil stiffness are shown in Tables 1.1 and 1.2, respectively. For pipe joint stiffness, Singhal [39, 40] presented some experimental results of rubber-gasket joints in tension, compression and rotation. The results are shown in Figs. 1.1 and 1.2. Ishibashi et al. [17] presented some dynamic characteristics of a flexible joint. For other types of joints, no existing data is available.

Another important factor is the seismic wave velocity which depends on the geological condition of the seismic area. There is a wide range of seismic wave velocities presented in the literature. From published papers the shear wave velocity ranges from 80 to 6500 ft/sec [7, 25, 29, 30, 31, 53] and compression wave velocity is usually considered as twice as shear wave velocity [14]. The existing data on shear wave velocity are listed in Table 1.3.

Published rearch papers fail to fully explain the behavior of buried pipeline systems subjected to seismic shaking. There is no design code for buried pipelines considering seismic effects at the present time. Further analytical studies on buried pipeline systems as well as more laboratory and in-situ testings certainly will aid to establish aseismic design code for buried pipelines in the future.

1.3 Assumptions and Conditions

The assumptions and conditions in this study are:

1. The surrounding soil is simulated by a series of longitudinal and lateral springs uniformly distributed along the pipe.
2. The joints are represented by longitudinal and rotational springs only; lateral spring is considered infinitely rigid.
3. The force-displacement relationship is assumed to be elasto-plastic for soil and bilinear for rotational joint springs with elastic unloading characteristics. Longitudinal joint spring is a special spring that has different tensile and compressive resistant characteristics.
4. The pipeline system is assumed to be empty; no water pressure is considered.
5. Circumferential strain or stress of pipe is not considered.
6. The wave propagation is in the same plane of the pipeline system; no torsional effect on the pipeline system is considered.
7. The system response is considered quasi-static.

1.4 Description of Models

A general buried pipeline system subjected to an arbitrary seismic ground shaking is shown in Fig. 1.3. The

system includes such important parameters as seismic ground motions, pipe segment properties and surrounding soil, the resistant characteristics of joints and junctions. For such a complicated buried pipeline system, the important parameters are described as follows:

1.4.1 Seismic Ground Motion

A lot of energy will be released as an earthquake occurs in the form of wave propagation from the source of the earthquake (hypocenter). There are several types of ground waves due to an earthquake (e.g., shear, primary, Love and Rayleigh waves); however, to the buried pipeline system only the characteristics (i.e. the magnitude, the traveling direction and the speed) of the waves are of interest. For example, a characteristic of the shear wave (S-wave) is that the vibration direction is perpendicular to the traveling direction. For a primary or compression wave (P-wave), the vibration direction is in the traveling direction, but with much higher speed than the shear wave.

Since the strong ground motion usually affects possibly hundreds of square miles in the vicinity of the epicenter, the spatial and temporal variations of wave propagation and the angles of incidence of the seismic waves should be taken into consideration in the analysis of buried pipeline systems. It should be noted that ground motion data records three components, i.e. two horizontal and one vertical

components. In this study only horizontal motion is considered since the vertical component is usually much smaller than the horizontal components. Other effects such as reflections, refractions and scattering of the waves are out of the scope of this research.

1.4.2 Model for Pipe and Surrounding Soils

Figure 1.3 shows an analytical model of a buried pipeline system under a seismic wave. To analyze the system by the finite element technique, the pipe element shown in Fig. 1.4a is modeled as a beam element with three degrees of freedom, two translations (longitudinal and lateral) and one rotation, at each end (node). It is also shown in Fig. 1.4a that the surrounding soil is represented by a series of elasto-plastic longitudinal and lateral springs with their initial spring constants k_{SA} and k_{SL}, respectively, uniformly distributed along the pipe element.

1.4.3 Model for Joints

In general, five types of joints, namely, (I) continuous, (II) linear, (III) elbow, (IV) T or Y, and (V) cross, as shown in Fig. 1.5, are used in a pipeline system. In Fig. 1.4b a simple analytical model of a linear joint is shown. Since most pipe joints are locked in space laterally, the relative lateral displacements between two segments are negligible at the joints. Hence, two springs, one

longitudinal translation and one rotation with spring constants k_{JA} and k_{JR} , respectively, are utilized to represent resistant properties of a pipe joint.

1.5 Objective and Scope

The purpose of this research consists of: first, to formulate the quasi-static equations of equilibrium for a general buried pipeline system under arbitrary wave propagation; secondly, to develop a general computer program with numerical schemes for the solutions of the desired pipeline responses (elastic and inelastic), such as the maximum pipe strain and pipe curvature, maximum relative joint displacement and rotation; and finally, to investigate the effects of various parameters by using the developed computer program.

In Chapter 2 the governing equilibrium equations of a buried pipeline system (segmented and continuous) are derived based on finite element method. The formulation includes important parameters such as seismic wave velocity and displacement, pipe and joint stiffness, soil resistant spring constants, and boundary conditions. Parametric behavior of buried pipelines was investigated and discussed by assuming that the whole system will behave elastically.

The basic formulation for solving the inelastic responses of the buried pipeline system is derived in Chapter 3. An iterative procedure considering the

hysteretic characteristics of soil and joint is described. Parametric behavior of buried pipelines was investigated and the comparison of elastic and inelastic solutions were also made.

Chapter 4 presents the summary and conclusions of this study and recommendations for future investigations.

Table 1.1 Longitudinal Soil Spring Constant (k_{SA})

Author	G_s (ksi)	Soil Condition	k^*_{SA} (ksi)
Berger et al. (1977) [4]	1.4 12.5 16.7 48.6	Soft Clay Stiff Clay Very Stiff Clay	1.4-4.2 12.5-37.5 16.7-40.1 48.6-145.8
Hardin et al. (1972) [12]	3-18 24-31 10-18	Clean Dry Sand Dry 60-100 Silica Sand Lick Creak-Silt	3-54 24-93 10-54
Tamura et al. (1976) [43]	17.6 6.7	Fine Sand Silt	17.6-52.9 6.7-20.3

*Note : The values of k_{SA} are obtained by means of following informations:

O'Rourke and Wang (1978) [28]: $k_{SA} = 2\ G$

Colton (1978) [6]: $k_{SA} = 3.98$ kips/in/in

Toki, et al. (1983) [46]: $k_{SA} = 3\ G$

O'Leary and Datta (1985) [27]: $k_{SA} = 2\ G$

Shibata et al. (1987) [36]: $k_{SA} = G$

Takada et al. (1987) [42]: $k_{SA} = 1.65\ MN/m^2$ (0.24kip/in/in)

k_{SA} is in the range of 10^{-1} - 10^2 ksi.

Table 1.2 Lateral Soil Spring Constant (k_{SL})

Author	k_{SL} (ksi)	Soil Condition
McClure et al. (1964) [23]	0.43	Light Dry Topsoil
	1.09	Moist Loaming Silty Topsoil
	2.40	Clayey Topsoil
	2.83	Semi-consolidated Sandy Clay Topsoil
	5.60	Wet Loam
	8.75	Rubble or Gravel
	11.15	Cemented Sand
	11.95	Sandy Clay
	19.75	Cemented Sandy Clay
	21.48	Dense Wet Clay
	22.50	Saturated Sand
	45.0	Clayey Sandstone Clay
	56.6	Sand
Tamura et al. (1976) [43]	11.38	Silty Clay
	17.08	Silty Clay
Audibert et al. (1976) [2, 3]	0.34	Loose Sand
	1.35	Dense Sand
	1.8	Backfill
Trautmann et al. (1983) [47, 48]	0.79	Loose Sand
	0.94	Dense Sand
Takada et al. (1987) [42]	0.24	-

Note: k_{SL} is in the range of 10^{-1} - 10^{2} kip/in/in

Table 1.3 Shear Wave Velocity of Soil (C_s)

Author	C_s ft/sec	Soil Condition
Abe & Ang (1974) [1]	80 400 750 1400 2900 3500	Banking Loam Clay Sandy Clay Gravel Silt Stone
Hakuno (1974) [10]	330	Fine Stone
Kubo (1973) [22]	210 210 - 660 1980	Very Soft Soil Soft Layer Hard Ground
McClure et al. (1964) [23]	750 1150 1650 1700 2500 2290 3000 3500 4000 4450 4600 5900 6500	Light Dry Topsoil Moist Loaming Silty Topsoil Clayey Topsoil Semiconsolidated Sandy Clay Topsoil Wet Loam Rubble or Gravel Cemented Sand Sandy Clay Cemented Sandy Clay Dense Wet Clay Saturated Sand Clayey Sandstone Clay Sand
Tamura et al. (1976) [43]	410 710 1130 850 520	Depth 0 - 80 ft Depth 80 - 200 ft Depth 200 - 380 ft Fine Sand Silt
Hall et al. (1978) [11]	3000 3500 4000	Sand and Competent Soil Massive Gravel Rock or Permafrost

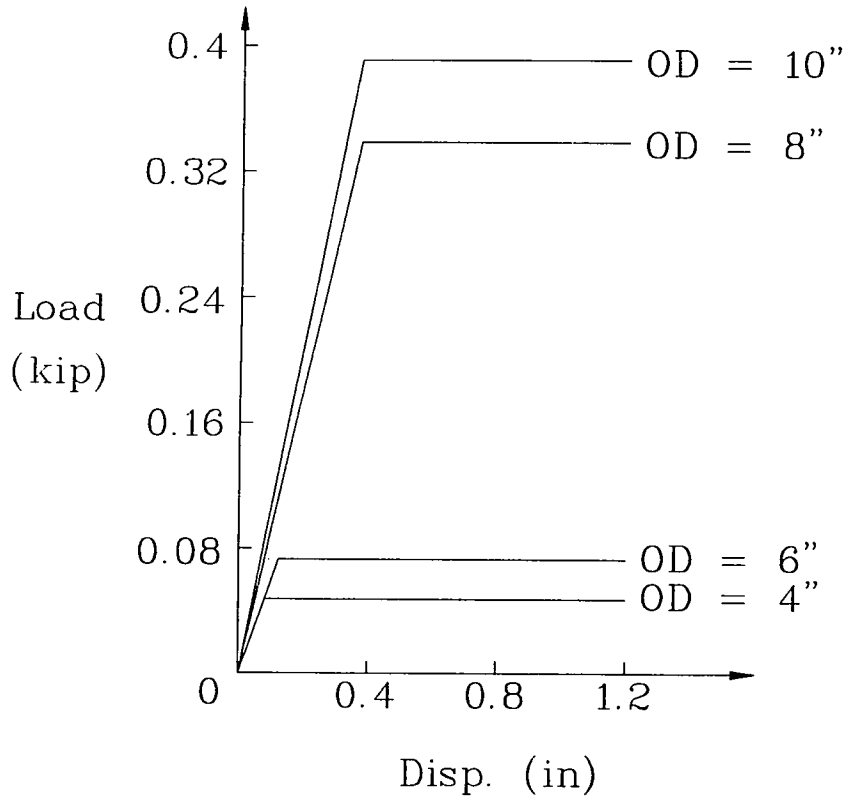

Fig. 1.1 Axial Pull Out Joint Stiffness [39, 40]

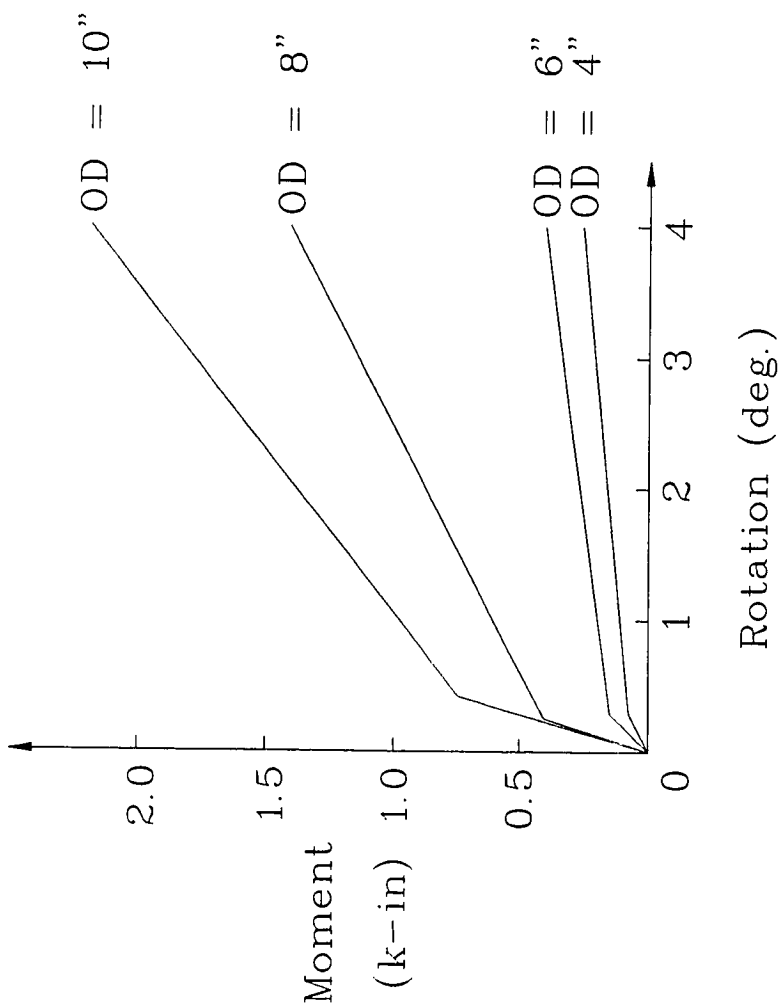

Fig. 1.2 Joint Bending Stiffness [39,40]

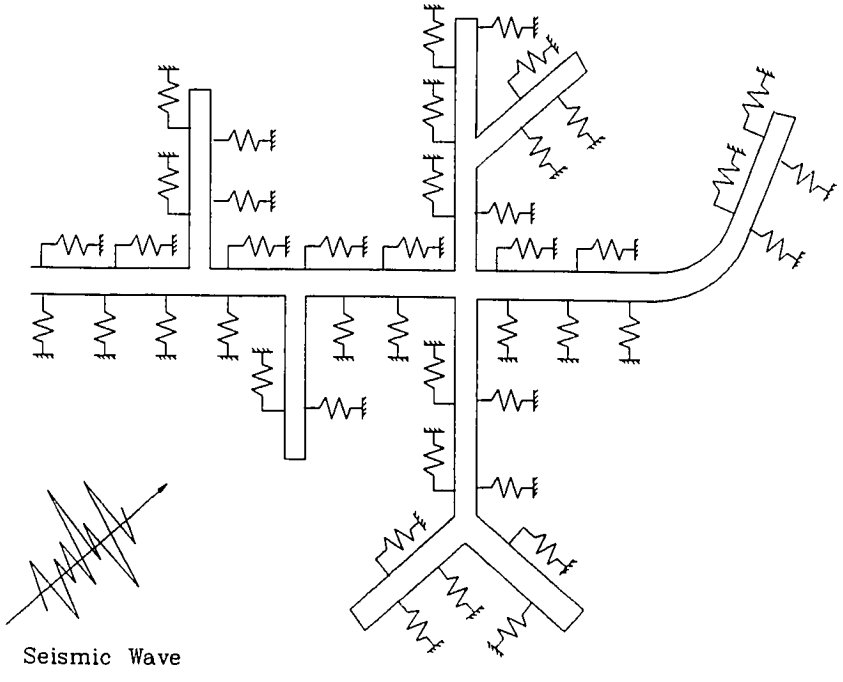

Fig. 1.3 Model of Buried Pipeline System under Seismic Wave

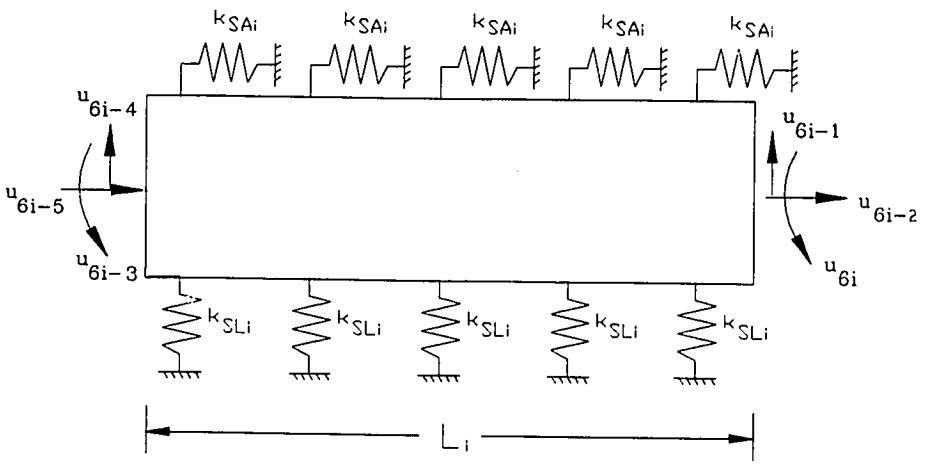

Fig. 1.4a Model for Pipe Element and Surrounding soil

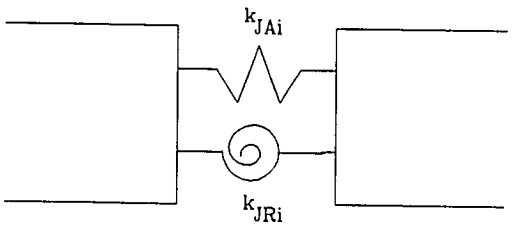

Fig. 1.4b Model for Joint

Fig. 1.5 Types of Joint

Chapter 2

ELASTIC ANALYSIS

It is assumed that the pipes will move along with the surrounding soils as long as the ground strain is in the elastic range. For buried pipeline problem, the dynamic effects (inertia and damping forces) are found to be negligible [34, 38]. However, since the input ground motion is time dependent, the so-called quasi-static method is adopted in the analysis.

2.1 Finite Element Formulation

A segmented (jointed) pipeline is considered to formulate the governing equation of equilibrium of the buried pipeline systems. The continuous pipeline system can be considered as a special case where the joint stiffnesses approach infinity. For a segmented pipeline system, three major parts, i.e. pipe members, surrounding soil and joints, are included in the analysis. Applying the energy approach, the total potential energy of the system which includes the strain energies of all three major parts (i.e., soil, pipes and joints) is obtained. Then, using the principle of

variations, the equations of equilibrium are constructed. The formulation for the quasi-static equilibrium equations is shown in the following sections.

2.1.1 Strain Energy of the Pipe

As shown in Fig. 1.4a, the pipe element is modeled as a beam element with three-degree-of-freedom at each end. The strain energy of the ith pipe element can be obtained as:

$$U^{i}_{Pipe} = \frac{1}{2} \underset{1x6}{\{u_{Pi}\}^{T}} \underset{6x6}{[k_{Pi}]} \underset{6x1}{\{u_{Pi}\}} \qquad i=1, 2,..., NM \quad (2.1)$$

where

$$\underset{1x6}{\{u_{Pi}\}^{T}} = [u_{6i-5}\ u_{6i-4}\ u_{6i-3}\ u_{6i-2}\ u_{6i-1}\ u_{6i}] \quad (2.1a)$$

is the nodal displacement vector and

$$\underset{6x6}{[k_{Pi}]} = \begin{bmatrix} \frac{E_iA_i}{L_i} & 0 & 0 & -\frac{E_iA_i}{L_i} & 0 & 0 \\ & \frac{12E_iI_i}{L_i^3} & \frac{6E_iI_i}{L_i^2} & 0 & -\frac{12E_iI_i}{L_i^3} & \frac{6E_iI_i}{L_i^2} \\ & & \frac{4E_iI_i}{L_i} & 0 & -\frac{6E_iI_i}{L_i^2} & \frac{2E_iI_i}{L_i} \\ & & & \frac{E_iA_i}{L_i} & 0 & 0 \\ & \text{Symmetric} & & & \frac{12E_iI_i}{L_i^3} & \frac{6E_iI_i}{L_i^2} \\ & & & & & \frac{4E_iI_i}{L_i} \end{bmatrix} \quad (2.1b)$$

is the standard member stiffness matrix of the ith pipe element, NM is the total number of pipe elements, E_i, Young's modulus, A_i, area, I_i, moment of inertia and L_i, segment length of the ith pipe.

It should be noted that Eq. (2.1b) is obtained in local coordinates. The relationship between local and global coordinates is shown in Fig. 2.1 where x-y-z and X-Y-Z represent the local and global coordinates, respectively. In order to obtain the system stiffness matrix, all element stiffnesses shown by Eq. (2.1b) have to be transformed to global coordinates by the following equation:

$$\underset{6x6}{[K_{pi}]} = \underset{6x6}{[T_i]^T}\ \underset{6x6}{[k_{pi}]}\ \underset{6x6}{[T_i]} \qquad (2.1c)$$

where $[K_{pi}]$ is the element stiffness matrix in global coordinates and $[T_i]$ is the transformation matrix given below:

$$\underset{6x6}{[T_i]} = \begin{bmatrix} \cos\theta_i & \sin\theta_i & 0 & 0 & 0 & 0 \\ -\sin\theta_i & \cos\theta_i & 0 & 0 & 0 & 0 \\ 0 & 0 & 1 & 0 & 0 & 0 \\ 0 & 0 & 0 & \cos\theta_i & \sin\theta_i & 0 \\ 0 & 0 & 0 & -\sin\theta_i & \cos\theta_i & 0 \\ 0 & 0 & 0 & 0 & 0 & 1 \end{bmatrix} \qquad (2.1d)$$

where θ_i is the angle between global and local coordinates and measured counterclockwise as shown in Fig. 2.1. The subscript i represents ith element.

By assembling the strain energies of all pipe elements, the total strain energy of pipe elements can be obtained in

the form of

$$U_{Pipe}^{Total} = \sum_{i=1}^{NM} U_{Pipe}^{i}$$

$$= \sum_{i=1}^{NM} \frac{1}{2} \underset{1x6}{(U_{Pi})^T} \underset{6x6}{[K_{Pi}]} \underset{6x1}{(U_{Pi})} \qquad (2.2)$$

or

$$U_{Pipe}^{Total} = \frac{1}{2} \underset{1xn}{(U_p)^T} \underset{nxn}{[K_p]} \underset{nx1}{(U_p)} \qquad (2.3)$$

where $[K_p]$ is system stiffness matrix of pipe; (U_p), system displacement vector in global coordinates; and n, the total number of degree of freedom.

2.1.2 Strain Energy of Surrounding Soil

The relative soil-pipe displacement (u_s) is defined as:

$$(u_s) = (u_p) - (x_G) \qquad (2.4)$$

where (x_G) is displacement vector of the ground. The strain energy of soil can be derived in longitudinal and lateral directions, respectively, as shown in the following sections.

In Longitudinal Direction

The relative displacement function defined by the discrete displacements at the nodes between a pipe element

and the ground (surrounding soils) in longitudinal direction can be expressed as:

$$y_A^i(x) = \left[\left(1 - \frac{x}{L_i}\right) \quad \frac{x}{L_i}\right] \left(\begin{Bmatrix} u_{6i-5} \\ u_{6i-2} \end{Bmatrix} - \begin{Bmatrix} x_{GA2i-1} \\ x_{GA2i} \end{Bmatrix} \right)$$

$$= [N_{Ai}] \left(\{u_{PAi}\} - \{x_{GAi}\}\right) = [N_{Ai}] \{u_{SAi}\} \quad (2.5)$$

where $\{u_{PAi}\}$ and $\{x_{GAi}\}$ are the longitudinal components of the ith pipe displacement and the corresponding ground displacement, respectively, as shown in Fig. 1.4a; $\{u_{SAi}\}$ is the relative soil-pipe displacement vector and $[N_{Ai}]$ is the assumed linear displacement function in longitudinal direction. Then the soil strain energy in the longitudinal direction of the ith element can be obtained as:

$$U^i_{Soil,Long} = \frac{1}{2} \int_0^{L_i} k_{SAi} (y_A^i)^2 dx \quad (2.6)$$

Substituting Eq. (2.5) into Eq. (2.6), one obtains

$$U^i_{Soil,Long} = \frac{k_{SAi}}{2} \int_0^{L_i} \left([N_{Ai}] \{u_{SAi}\}\right)^2 dx$$

$$= \frac{k_{SAi}}{2} \int_0^{L_i} \{u_{SAi}\}^T [N_{Ai}]^T [N_{Ai}] \{u_{SAi}\} dx \quad (2.7)$$

In view of Eq. (2.4), the terms inside the integral on the right hand side of Eq. (2.7) can be expanded as:

$$\{u_{PAi}\}^T [N_{Ai}]^T [N_{Ai}] \{u_{PAi}\} - 2\{u_{PAi}\}^T [N_{Ai}]^T [N_{Ai}] \{x_{GAi}\}$$

$$+ \{x_{GAi}\}^T [N_{Ai}]^T [N_{Ai}] \{x_{GAi}\}$$

Plugging these terms into Eq. (2.7), one obtains:

$$U^i_{Soil,Long} = \frac{1}{2} k_{SAi}\{u_{PAi}\}^T \int_0^{L_i} [N_{Ai}]^T[N_{Ai}]\, dx\, \{u_{PAi}\}$$

$$- k_{SAi}\{u_{PAi}\}^T \int_0^{L_i} [N_{Ai}]^T[N_{Ai}]\, dx\, \{x_{GAi}\}$$

$$+ \frac{1}{2} k_{SAi}\{x_{GAi}\}^T \int_0^{L_i} [N_{Ai}]^T[N_{Ai}]\, dx\, \{x_{GAi}\} \quad (2.8)$$

Note that the last term on the right hand side does not contain unknown nodal displacement. There is no need of carrying out the integration since this term will go out upon its variation. It can be simply represented by a constant a_i. Thus, Eq. (2.8) can be rewritten after integration as:

$$U^i_{Soil,Long} = \frac{1}{2} \underset{1x2}{\{u_{PAi}\}^T} \underset{2x2}{[k^i_{SA}]} \underset{2x1}{\{u_{PAi}\}}$$

$$- \underset{1x2}{\{u_{PAi}\}^T} \underset{2x2}{[k^i_{SA}]} \underset{2x1}{\{x_{GAi}\}} + a_i \quad (2.9)$$

where

$$\underset{2x2}{[k^i_{SA}]} = k_{SAi}\int_0^{L_i} [N_{Ai}]^T[N_{Ai}]dx$$

$$= \frac{1}{3} k_{SAi}L_i \begin{bmatrix} 1 & 0.5 \\ 0.5 & 1 \end{bmatrix} \quad (2.9a)$$

In Lateral Direction

The relative displacement between pipe element and surrounding soil in lateral direction can be written as:

$$y_L^i(x) = [N_1\ N_2\ N_3\ N_4]\ \left(\begin{Bmatrix} u_{6i-4} \\ u_{6i-3} \\ u_{6i-1} \\ u_{6i} \end{Bmatrix} - \begin{Bmatrix} x_{GL2i-1} \\ 0 \\ x_{GL2i} \\ 0 \end{Bmatrix} \right)$$

$$= [N_{Li}]\ (\{u_{PLi}\} - \{x_{GLi}\}) = [N_{Li}]\ \{u_{SLi}\} \quad (2.10)$$

where $\{u_{PLi}\}$ and $\{x_{GLi}\}$ are the lateral and rotational components of the ith pipe displacement and the corresponding ground displacement, respectively, as shown in Fig. 1.4a. $\{u_{SLi}\}$ is the relative soil-pipe displacement vector and $[N_{Li}]$ is the assumed displacement function in the lateral direction and is given in the form of:

$$[N_{Li}] = [(1 - \frac{3x^2}{L_i^2} + \frac{2x^3}{L_i^3}),\ (x - \frac{2x^2}{L_i} + \frac{x^3}{L_i^2}),$$

$$(\frac{3x^2}{L_i^2} - \frac{2x^3}{L_i^3}),\ (-\frac{x^2}{L_i} + \frac{x^3}{L_i^2})] \quad (2.11)$$

Then the soil strain energy in the lateral direction within the ith element can be formulated as:

$$U^i_{Soil,Lateral} = \frac{1}{2} k_{SLi} \int_0^{L_i} (y_L^i)^2 dx \quad (2.12)$$

Substituting Eq. (2.10) into Eq. (2.12) yields:

$$U^i_{Soil,Lateral} = \frac{1}{2} k_{SLi} \int_0^{L_i} ([N_{Li}]\ \{u_{SLi}\})^2\ dx$$

$$= \frac{1}{2} k_{SLi} \int_0^{L_i} \{u_{SLi}\}^T [N_{Li}]^T [N_{Li}]\ \{u_{SLi}\}\ dx \quad (2.13)$$

In view of Eq. (2.4), the terms inside the integral on the right hand side of Eq. (2.13) can be expanded as:

$$\{u_{PLi}\}^T[N_{Li}]^T[N_{Li}]\{u_{PLi}\} - 2\{u_{PLi}\}^T[N_{Li}]^T[N_{Li}]\{x_{GLi}\} + \{x_{GLi}\}^T[N_{Li}]^T[N_{Li}]\{x_{GLi}\}$$

Plugging these terms into Eq. (2.13) obtains:

$$U^i_{Soil,Lateral} = \frac{1}{2} k_{SLi}\{u_{PLi}\}^T \int_0^{L_i}[N_{Li}]^T[N_{Li}]\,dx\,\{u_{PLi}\} - k_{SLi}\{u_{PLi}\}^T \int_0^{L_i}[N_{Li}]^T[N_{Li}]\,dx\,\{x_{GLi}\} + \frac{1}{2} k_{SLi}\{x_{GLi}\}^T \int_0^{L_i}[N_{Li}]^T[N_{Li}]\,dx\,\{x_{GLi}\} \quad (2.14)$$

Again, as mentioned before the last term on the right hand side of Eq. (2.14) can be represented by a constant b_i. Thus, after integrating Eq. (2.14) can be rewritten as:

$$U^i_{Soil,Lateral} = \frac{1}{2} \underset{1x4}{\{u_{PLi}\}^T} \underset{4x4}{[k^i_{SL}]} \underset{4x1}{\{u_{PLi}\}} - \underset{1x4}{\{u_{PLi}\}^T} \underset{4x4}{[k^i_{SL}]} \underset{4x1}{\{x_{GLi}\}} + b_i \quad (2.15)$$

where

$$[k^i_{SL}]_{4x4} = k_{SLi}\int_0^{L_i}[N_{Li}]^T[N_{Li}]\,dx$$

$$= k_{SLi}L_i\begin{bmatrix} \frac{13}{35} & \frac{11}{210}L_i & \frac{9}{70} & -\frac{13}{420}L_i \\ & \frac{L_i^2}{105} & \frac{13}{420}L_i & \frac{L_i^2}{140} \\ & & \frac{13}{35} & -\frac{11}{210}L_i \\ & \text{Symmetric} & & \frac{L_i^2}{105} \end{bmatrix} \qquad (2.15a)$$

and b_i is a constant. Combining Eqs. (2.9) and (2.15), the total soil strain energy within the ith element can be obtained as:

$$U^i_{Soil} = U^i_{Soil,Long} + U^i_{Soil,Lateral} \qquad (2.16)$$

or

$$U^i_{Soil} = \frac{1}{2}\underset{1x2}{\{u_{PAi}\}^T}\underset{2x2}{[k^i_{SA}]}\underset{2x1}{\{u_{PAi}\}} + \frac{1}{2}\underset{1x4}{\{u_{PLi}\}^T}\underset{4x4}{[k^i_{SL}]}\underset{4x1}{\{u_{PLi}\}}$$

$$- \underset{1x2}{\{u_{PAi}\}^T}\underset{2x2}{[k^i_{SA}]}\underset{2x1}{\{x_{GAi}\}} - \underset{1x4}{\{u_{PLi}\}^T}\underset{4x4}{[k^i_{SL}]}\underset{4x1}{\{x_{GLi}\}}$$

$$+ a_i + b_i \qquad (2.17)$$

Note that the first four terms on the right hand side of Eq. (2.17) can be expanded to the same dimension and then the first two terms and the next two terms can be composed

together, respectively. Eq. (2.17) can be rewritten as:

$$U^i_{Soil} = \underset{1x6}{\frac{1}{2}\{u_{Pi}\}^T} \underset{6x6}{[k^i_S]} \underset{6x1}{\{u_{Pi}\}} - \underset{1x6}{\{u_{Pi}\}^T} \underset{6x6}{[k^i_S]} \underset{6x1}{\{x_{Gi}\}} + c_i \tag{2.18}$$

where $[k_{Si}]$ is the element stiffness of surrounding soil along the ith pipe element and $c_i = a_i + b_i$ is a constant.

After transforming the soil stiffness matrix $[k_S]$ of local coordinate into $[K_S]$ of global coordinate in view of Eqs. (2.1c) and (2.1d), the total strain energy of surrounding soil can be obtained by adding Eq. (2.17) or Eq. (2.18) through all elements:

$$U^{Total}_{Soil} = \sum_{i=1}^{NM} U^i_{Soil}$$

$$= \sum_{i=1}^{NM} \left(\underset{1x6}{\frac{1}{2}\{U_{Pi}\}^T} \underset{6x6}{[K_{Si}]} \underset{6x1}{\{U_{Pi}\}} - \underset{1x6}{\{U_{Pi}\}^T} \underset{6x6}{[K_{Si}]} \underset{6x1}{\{X_{Gi}\}} + c_i \right) \tag{2.19}$$

or

$$U^{Total}_{Soil} = \underset{1xn}{\frac{1}{2}\{U_P\}^T} \underset{nxn}{[K_S]} \underset{nx1}{\{U_P\}} - \underset{1xn}{\{U_P\}^T} \underset{nxn}{[K_S]} \underset{nx1}{\{X_G\}} + c \tag{2.20}$$

where $[K_S]$ is the system stiffness matrix of surrounding soil and c is a constant.

2.1.3 Strain Energy of Joints

As shown in Fig. 1.4b, the relative displacement of the ith intermediate linear joint can be written as:

$$U^i_{Joint} = \frac{1}{2} k_{JAi}(u_{6i+1} - u_{6i-2})^2 + \frac{1}{2} k_{JRi}(u_{6i+3} - u_{6i})^2 \tag{2.21}$$

or in matrix form:

$$U^i_{Joint} = \frac{1}{2} \underset{1x4}{\{u_{Ji}\}^T} \underset{4x4}{[k^i_J]} \underset{4x1}{\{u_{Ji}\}} \qquad i=1, 2, \ldots, NJ-NBJ \tag{2.22}$$

where

$$\underset{1x4}{\{u_{Ji}\}^T} = [u_{6i+1},\ u_{6i+3},\ u_{6i-2},\ u_{6i}] \tag{2.22a}$$

$$\underset{4x4}{[k^i_J]} = \begin{bmatrix} k_{JAi} & 0 & -k_{JAi} & 0 \\ & k_{JRi} & 0 & -k_{JRi} \\ & & k_{JAi} & 0 \\ \text{Symmetric} & & & k_{JRi} \end{bmatrix} \tag{2.22b}$$

NJ is the total number of joints in the system in which the number of boundary joints is denoted as NBJ. k_{JAi} and k_{JRi} are longitudinal and rotational spring constants of ith joint, respectively. Note that there is no lateral displacement component involved in Eq. (2.21), since no relative joint displacement in lateral direction at each

joint is assumed. The detail of stiffness matrices of other types of joints are shown in Appendix. For the boundary joints, which are connected to the station, building or free, the strain energy at each boundary joint can be written as:

$$U^j_{Joint} = \frac{1}{2} k_{JAj}(u_{6i-5} - x_{GAj})^2 + \frac{1}{2} k_{JRj} u^2_{6i-3} \quad (2.23)$$

or in matrix form:

$$U^j_{Joint} = \frac{1}{2} \underset{1x2}{\{u_{Jj}\}^T} \underset{2x2}{[k^j_{BJ}]} \underset{2x1}{\{u_{Jj}\}} - \underset{1x2}{\{u_{Jj}\}^T} \underset{2x2}{[k^j_{BJ}]} \underset{2x1}{\{x_{GBj}\}}$$

$$+ \frac{1}{2} \underset{1x2}{\{x_{GBj}\}^T} \underset{2x2}{[k^j_{BJ}]} \underset{2x1}{\{x_{GBj}\}} \qquad j=1, 2, \ldots, NBJ \quad (2.24)$$

where i is the nodal number of the pipe adjacent to boundary joint j;

$$\underset{1x2}{\{u_{Jj}\}^T} = [u_{6i-5}, u_{6i-3}]; \quad \underset{1x2}{\{x_{GBj}\}^T} = [x_{GAj}, 0] \quad (2.25a)$$

are the boundary joint displacement vector and the corresponding ground displacement vector, respectively, as shown in Fig. 2.2, and

$$\underset{2x2}{[k^j_{BJ}]} = \begin{bmatrix} k_{JAj} & 0 \\ 0 & k_{JRj} \end{bmatrix} \quad (2.25b)$$

is the stiffness matrix of the jth boundary joint. Note that the last term on the right hand side of Eq. (2.24) is

independent of unknown nodal displacements and can be represented by a constant d_j.

After transformation of axes and assembly, the total strain energy of joints can be obtained in the form of:

$$U_{Joint}^{Total} = \sum_{i=1}^{NJ-NBJ} U_{Joint}^{i} + \sum_{j=1}^{NBJ} U_{Joint}^{j}$$

$$= \sum_{i=1}^{NJ-NBJ} \frac{1}{2} \underset{1x4}{\{U_{Ji}\}^T} \underset{4x4}{[K_J^i]} \underset{4x1}{\{U_{Ji}\}} + \sum_{j=1}^{NBJ} \left(\frac{1}{2} \underset{1x2}{\{U_{Jj}\}^T} \underset{2x2}{[K_{BJ}^j]} \underset{2x1}{\{U_{Jj}\}} \right.$$

$$\left. - \underset{1x2}{\{U_{Jj}\}^T} \underset{2x2}{[K_{BJ}^j]} \underset{2x1}{\{X_{GBj}\}} + d_j \right) \qquad (2.26)$$

or

$$U_{Joint}^{Total} = \frac{1}{2} \underset{1xn}{\{U_P\}^T} \underset{nxn}{[K_J]} \underset{nx1}{\{U_P\}} - \sum_{i=1}^{NBJ} \underset{1x1}{\{U_{JAi}\}^T} \underset{1x1}{[K_{JAi}]} \underset{1x1}{\{X_{GAi}\}} + d$$

(2.27)

where $[K_J]$ is the system stiffness matrix of joints. Note that the second term on the right hand side of Eq. (2.27) contains only the longitudinal strain energy of boundary joints since the rotational component of ground displacement is zero; the boundary conditions of the system are imposed at this term.

2.1.4 Total Potential Energy of the Pipeline System

Adding Eqs. (2.3), (2.20), and (2.27), one obtains the total strain energy of the pipeline system in the form of:

$$U^{Total} = U^{Total}_{Pipe} + U^{Total}_{Soil} + U^{Total}_{Joint} \qquad (2.28)$$

or

$$U^{Total} = \underset{1xn\ \ nxn\ \ nx1}{\frac{1}{2}\{U_P\}^T[K_P]\{U_P\}} + \underset{1xn\ \ nxn\ \ nx1}{\frac{1}{2}\{U_P\}^T[K_S]\{U_P\}}$$

$$+ \underset{1xn\ \ nxn\ \ nx1}{\frac{1}{2}\{U_P\}^T[K_J]\{U_P\}} - \underset{1xn\ \ nxn\ \ nx1}{\{U_P\}^T[K_S]\{X_G\}}$$

$$- \sum_{i=1}^{NBJ} \underset{1x1\ \ 1x1\ \ 1x1}{\{U_{JAi}\}^T[K_{JAi}]\{X_{GAi}\}} + c + d \qquad (2.29)$$

Note that on the right hand side of Eq. (2.29) the first three terms can be combined together as well as the fourth and fifth terms. Then Eq. (2.29) can be expressed in a simple form as:

$$U^{Total} = \underset{1xn\ \ nxn\ \ nx1}{\frac{1}{2}\{U_P\}^T[K_{SYS}]\{U_P\}} - \underset{1xn\ \ nxn\ \ nx1}{\{U_P\}^T[K]\{X_G\}} + h \qquad (2.30)$$

where

$$\underset{nxn}{[K_{SYS}]} = \underset{nxn}{[K_P]} + \underset{nxn}{[K_S]} + \underset{nxn}{[K_J]} \qquad (2.30a)$$

is the system stiffness matrix of the buried pipeline system and [K] is a coefficient matrix consisting of system stiffness of surrounding soil, $[K_S]$, and longitudinal stiffness of boundary joints, and h is a constant.

2.1.5 Governing Equations of Equilibrium of a Buried Pipeline System

Based on the principle of variation, the first variation of the total potential energy of an equilibrium system should be equal to zero. Thus,

$$\delta\, U^{Total} = 0 \tag{2.31}$$

or

$$\frac{\partial\, U^{Total}}{\partial\, \{U_P\}} = 0 \tag{2.32}$$

where $\{U_P\}$ is the unknown nodal displacement. Then in view of Eq. (2.30) one obtains the following equation:

$$\underset{nxn}{[K_{SYS}]}\ \underset{nx1}{\{U_P\}} = \underset{nxn}{[K]}\ \underset{nx1}{\{X_G\}} = \underset{nx1}{\{F(t)\}} \tag{2.33}$$

where $\{F(t)\}$ is the equivalent force vector. Since $\{X_G\}$ is a function of time, then the forcing function $\{F(t)\}$ is a function of time.

Solving Eq. (2.33), the displacement responses of the pipeline, $\{U_P\}$, can be obtained. Then the pipe responses in local coordinates, $\{u_P\}$, can be obtained by following equations:

$$\underset{6x1}{\{u_{Pi}\}} = \underset{6x6}{[T]}\ \underset{6x1}{\{U_{Pi}\}} \qquad i = 1, 2, \ldots, NM \tag{2.34}$$

where [T] is the transformation matrix as shown in Eq.

(2.1d). The relative joint displacement can be obtained by subtracting the corresponding displacements, longitudinal and rotational displacements, at each joint. The strain and curvature of pipe can be obtained from the strain- and curvature-displacement relationships [56], respectively, which are given as:

$$\{\varepsilon_i(x)\} = [-\frac{1}{L_i}, \frac{1}{L_i}]\{u_{PAi}\}_{2x1} \quad i=1,2,...,NM \quad (2.35)$$

and

$$\{\chi_i(x)\} = [(-\frac{6}{L_i^2} + \frac{12x}{L_i^3}), (-\frac{4}{L_i} + \frac{6x}{L_i^2}), (\frac{6}{L_i^2} - \frac{12x}{L_i^3}), (-\frac{2}{L_i} + \frac{6x}{L_i^2})]\{u_{PLi}\}_{4x1} \quad i=1,2,...,NM \quad (2.36)$$

2.1.6 Special Case (Continuous Pipeline System)

For a continuous pipeline system, the same governing equilibrium equation, Eq. (2.33), for the segmented pipeline is also applicable as long as the joint stiffness is close to infinite. However, in order to save computational time, the governing equilibrium equation for a continuous pipeline can be formulated without consideration of joints (except boundary joints) just like the traditional structural analysis. Therefore, the detail will not be shown here and the governing equilibrium equation is given in the form of:

$$[K_{SYS}]_{nxn}\{U_p\}_{nx1} = [K]_{nxn}\{X_G\}_{nx1} = \{F(t)\}_{nx1} \quad (2.37)$$

where

$$[K_{SYS}]_{nxn} = [K_P]_{nxn} + [K_S]_{nxn} \tag{2.37a}$$

and

$$[K]_{nxn} = [K_S]_{nxn} + [K_{BJ}]_{nxn} \tag{2.37b}$$

and n is the total number of degree of freedom of the continuous buried pipeline system. In view of Eq. (2.34), the pipe responses in local coordinates, $\{u_p\}$, can be obtained. Then Eqs. (2.35 and 2.36) can be applied to obtain the pipe strain and curvature.

2.1.7 Ground Motion Input

The solution for pipe response, $\{U_p\}$, given in Eqs. (2.33 or 2.37) depends on the inputs of the ground motion, $\{X_G\}$. Since $\{X_G\}$ is a function of time, the solution of $\{U_p\}$ is also a function of time.

Assuming that the wave form of the traveling seismic excitation remains constant over the entire pipeline system, the inputs of the time-space varying ground motions starting from the first node are:

$$\{X_{Gi}(t)\} = \begin{Bmatrix} X_{GAi} \\ X_{GLi} \\ 0 \end{Bmatrix} = A_{max} g(t - \Delta t_i) \tag{2.38}$$

where A_{max} is the amplitude of ground displacement; g(t) is

the displacement time function which equals 0 as $t \leq \Delta t_i$; Δt_i is the delay time of seismic wave traveling from the first node to the end face of the ith node and is given in the form of:

$$\Delta t_i = \sum_{j=1}^{i} L_j/C_j \qquad (2.39)$$

and C_j is the propagation velocity of seismic wave with respect to the jth pipe segment. Note that in Eq. (2.38) there is no rotational component in the ground displacement input.

2.2 Solution and Computer Program

A computer program is developed to solve the elastic responses of buried pipeline system (continuous and segmented). For a given buried pipeline system, the coordinates of each node, and information on the pipe (Young's modulus, outer and inner diameter), surrounding soil (longitudinal and lateral spring constants), joint (longitudinal and rotational spring constants) and ground motion (wave velocity, incident angle, types of wave, displacement data such as number of records, time step and magnitude) are required as input data. Then the stiffness matrices, $[K_{SYS}]$, $[K_S]$, $[K_J]$ and $[K]$ are constructed automatically. Because of the symmetric characteristics of the stiffness matrices, the Choleski scheme is applied to

solve for the pipe responses in global coordinates, $\{U_p\}$ as shown in Eqs. (2.33) and (2.37). Then, converting $\{U_p\}$ to local coordinates, $\{u_p\}$, the joint responses for segmented pipes, $\{u_{JA}\}$ and $\{u_{JR}\}$, can be obtained and so can the pipe strains and curvatures (Eqs. (2.35) and (2.36)).

Note that this program has been modified for studying inelastic analysis. For more information about this program, one can refer to Sec. 3.7 and the details of input/output data and listing of the computer program will be given in a separate report [55].

2.2.1 Verification of the Developed Computer Program for Elastic Analysis

The developed program has been verified by comparing the results with those obtained by traditional structural analysis and Wang's program [52].

Considering a plane frame structure as shown in Table 2.1 subjected to a unit vertical displacement at support A, the responses at node B by using the developed program and traditional plane frame analysis are shown in Table 2.1. From this table one can see that the results obtained by the developed program is almost the same as those obtained by plane frame analysis.

Another comparison is made by considering a straight buried pipeline with both ends fixed as shown in Table 2.2 subjected to a sinusoidal P-wave with traveling velocity of

2400 in/sec, amplitude of 1 inch, period of 0.8 sec., time step of 0.1 sec. and duration of 4 sec. The maximum compressive pipe strain responses with various longitudinal soil spring constants, k_{SA} = 0.001 to 1000 ksi, obtained by the developed program as well as by Wang's program are shown in Table 2.2. It is shown in this table that the results obtained by both programs are almost exactly the same.

The above comparisons verify the accuracy of the developed program. Using this program, a series of parametric studies have been studied and shown in the following section.

2.3 Parametric Study

To study the effects of various parameters in a buried pipeline system, a cross type pipeline with 10 segments for each leg (East, West, North and South) as shown in Fig. 2.3 is used as a referenced system for the parametric study. Three types of wave form, trapezoidal, sinusoidal and triangular waves as shown in Fig. 2.4 are used as input ground motions. They have the same amplitude of 1 inch, period of 0.8 seconds, duration of 4 seconds and time step of 0.1 seconds. Later on only the sinusoidal wave is used as the input ground displacement for the rest of parametric study. The referenced and the parametric conditions set for the comparison of results are given in Table 2.3.

2.4 Results and Discussion

Using the developed computer program [55], a series of parametric studies have been done. For comparison purposes only the maximum responses, i.e., maximum pipe strains, pipe curvatures, joint displacements and rotational angles are plotted versus various soil conditions. The results and discussion of continuous and segmented pipeline system are presented in the following sub-sections, respectively.

2.4.1 Continuous Pipeline System Responses

The results of the parametric study for continuous pipeline system are given in Figs. 2.5 to 2.12. Figures 2.5 and 2.6 show the effects of wave forms on the maximum pipe responses; Figs. 2.7 and 2.8, the effects of pipe sizes; Figs. 2.9 and 2.10, the effects of wave velocities; Fig. 2.11, the effects of incident angles of ground waves; and Fig. 2.12, the effects of pipe materials. The longitudinal and lateral soil spring constants are varied from 0.00001 to 100,000 ksi for Figs. 2.5 and 2.6. Because of the effect of low spring constant, the value of 0.1 to 100,000 ksi for soil spring constants were used for subsequent studies as shown in Figs. 2.7 to 2.12.

For continuous pipelines, one can see that the maximum pipe strain increases as the soil longitudinal stiffness increases as shown in Figs. 2.5, 2.7, 2.9, 2.11 and 2.12 while the maximum pipe curvature increases as the soil

lateral stiffness increases as shown in Figs. 2.6, 2.8, and 2.10. As the soil stiffnesses approach to zero, $k_{SA} = k_{SL} \leq$ 0.01 ksi, the pipe responses will approach to zero since there is no interaction between the soil and the pipe. As the soil stiffnesses approach to a large value, i.e., $k_{SA} = k_{SL} \geq 1000$ ksi, the maximum pipe strain will approach to the upper bound, the maximum ground strain, since the soil is so rigid that no relative soil-pipe displacement is created. In other words, the pipe responses will be identical to the ground movement.

Figures 2.5 and 2.6 show that the trapezoidal wave will create higher pipe responses than the sinusoidal and triangular waves since the trapezoidal displacement wave form produces a greater peak ground velocity than that of the triangular and sinusoidal waves with the same amplitude, period and duration. It is known that higher peak ground velocity produces higher ground strains. Because of high ground strains imposed on the buried pipeline, the pipe responses would also be high. For the same reason the sinusoidal wave produces larger pipe responses than the triangular wave. The maximum velocities of the three different wave forms are presented in Table 2.4.

The effects of pipe sizes on the maximum pipe responses, strain and curvature, are shown in Figs. 2.7 and 2.8, respectively. As shown in Fig. 2.7, the maximum pipe strain decreases as the pipe diameter increases. Since a

larger diameter pipe is stiffer, it is more difficult to be stressed by the imposed ground strain. Therefore, the pipe strain becomes less. Similarly, as shown in Fig. 2.8, the bending rigidity will increase as the pipe diameter increases. Therefore a larger diameter pipe is more difficult to be bent by the imposed ground curvature. A smaller value of the curvature is expected as the pipe diameter increases.

From the responses shown in Figs. 2.9 and 2.10, one can conclude that the lower propagation velocity (P- and S-wave) of the soil (soft soil) at the site will produce higher pipeline responses. This is because the higher wave propagation velocity would allow the ground displacement to travel a longer distance, thus there would be less ground strains and curvatures imposed on the buried pipes.

The effect of the ground wave incident angles, ϕ, on the maximum pipe strains is displayed in Fig. 2.11. In Fig. 2.11 a sinusoidal P-wave with various incident angles, i.e., $\phi = 0°$, 15°, 30° and 45°, is used and the maximum pipe strains are obtained for pipelines in North-South (N-S) and East-West (E-W) directions. One can see from this figure that when $\phi = 0°$, E-W pipe has the highest strain, while N-S the lowest since longitudinal strain dominated the response behavior. At $\phi = 45°$, both E-W and N-S pipes have the same maximum pipe strains because the pipeline system used is symmetrical.

It is also shown in Fig. 2.12 for different pipe materials, i.e., steel, concrete and cast iron, but the same soil conditions, element length, pipe size and ground motion input, the maximum pipe strain increases as the material becomes softer (the smaller value of Young's modulus). This is the same reason related to the relative stiffnesses between the pipe and the surrounding soil.

2.4.2 Segmented Pipeline System Responses

In addition to the parameters used in parametric study for continuous pipelines, the value of joint spring constants, k_{JA} and k_{JR}, varying from 0.1 to 10,000 k/in and k-in/deg are also included for parametric study of segmented pipelines. The results of parametric study for segmented pipeline system are given in Figs. 2.13 to 2.23.

For segmented pipeline systems, in general, as for continuous pipelines, the maximum pipe strain increases as the longitudinal soil stiffness increases as shown in Figs. 2.13, 2.15, 2.18 and 2.20 while the maximum relative joint displacements decreases as the longitudinal soil stiffness increases as shown in Figs. 2.14, 2.16, 2.17, 2.19 and 2.21.

Figures 2.13 and 2.14 present the effects of pipe sizes on the pipe strain and relative joint displacements responses. As shown in these figures, the larger the pipe

size, the larger the maximum relative joint displacement and the smaller the maximum pipe strain will be.

The maximum pipe strain and relative joint displacement responses for different wave velocities are shown in Figs. 2.15 to 2.17. It is shown in these figures that the lower propagation velocity (P- and S-wave) of the soil will cause larger pipeline responses, i.e., pipe strains, joint displacements and rotations.

As shown in Figs. 2.18 and 2.19, the pipe strain and relative joint displacement responses will decrease as the incident angle of ground motion increases. As the incident angle increases, the apparent wave velocity increases (shorter delay time) and the ground displacement component imposed on the pipe decreases (smaller ground strain). Thus, smaller pipe strain responses and relative joint displacements are expected.

In Figs. 2.20 and 2.21 the effects of pipe materials are shown, i.e., the stiffer the pipe material is (larger value of Young's modulus) the smaller the pipe responses and relative joint displacements will be.

The effects of joint stiffness on pipe strain and relative joint displacement responses are shown in Figs. 2.22 and 2.23. From these figures one can see that the pipe strain responses increase, but the relative joint displacement responses decrease, as the joint stiffness

increases. In other words, the more flexible the joint is, the smaller the pipe strain and the larger the relative joint displacement responses will be.

Table 2.1 Comparison of the Responses of a Plane Frame Subjected to a Unit Vertical Displacement at Support A

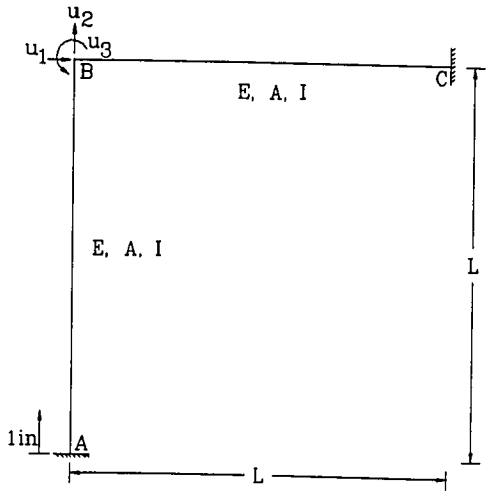

E = 10 ksi

A = 13.94 in^2

I = 549.1 in^4

	Responses at Node B					
	u_1(in)		u_2(in)		u_3(rad)	
L (ft)	(1)*	(2)**	(1)*	(2)**	(1)*	(2)**
12	0.166	0.166	0.519	0.520	-0.043	-0.043
24	0.104	0.105	0.787	0.792	-0.028	-0.028
36	0.059	0.060	0.885	0.892	-0.020	-0.020
60	0.025	0.025	0.954	0.957	-0.012	-0.012
72	0.018	0.018	0.963	0.970	-0.010	-0.010

* Obtained by Developed Program

** Obtained by Plane Frame Analysis

Table 2.2 Comparison of the Maximum Compressive Pipe Strain Responses of a Straight Buried Pipeline Subjected to a Sinusoidal P-wave

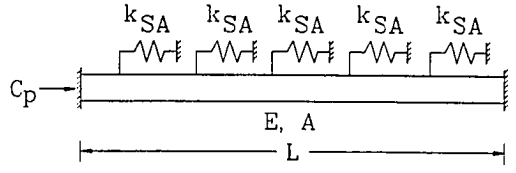

E = 30,000 ksi

A = 13.94 in^2

C_p = 2400 in/sec

k_{SA} (ksi)	Maximum Compressive Pipe Strain ($x10^{-3}$)	
	Developed Program	Wang's Program
0.001	0.42	0.421
0.01	0.447	0.427
0.1	0.678	0.674
1.0	1.70	1.70
10.0	2.84	2.84
100.0	2.96	2.959
1000.0	2.95	2.95

Table 2.3 Referenced and Parametric Conditions

Used in Elastic Parametric Study

Physical Parameter	Referenced Condition	Parametric Conditions
Pipe Material	Steel E=30,000 ksi	Concrete E=3,000 ksi C. I. E = 13,000 ksi
Diameter	OD = 6"	12", 18", 24"
Soil Stiffness	$k_{SA} = k_{SL} = 1$ ksi	k_{SA} = 0.1 to 100,000 ksi k_{SL} = 0.1 to 100,000 ksi
Joint Stiffness	Continuous	k_{JA} = 0.1 to 10,000 k/in k_{JR} = 0.1 to 10,000 k-in/deg
Wave Velocity	C_p = 2400 in/sec C_s = 1200 in/sec	C_p = 1200 to 12,000 in/sec C_s = 600 to 6,000 in/sec
Incident Angle	$\phi = 0°$	$\phi = 0°, 15°, 30°, 45°$
Wave Form	Sinusoidal	Triangular, Trapezoidal

Table 2.4 The Maximum Velocities of Three Types of Wave Form

	Trapezoidal	Sinusoidal	Triangular
Maximum Wave Velocity (in/sec)	10.0	7.07	5.0

Fig. 2.1 Relationship between Local and Global Coordinates

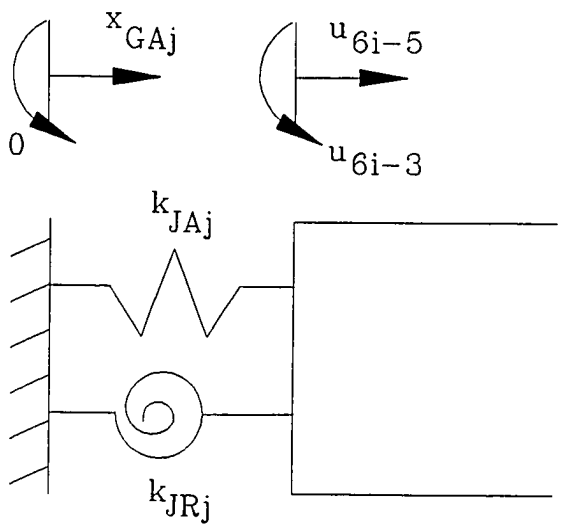

Fig. 2.2 Model for Boundary Joint

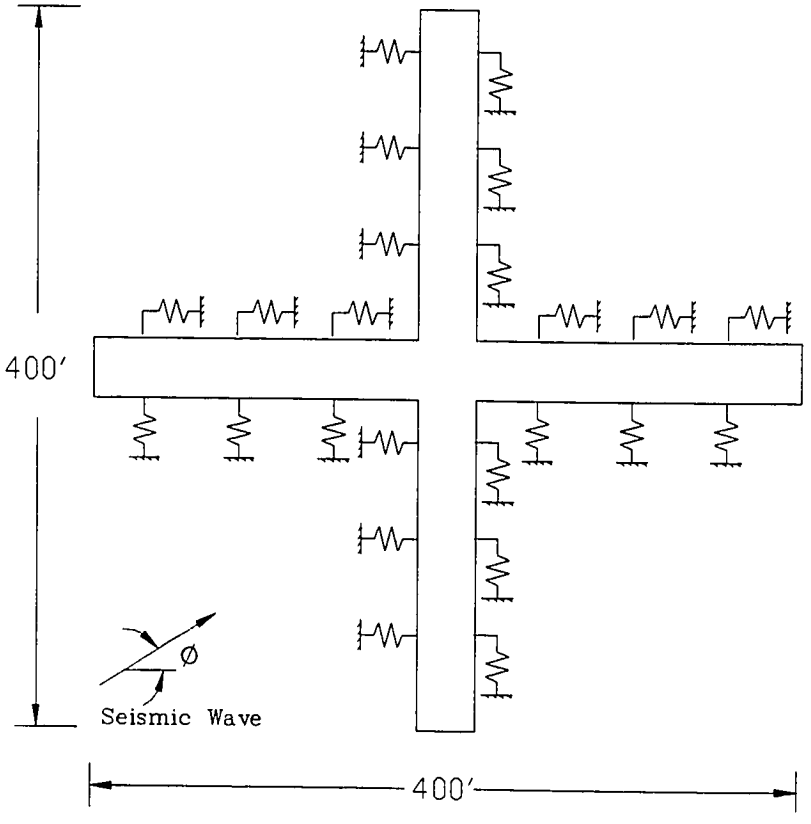

Fig. 2.3 Referenced Pipeline System for Parametric Study

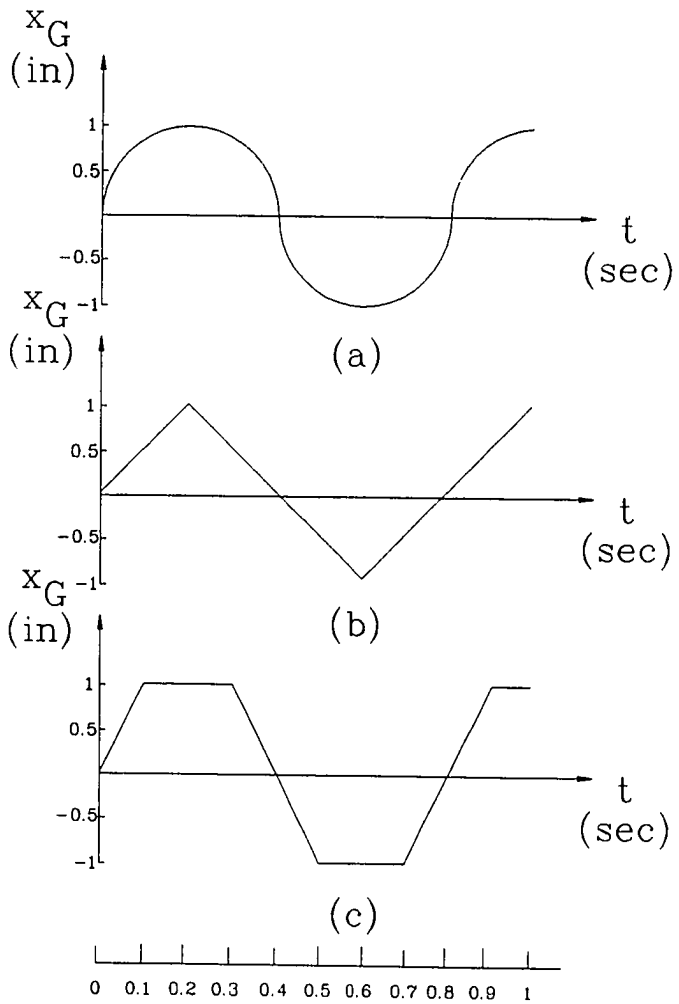

Fig. 2.4 Wave Forms (a) Sinusoidal (b) Triangular (c) Trapezoidal

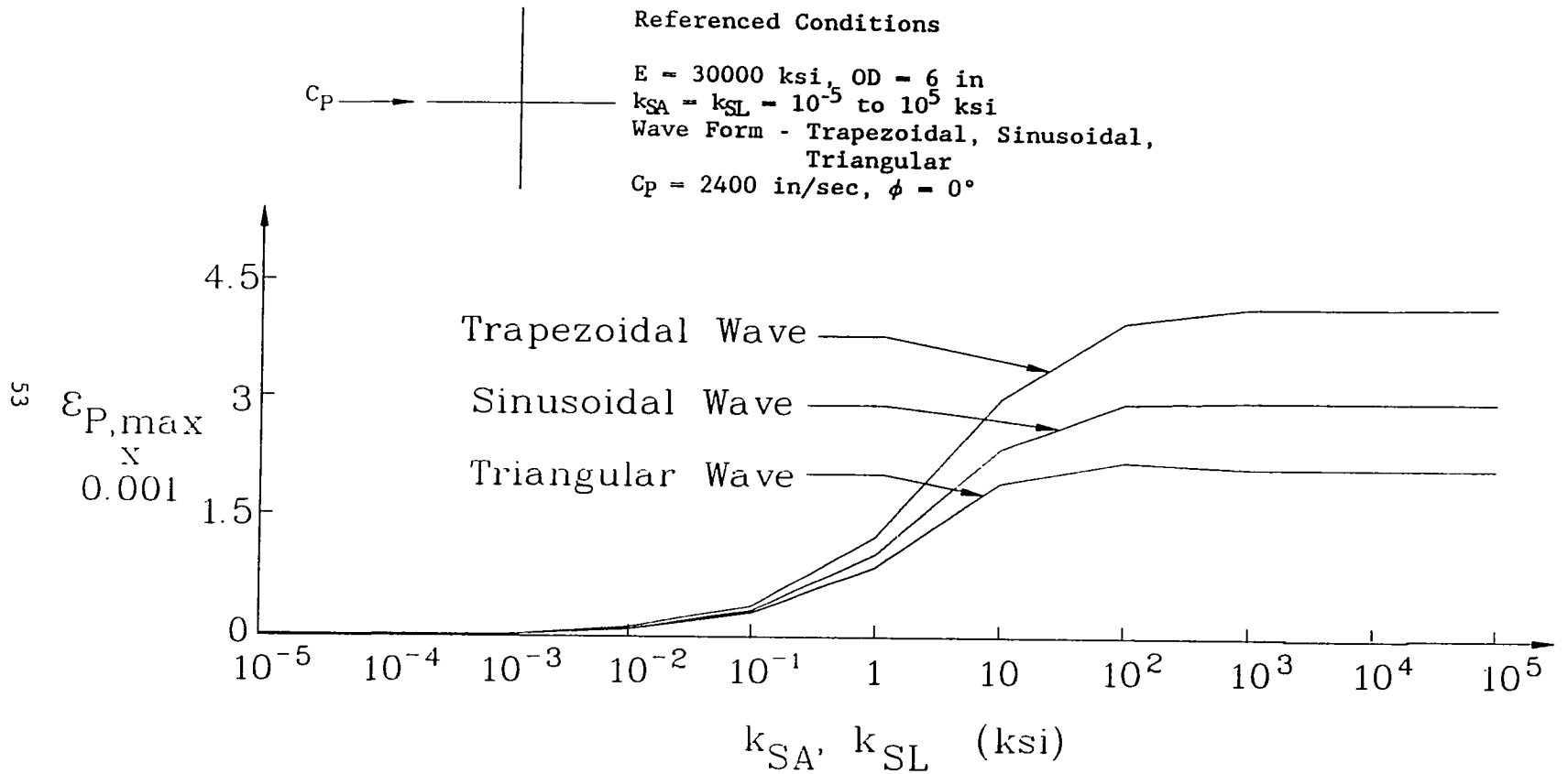

Fig. 2.5 Effect of Wave Form on Pipe Strain Responses

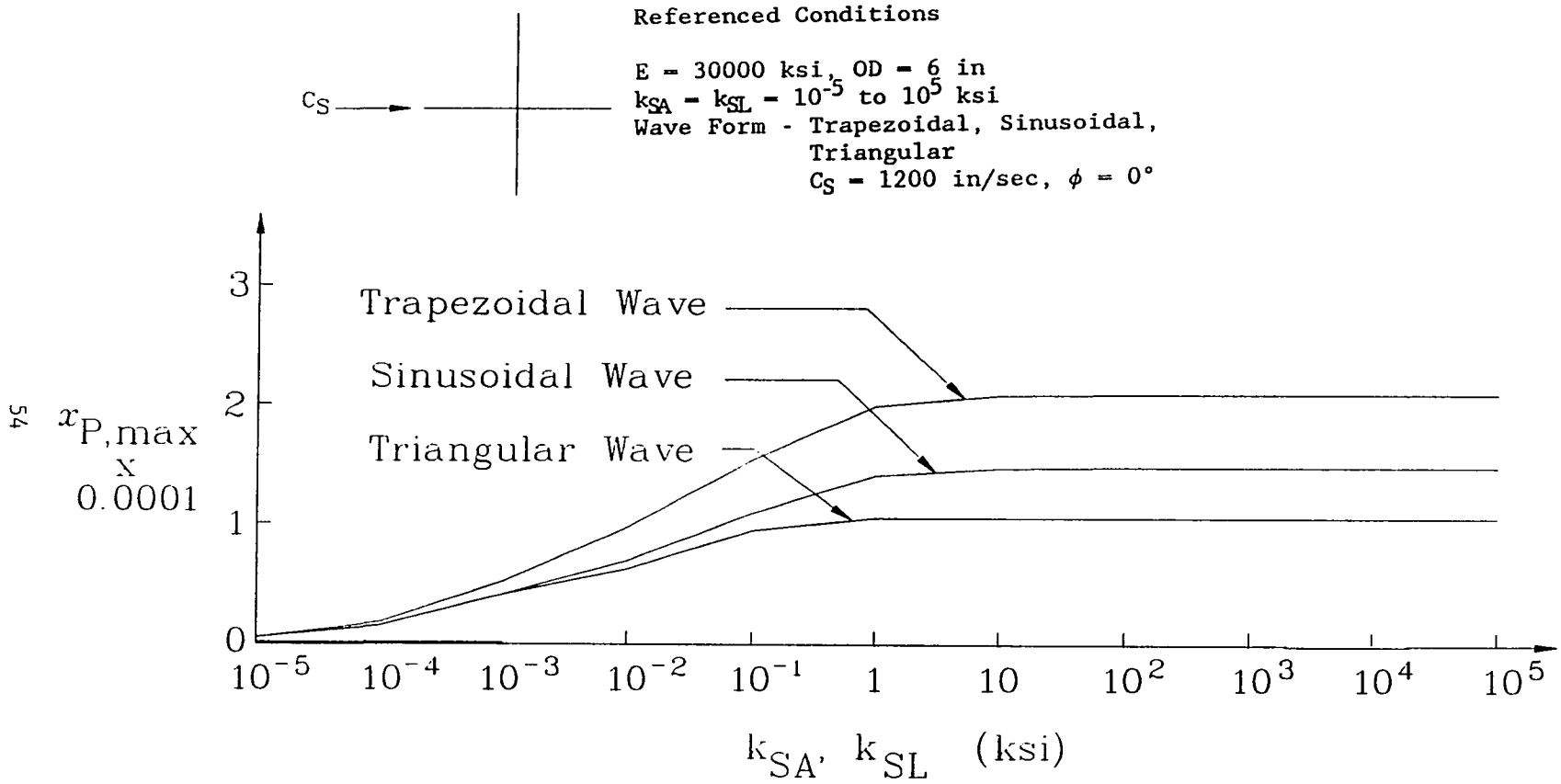

Fig. 2.6 Effect of Wave Form on Pipe Curvature Responses

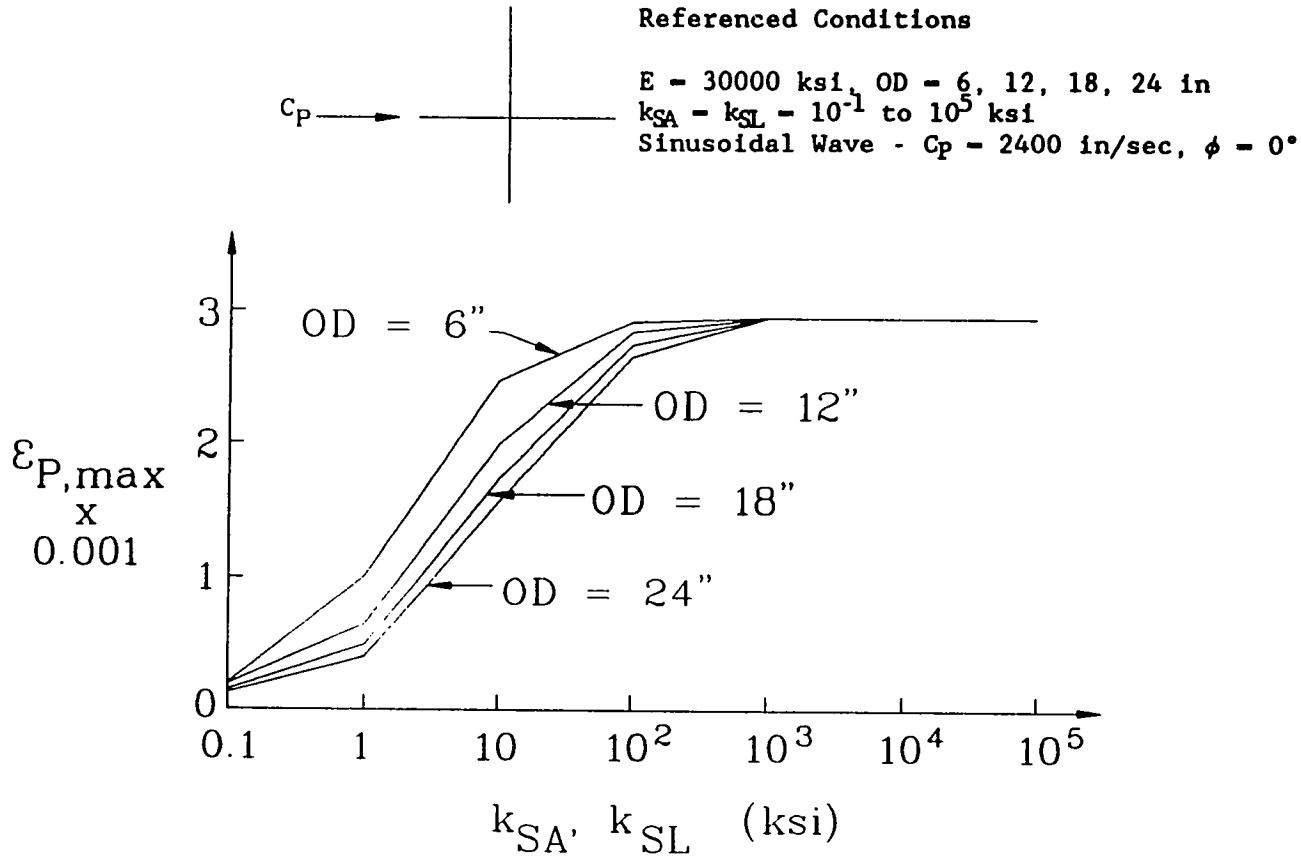

Fig. 2.7 Effect of Pipe Size on Pipe Strain Responses

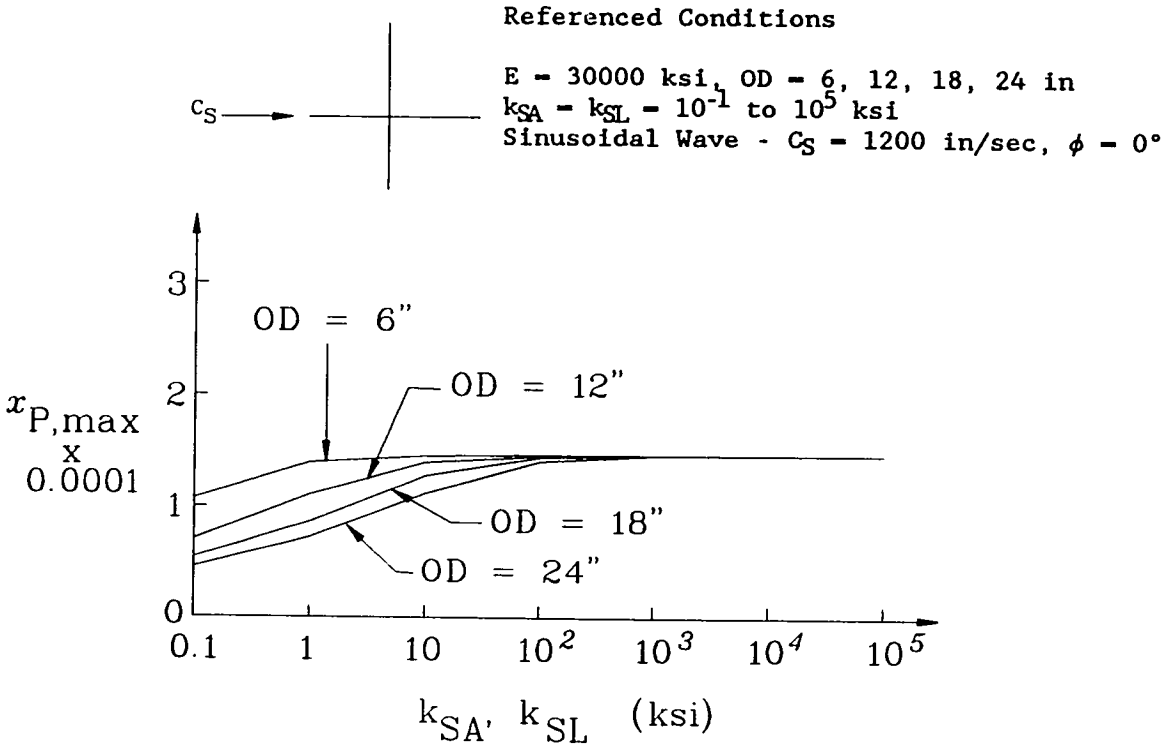

Fig. 2.8 Effect of Pipe Size on Pipe Curvature Responses

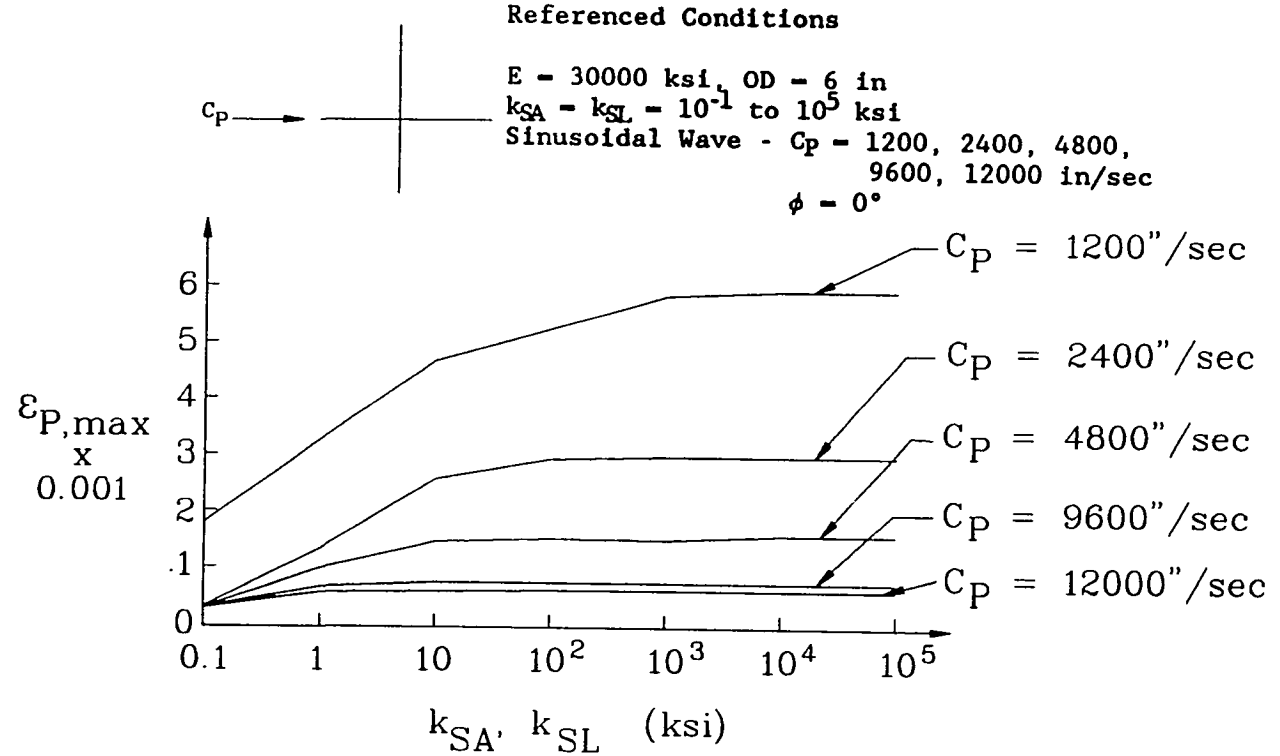

Fig. 2.9 Effect of Wave Velocity on Pipe Strain Responses

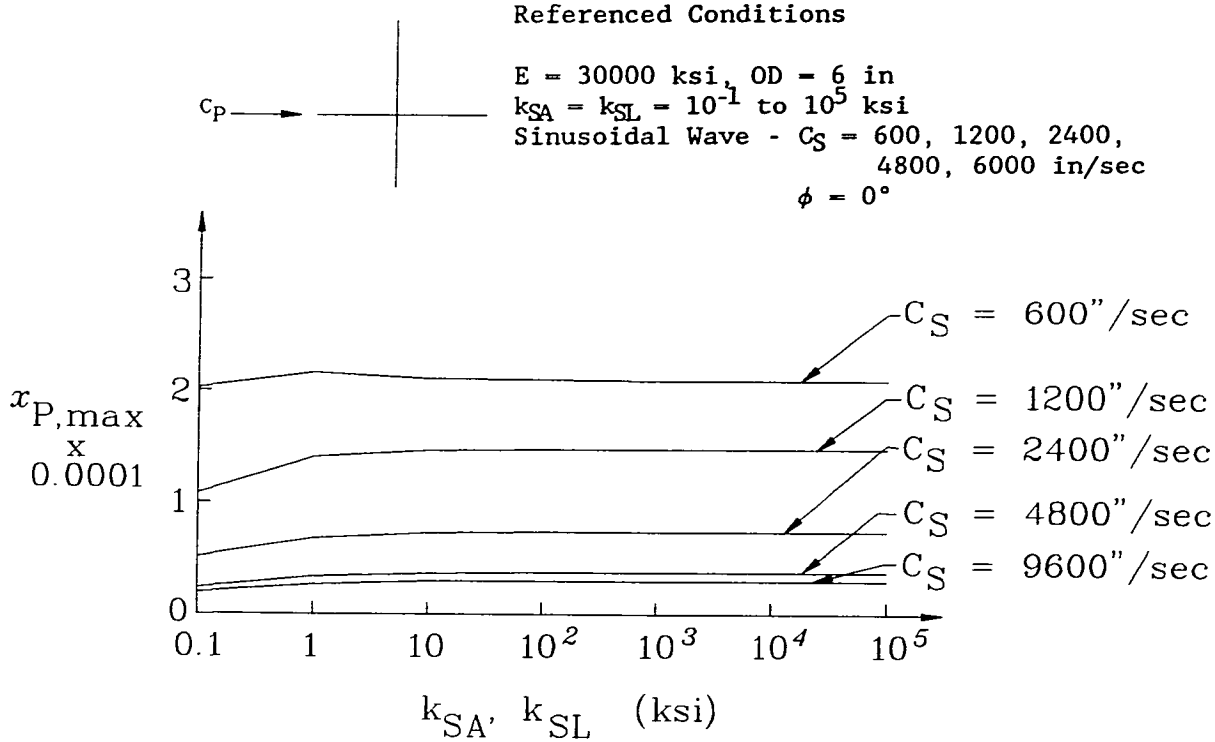

Fig. 2.10 Effect of Wave Velocity on Pipe Curvature Responses

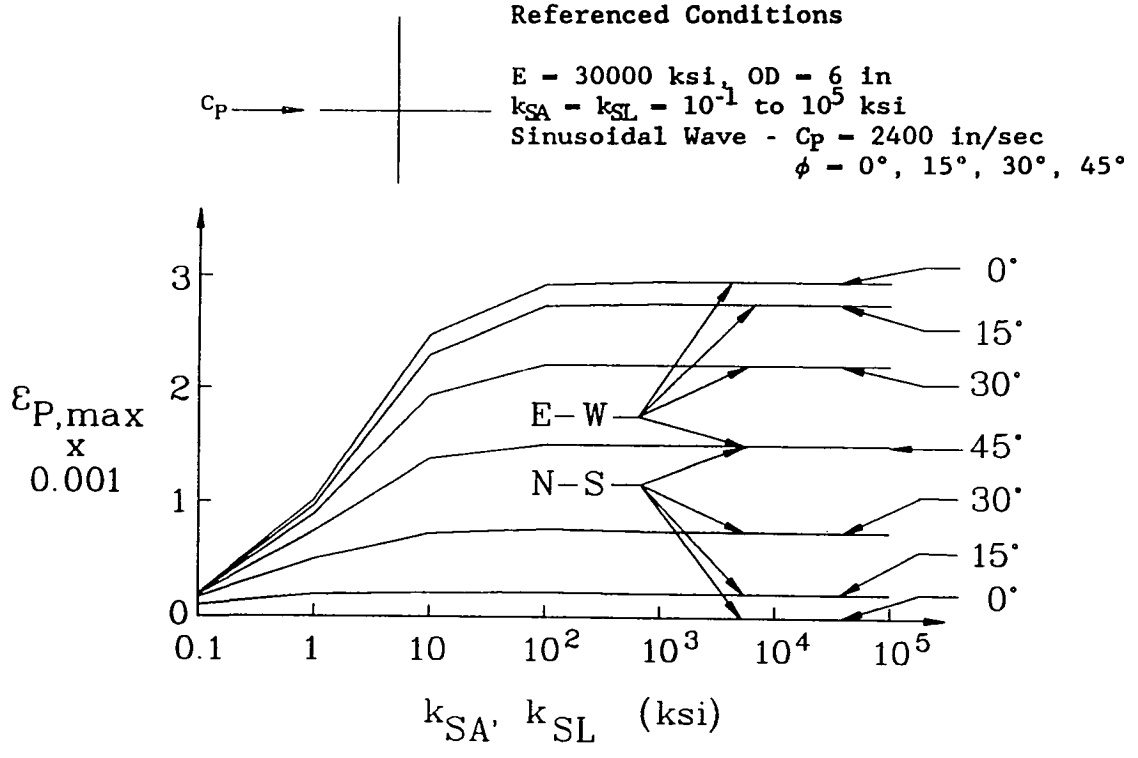

Fig. 2.11 Effect of Incident Angle on Pipe Strain Responses

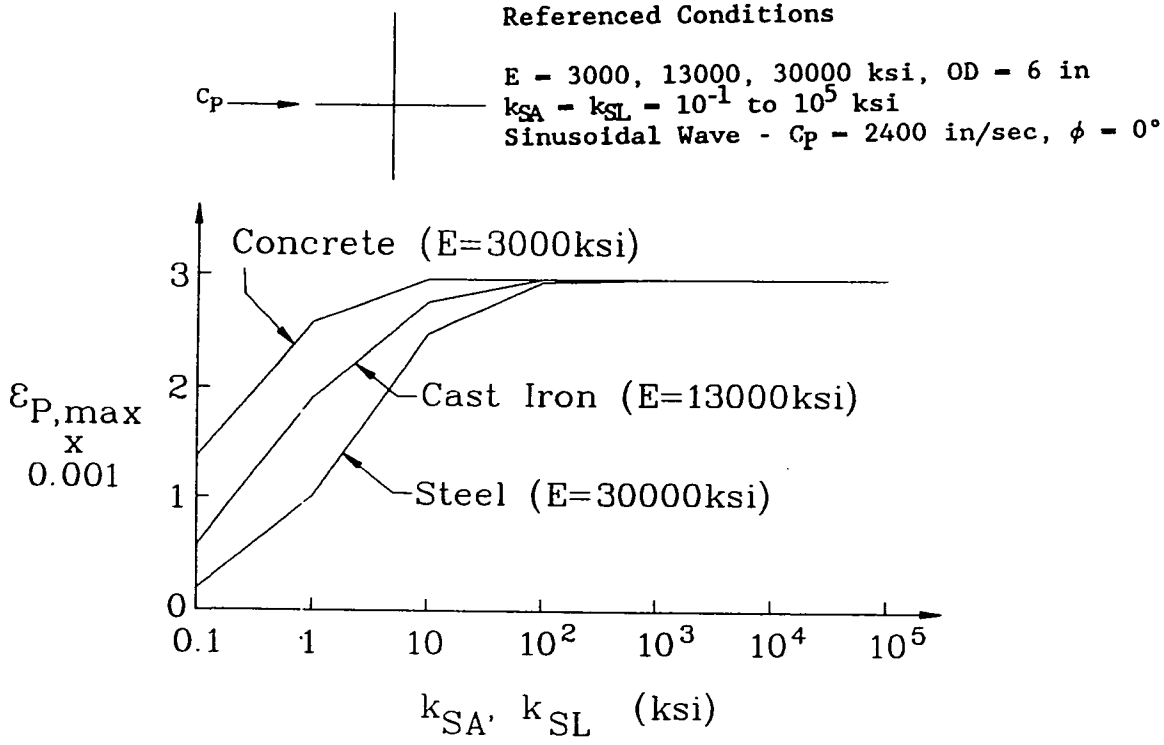

Fig. 2.12 Effect of Material on Pipe Strain Responses

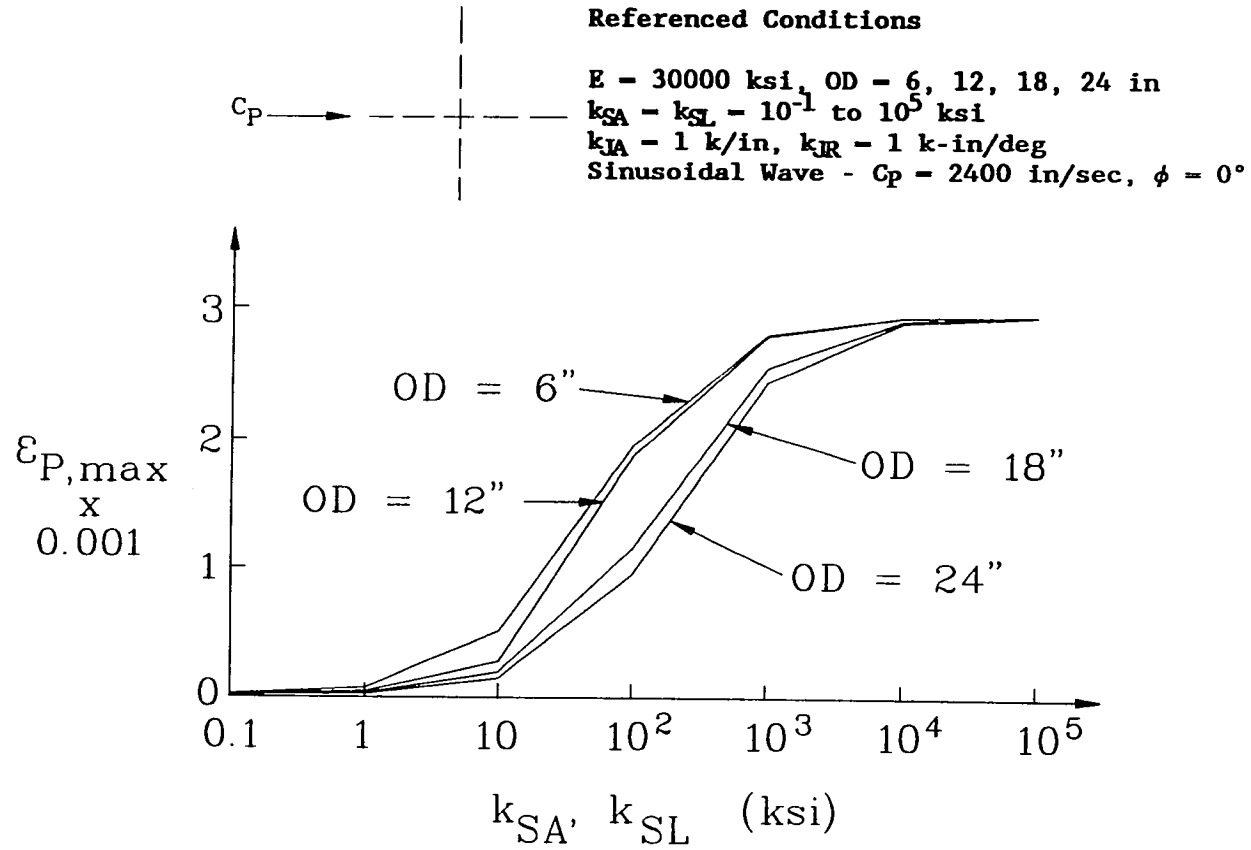

Fig. 2.13 Effect of Pipe Size on Pipe Strain Responses

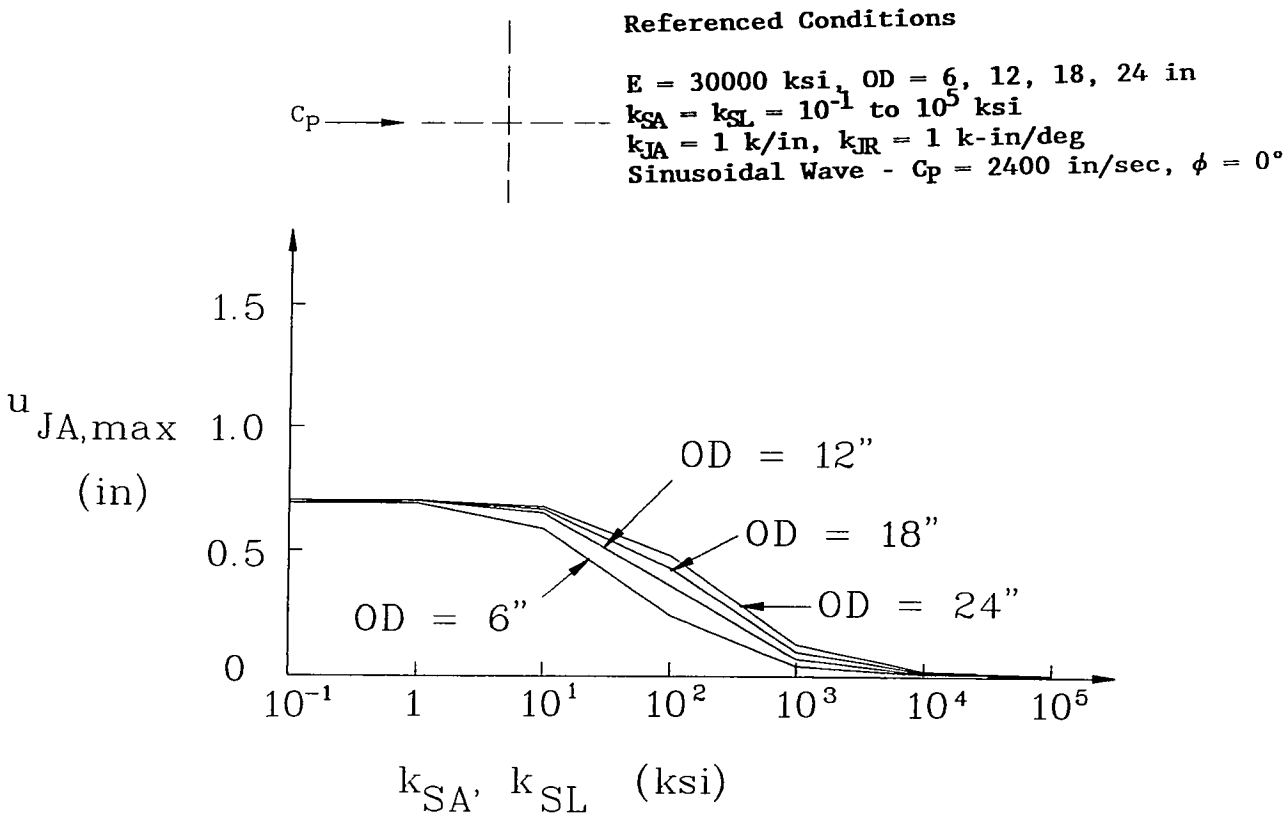

Fig. 2.14 Effect of Pipe Size on Relative Joint Displacement Responses

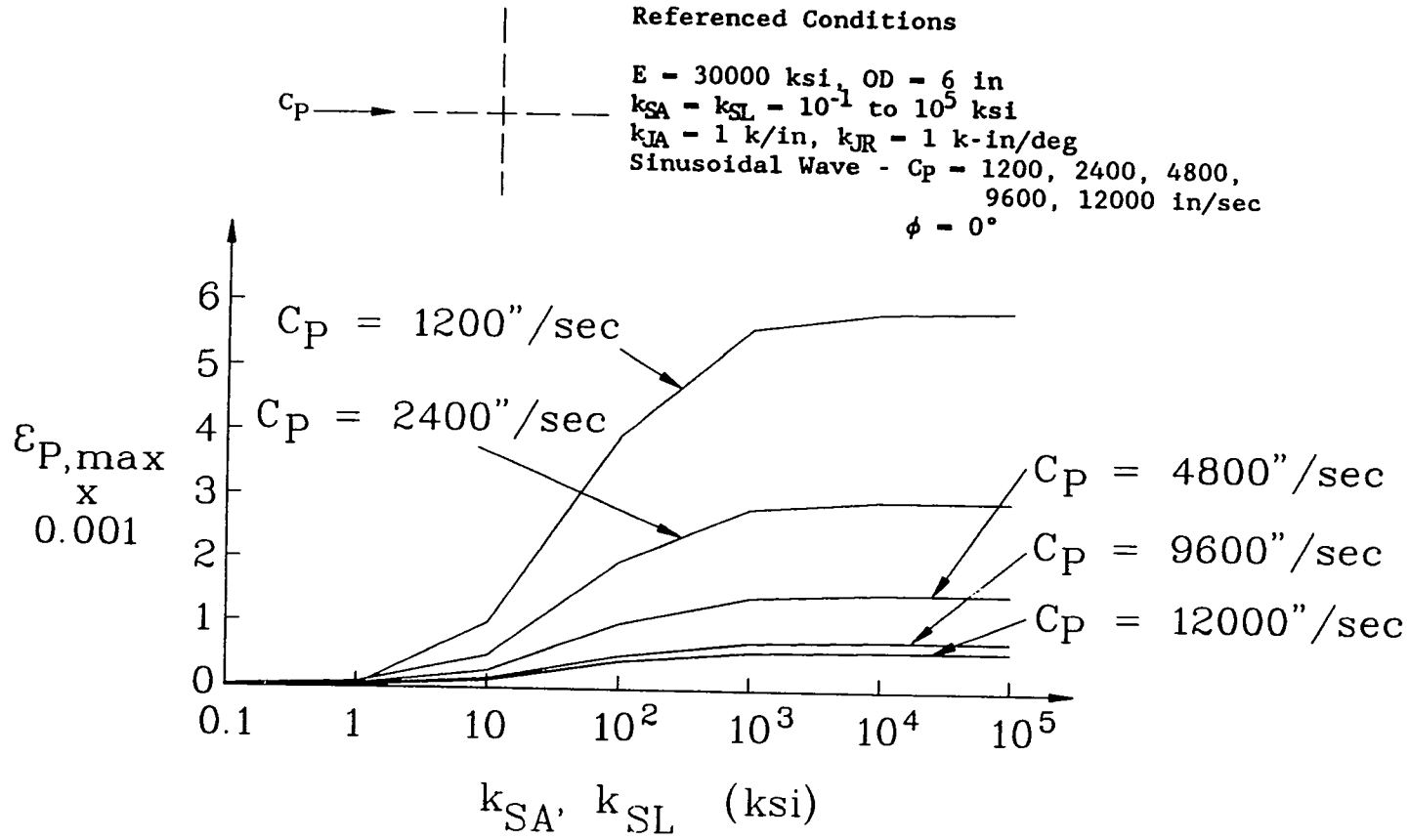

Fig. 2.15 Effect of Wave Velocity on Pipe Strain Responses

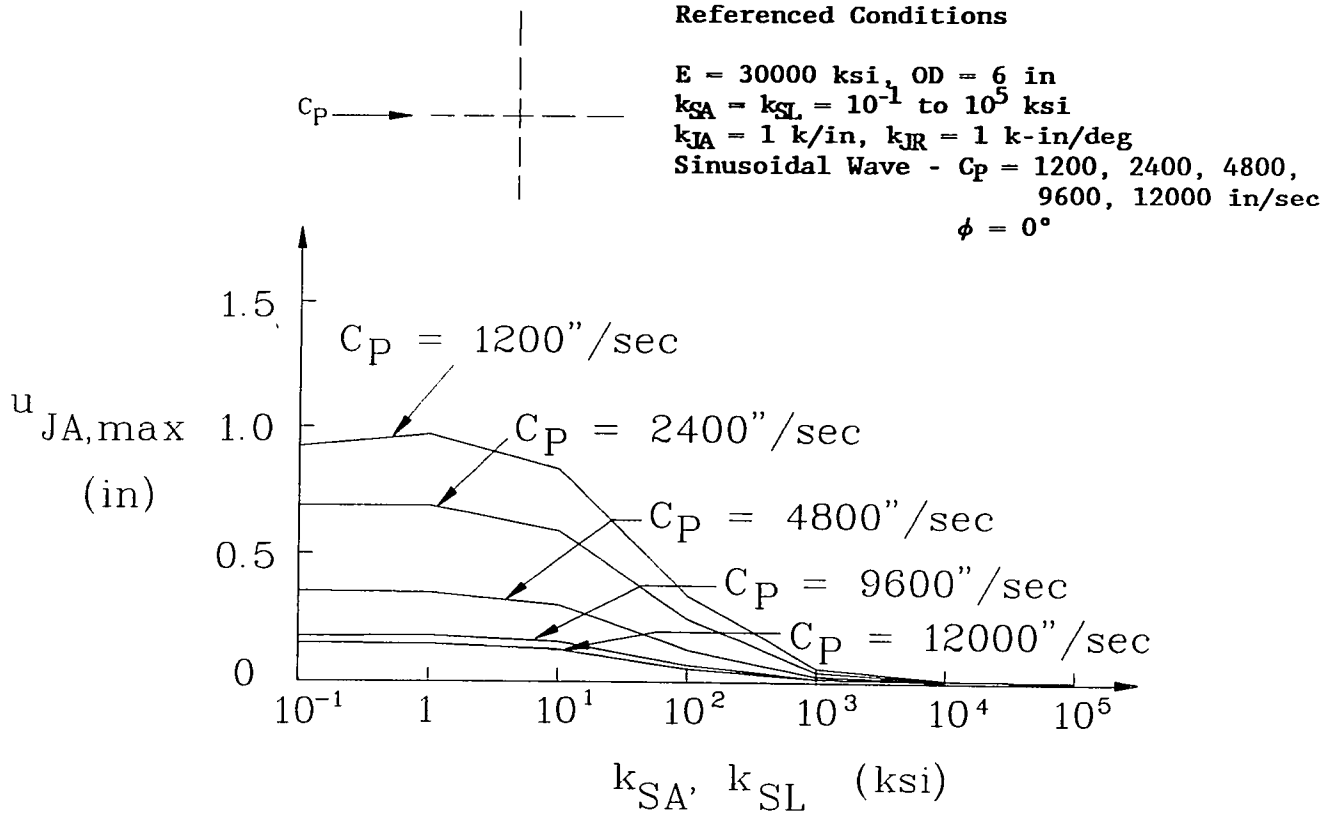

Fig. 2.16 Effect of Wave Velocity on Relative Joint Displacement Responses

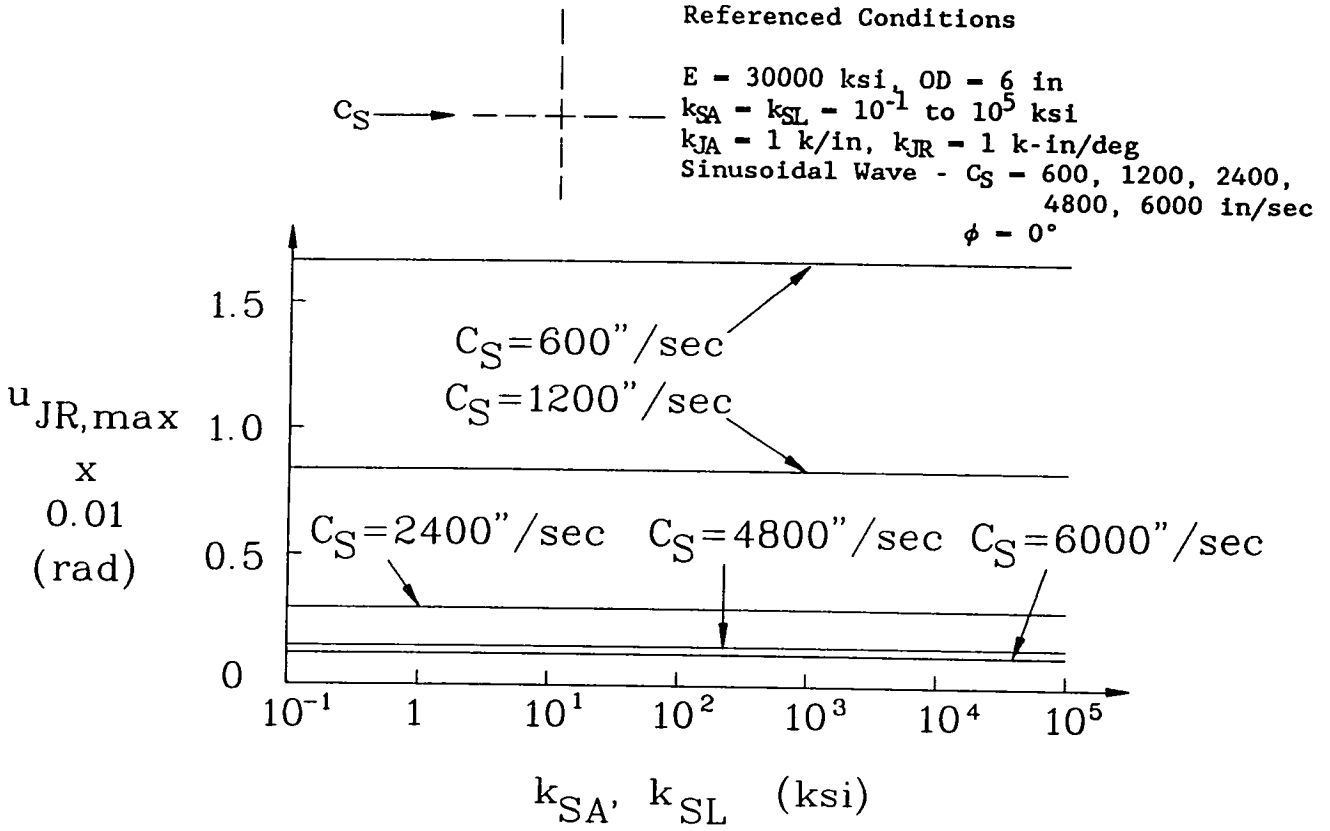

Fig. 2.17 Effect of Wave Velocity on Joint Rotation Responses

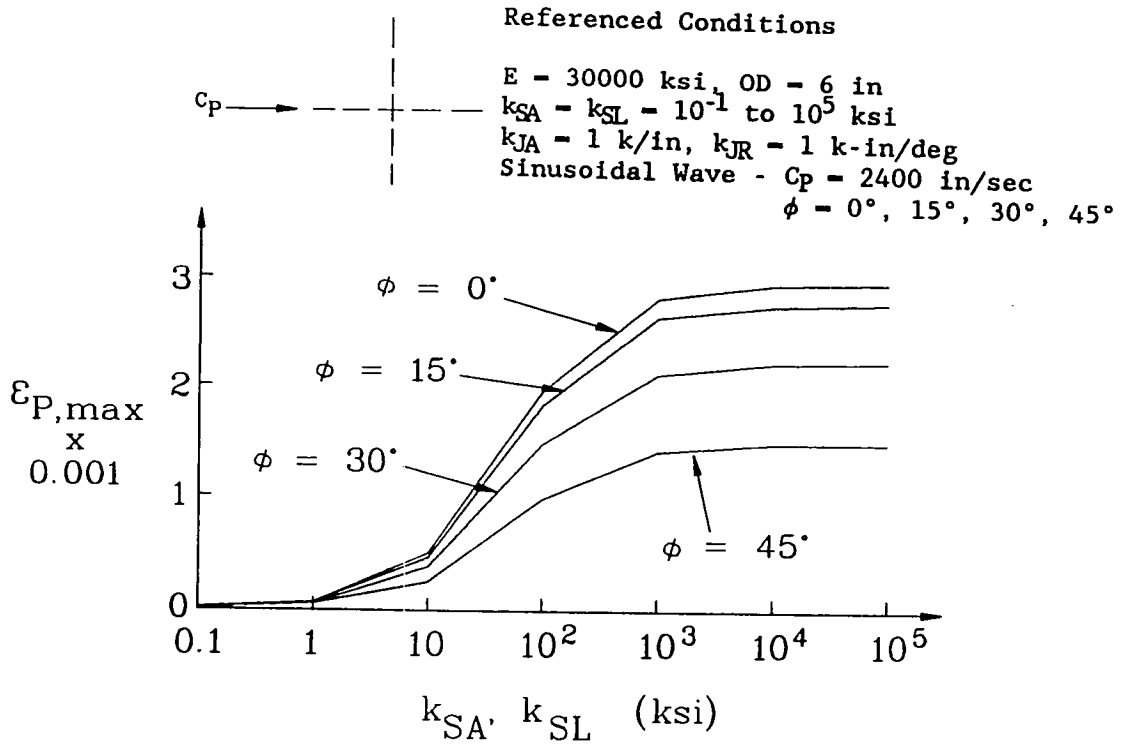

Fig. 2.18 Effect of Incident Angle on Pipe Strain Responses

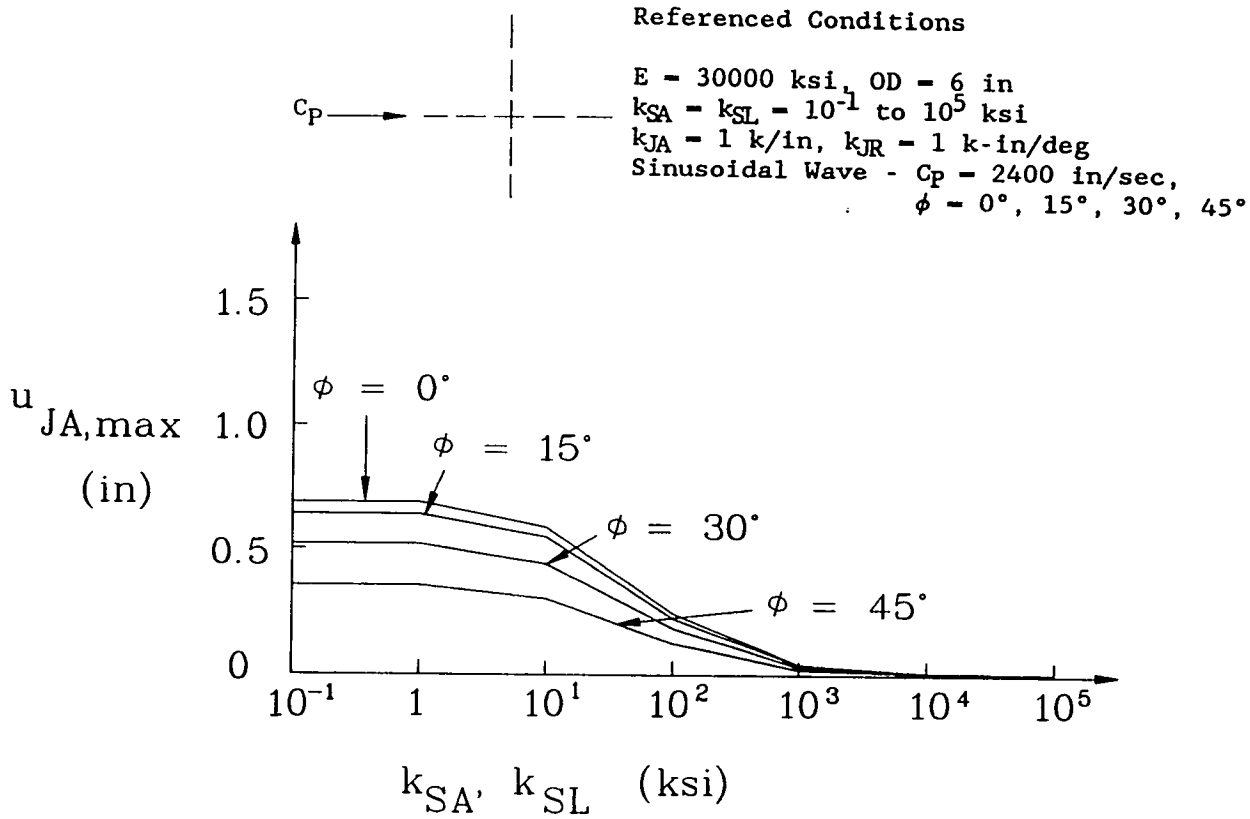

Fig. 2.19 Effect of Incident Angle on Relative Joint Displacement Responses

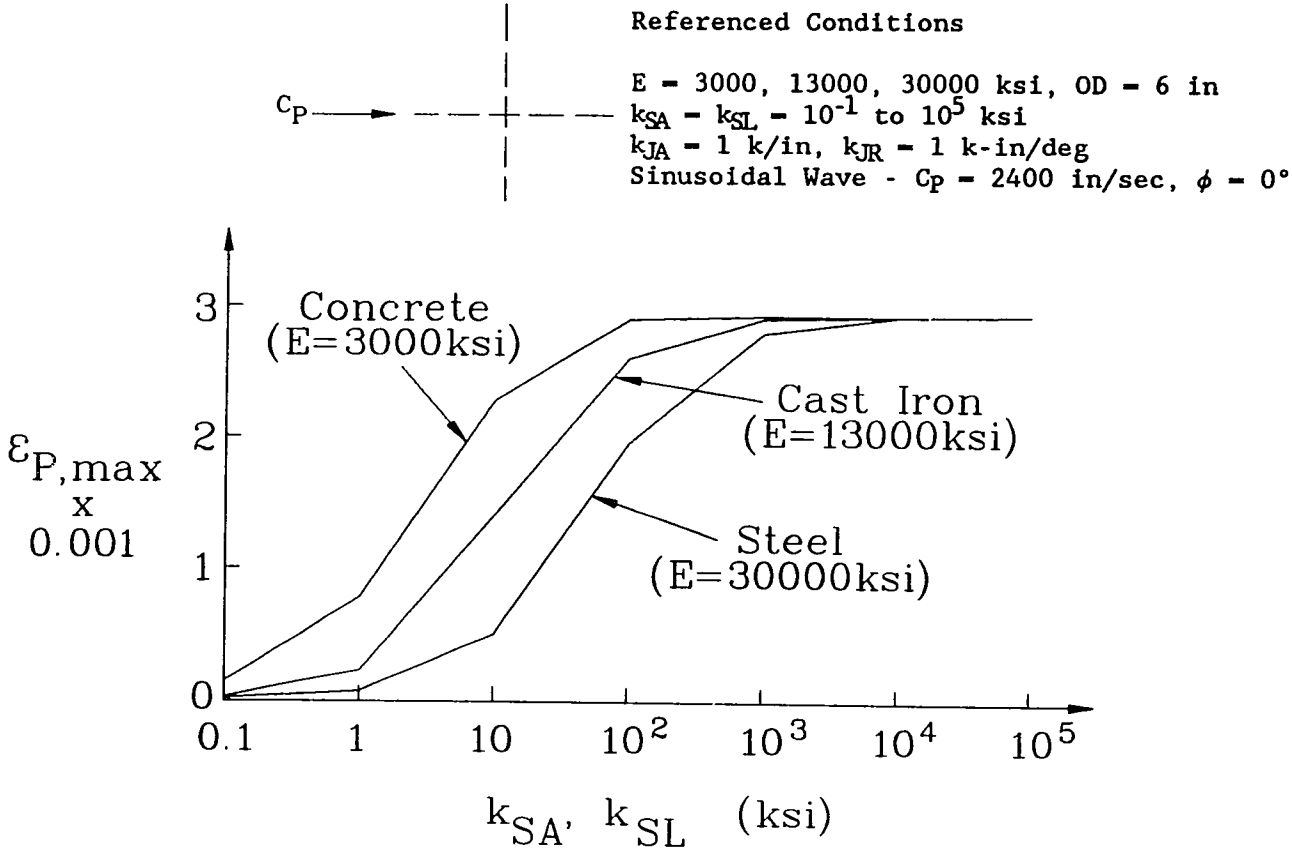

Fig. 2.20 Effect of Material on Pipe Strain Responses

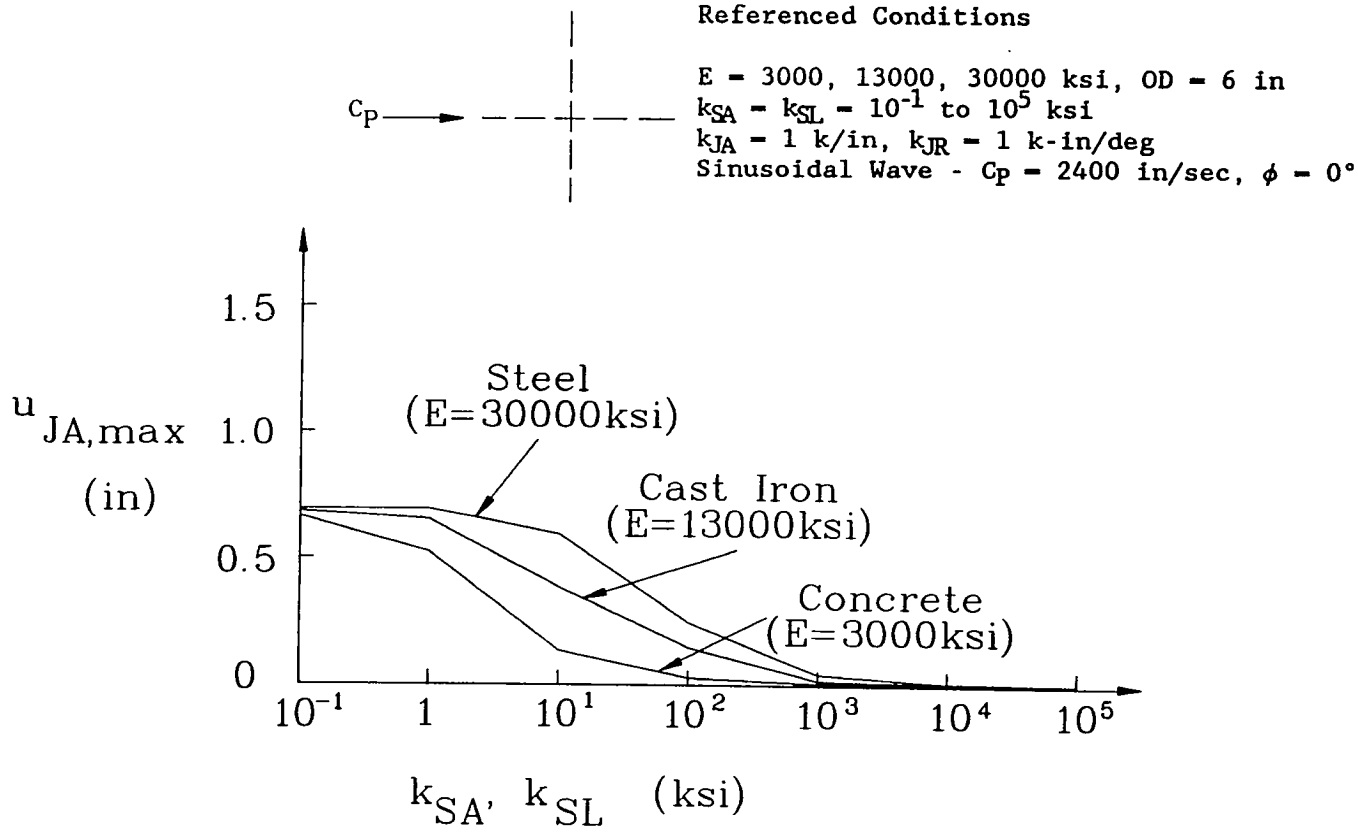

Fig. 2.21 Effect of Material on Relative Joint Displacement Responses

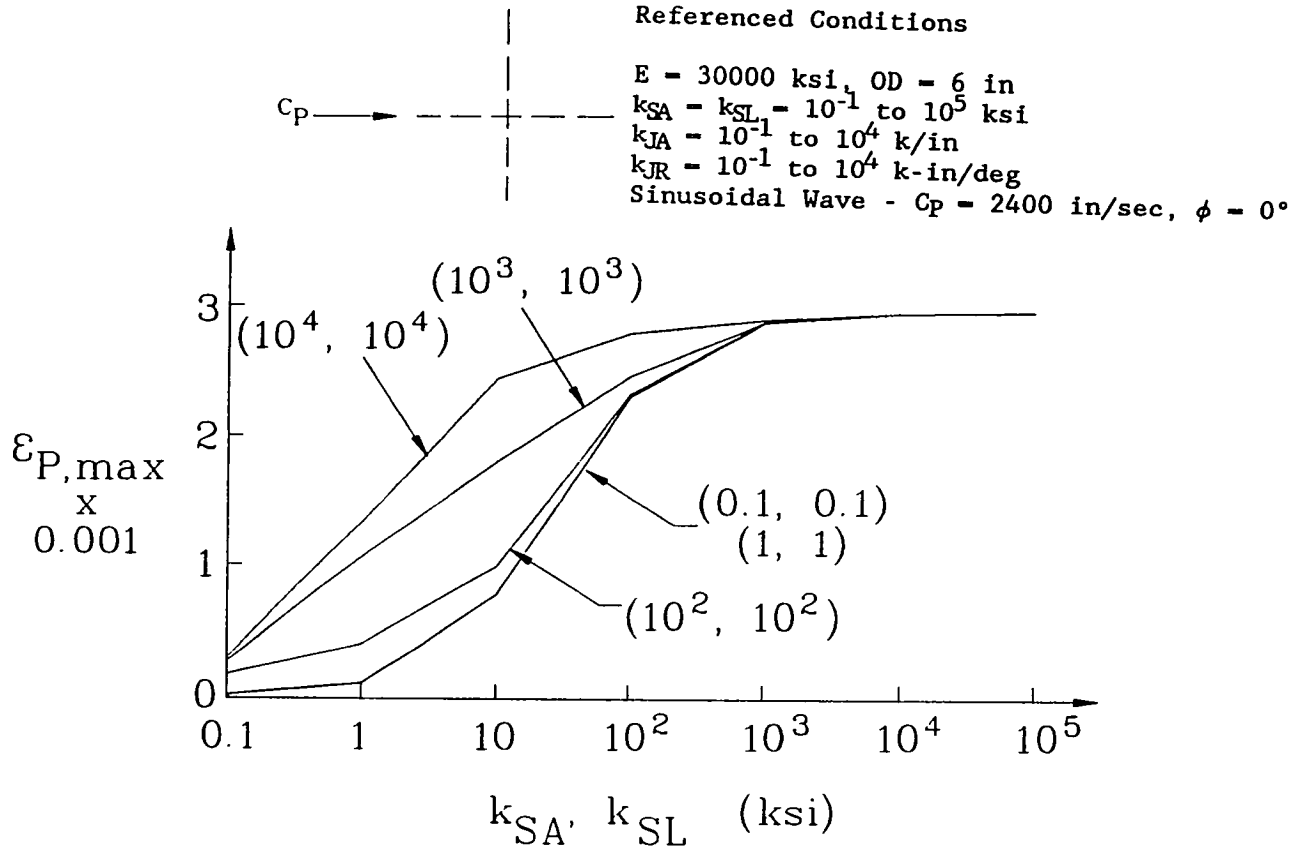

Fig. 2.22 Effect of Joint Stiffness on Pipe Strain Responses

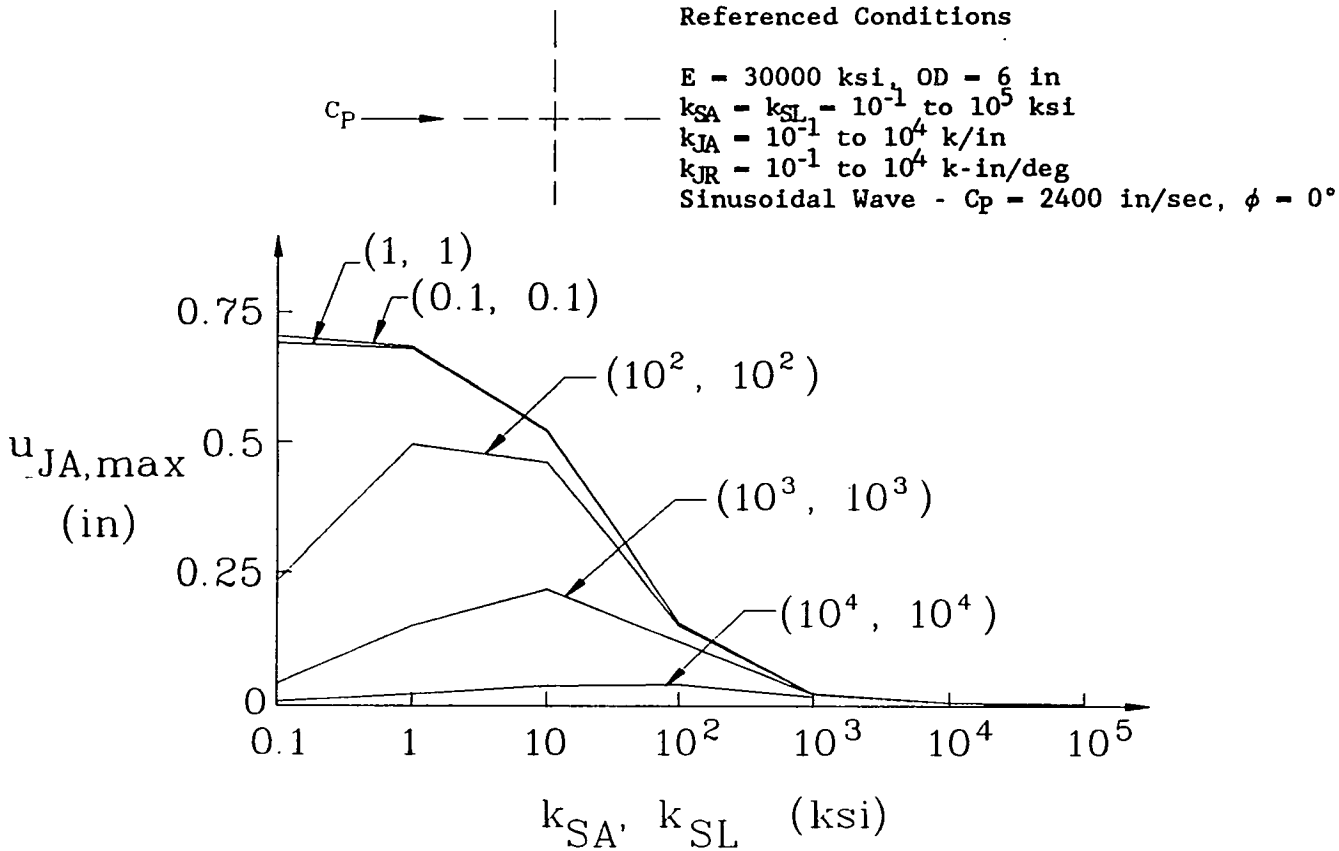

Fig. 2.23 Effect of Joint Stiffness on Relative Joint Displacement Response

Chapter 3

INELASTIC ANALYSIS

3.1 Basic Formulations

Due to the elasto-plastic behavior of soils and joints, a non-linear inelastic analysis of buried pipeline systems is necessary. To this end, it is convenient to reformulate the equilibrium equations, Eq. (2.33), in terms of the relative soil-pipe displacements, $\{U_S\}$, which are given by

$$\underset{nx1}{\{U_S\}} = \underset{nx1}{\{X_G\}} - \underset{nx1}{\{U_P\}} \tag{3.1}$$

Note that the relationship shown in Eq. (3.1) is also true for local coordinates. Substituting Eq.(3.1) into Eq.(2.33) one obtains

$$\underset{nxn}{[K_{SYS}]}\underset{nx1}{\{U_S\}} = \underset{nxn}{[K]}\ \underset{nx1}{\{X_G\}} = \underset{nx1}{\{F(t)\}} \tag{3.2}$$

where

$$\underset{nxn}{[K]} = \underset{nxn}{[K_P]} + \underset{nxn}{[K_J]} - \underset{nxn}{[K_{BJ}]} \tag{3.2a}$$

Eq. (3.2) can be solved for relative soil-pipe displacements, $\{U_S\}$, directly. Applying Eq. (2.34) the

relative soil-pipe displacements in local coordinates, $\{u_S\}$, can be obtained. Then through back-substitution the pipe responses, $\{u_P\}$, and relative joint displacements, $\{u_J\}$, can be obtained. Because the input ground displacement, $\{X_G(t)\}$, is time dependent, the equivalent force function, $\{F(t)\}$, will perform cyclic loading situations, i.e., loading, unloading and reloading, on the soil elements and joints once their elastic limits are exceeded. The idealized hysteretic characteristics of soil and joint springs are assumed as shown in Figs. 3.1 and 3.2. Once the responses of soil and/or joint exceed their elastic limits, the inelastic analysis considering the cyclic loading situations will begin.

3.2 Hysteretic Characteristic of Soil Springs

The assumed hysteretic characteristics (load-displacement relationship) of the soil (longitudinal or lateral) is shown in Fig. 3.1 under the loading, unloading and reloading situations.

When the tensile (positive) loading response, u_S, reaches and exceeds the elastic limit, $u_{S,y}$, the resistant force, f_S, acting on the pipe from the surrounding soil will keep at a constant limited value, $f_{S,y}$, while the pipe displacement increases. This is called the slippage or yielding of soil. As the loading decreases (unloading situation), the displacement will decrease elastically as

shown in Fig. 3.1. If the unloading continues until reaching its compressive (negative) limited resistant force, $f_{S,-y}$, compressive slippage or yielding of soil will occur. Again if the loading increases (reloading situation), at this stage, the displacement will increase linearly as shown in Fig. 3.1. This force-displacement (hysteretic) relationship is also applied to the compressive loading, unloading and reloading situations.

3.3 Hysteretic Characteristic of Joint Springs

Hysteretic characteristics of a joint for longitudinal (axial) and rotational resistances are shown in Figs. 3.2a and 3.2b, respectively. Singhal [39, 40] presented a set of experimental results that are shown in Figs. 1.1 and 1.2 for a rubber gasket joint. It is shown that the load-displacement relationship for longitudinal (axial) spring is elasto-plastic and bilinear for rotational spring.

3.3.1 Longitudinal Springs

Figure 3.2a shows the force-displacement relationship of a rubber gasket joint for longitudinal (axial) loading, unloading and reloading situations. Line FCDD' indicates the behavior of the joint after the contact of two connected pipe ends, i.e., the relative joint displacement is constant, $u_{J,c}$, while the force continues increasing. In general, two possible cases for longitudinal (axial)

loading-unloading situations shown in Fig. 3.2a, namely (1) OABCD' and (2) OAB'C'DD' are discussed. Case (1) represents that the ends-contact, BC, occurs before the joint yields, i.e., $f_J >$

$f_{J,-y}$, while in case (2), the joint yields, $f_J = f_{J,-y}$, before the ends contact, C'D. For reloading situation, case (1) will follow the direction of D'CB, while case (2) D'DE. The jumps, D'C and D'D, result from the sudden loss of ends-contact. Similarly, the compressive loading and unloading situations are demonstrated by OFD' and D'FAB(B'), respectively. For compressive reloading situation, two possible cases, i.e., BCD' and B'C'DD' could occur just like tensile unloading situation. Note that the joint is considered failure as the positive relative joint displacement, u_J, reaches the pull-out joint displacement, $u_{J,u}$, as shown in Fig. 3.2a.

3.3.2 Rotational Springs

Figure 3.2b shows the moment-rotation relationship for loading, unloading and reloading situations of a rotational joint spring. One can see that Figs. 3.1 and 3.2b have similar patterns. However, the soil spring has an elasto-plastic force-displacement relationship (Fig. 3.1), while a bilinear relationship (Fig. 3.2b) is adopted for rotational joint springs as suggested in Refs. [39, 40].

3.4 Modified Stiffness Matrices and Inelastic Nodal Force

Considering a pipe segment in which the surrounding soil is partially plastified in the longitudinal direction as shown in Fig. 3.3, the inelastic portions can be calculated by following equations:

$$x_{ti} = \frac{u_{S,y} - u_{S0}}{u_{S1} - u_{S0}} L_i \tag{3.3a}$$

$$x_{ci} = \frac{u_{S1} - u_{S,-y}}{u_{S1} - u_{S0}} L_i \tag{3.3b}$$

where x_{ti} and x_{ci} are the tensile and compressive inelastic length of soil, respectively, along the ith pipe element. $u_{S,y}$ and $u_{S,-y}$ are the tensile and compressive elastic limits, respectively, and u_{S0} and u_{S1} represent longitudinal nodal responses at the two ends of the ith segment. Then the potential energy of soil along the ith segment can be written as:

$$U^i_{Soil,Long} = \frac{k_{SAi}}{2} \int_0^{L_i} ([N_{Ai}]\{u_{SAi}\})^2 dx$$
$$- \frac{k_{SAi}}{2}\int_0^{x_{ti}} ([N_{Ai}]\{u_{SAi}\})^2 dx - \frac{k_{SAi}}{2}\int_{L_i-x_{ci}}^{L_i} ([N_{Ai}]\{u_{SAi}\})^2 dx$$
$$+ f_{SA,y} \int_0^{x_{ti}} [N_{Ai}]\{u_{SAi}\} dx + f_{SA,-y} \int_{L_i-x_{ci}}^{L_i} [N_{Ai}]\{u_{SAi}\} dx \tag{3.4}$$

where $f_{SA,y}$ and $f_{SA,-y}$ are the constant longitudinal tensile and the constant compressive resistant forces, respectively.

Observing Eq. (3.4), on the right hand side the first term represents the elastic energy of entire segment, the second and third terms represent the elastic energy of inelastic portions and the last two terms represent the work-done by the constant yield resistant forces, $f_{SA,y}$ and $f_{SA,-y}$, along the inelastic portions. Thus, Eq. (3.4) can be written in a short form as:

$$U^{i}_{Soil,Long} = A_i - B_i + C_i \qquad i=1, 2,..., NA \qquad (3.5)$$

where

$$A_i = \frac{k_{SAi}}{2} \int_0^{L_i} ([N_{Ai}]\{u_{SAi}\})^2 dx \qquad (3.5a)$$

$$B_i = \frac{k_{SAi}}{2} \left(\int_0^{x_{ti}} ([N_{Ai}]\{u_{SAi}\})^2 dx + \int_{L_i - x_{ci}}^{L_i} ([N_{Ai}]\{u_{SAi}\})^2 dx \right) \qquad (3.5b)$$

$$C_i = f_{SA,y} \int_0^{x_{ti}} [N_{Ai}]\{u_{SAi}\} dx + f_{SA,-y} \int_{L_i - x_{ci}}^{L_i} [N_{Ai}]\{u_{SAi}\} dx \qquad (3.5c)$$

and NA is the total number of segments in which the surrounding soil is partially plastified longitudinally. Note that for elastic case, both B_i and C_i vanish and Eq. (3.5) is the same as Eq. (2.9).

Similarly, the potential energy of soil, which is partially plastified in lateral direction, can be expressed as:

$$U^{j}_{Soil,Lateral} = D_j - E_j + F_j \qquad j=1, 2,..., NL \quad (3.6)$$

where

$$D_j = \frac{k_{SLj}}{2} \int_0^{L_j} ([N_{Lj}]\{u_{SLj}\})^2 dx \quad (3.6a)$$

$$E_j = \frac{k_{SLj}}{2} \left(\int_0^{x_{tj}} ([N_{Lj}]\{u_{SLj}\})^2 dx + \int_{L_j - x_{cj}}^{L_j} ([N_{Lj}]\{u_{SLj}\})^2 dx \right) \quad (3.6b)$$

$$F_j = f_{SL,y} \int_0^{x_{tj}} [N_{Lj}]\{u_{SLj}\} dx + f_{SL,-y} \int_{L_j - x_{cj}}^{L_j} [N_{Lj}]\{u_{SLj}\} dx \quad (3.6c)$$

and NL is the total number of segments in which the surrounding soil is partially plastified laterally. Again for elastic case, both E_j and F_j vanish and Eq. (3.6) is the same as Eq. (2.18).

Assuming the joint responses are in the elastic range, after transformation and assembly the total potential energy of the pipeline system can be expressed as:

$$U^{Total} = U^{Total}_{Pipe} + U^{Total}_{Joint} + U^{Total}_{Soil,m} \quad (3.7)$$

where

$$U^{Total}_{Soil,m} = U^{Total}_{Soil} - U^{Total}_{Soil,Inel} \quad (3.7a)$$

and

$$U^{Total}_{Soil,Inel} = \sum_{i=1}^{NA} (B_i - C_i) + \sum_{j=1}^{NL} (E_j - F_j) \qquad (3.7b)$$

It should be noted that for unloading and reloading situations, Eqs. (3.5b), (3.5c), (3.6b) and (3.6c) are still applicable as long as the inelastic portions, x_{ti} and x_{ci}, are known. However, these inelastic portions are not easy to calculate even after one cycle of loading. Therefore, an approximate approach is introduced to solve this complicated problem.

The element as shown in Fig. 3.4 is divided into a number of sub-elements. The displacements at the center points of all sub-elements are recorded in order to identify whether a sub-element is plastified or not. In other words, the behavior of each sub-element is represented by that of its center point. Once the behavior of each sub-element is known, the modified stiffness matrices and the nodal inelastic force vector can be constructed by Eqs. (3.5b, c and 3.6b, c), respectively.

Applying variational principle, the equilibrium equations of the pipeline system can be obtained as:

$$\underset{nxn}{([K_P]} + \underset{nxn}{[K_J]} + \underset{nxn}{[K_S]} - \underset{nxn}{[K_S]_{Inel}}) \underset{nx1}{\{U_S\}} = \underset{nxn}{[K]} \underset{nx1}{\{X_G\}} - \underset{nx1}{\{F\}_P} \qquad (3.8)$$

where $[K_S]_{Inel}$ is the soil stiffness matrix obtained from inelastic portions of soil, B_i and E_j, and $\{F\}_p$ is the inelastic nodal force vector from C_i and F_j. It should be noted that Eq. (3.8) is obtained by assuming that the joint responses are elastic. Therefore the joint stiffness matrix should be modified if any joint response is also in inelastic range.

In the case of inelastic joint response due to tensile or compressive loading, the secant modulus, k_{JAs}, are shown in Fig. 3.5a and given in the form of:

$$k_{JAs} = \frac{u_{JA,y}}{u_{JA,1}} k_{JA} \tag{3.9a}$$

for tensile yielding and

$$k_{JAs} = \frac{u_{JA,2}}{u_{JA,c}} k_{JA} \tag{3.9b}$$

for compressive yielding. This secant modulus will replace the elastic modulus, k_{JA}, in the computer analysis. Similarly, for the case of inelastic joint response due to bending, the secant modulus, k_{JRs}, as shown in Fig. 3.5b and given in the form of:

$$k_{JRs} = \frac{(1-\alpha)\ u_{JR,y} + \alpha\ u_{JR}}{u_{JR}} k_{JR} \tag{3.10}$$

will replace the elastic modulus, k_{JR}. $u_{JA,y}$ and $u_{JR,y}$ are the elastic limits for longitudinal and rotational joint

spring and u_{JA} and u_{JR} are the inelastic longitudinal and rotational joint responses, respectively. α is the ratio of rotational joint stiffness after yielding to the elastic rotational joint stiffness as defined by Singhal [39, 40], who found that α varies from 0.1 to 0.3 for a rubber gasket joint.

After constructing modified joint stiffness matrix by substituting the secant moduli, k_{JAs} and k_{JRs}, for the elastic moduli, k_{JA} and k_{JR}, respectively, Eq. (3.8) can be rewritten as:

$$\underset{nxn}{([K_P]} + \underset{nxn}{[K_J]_m} + \underset{nxn}{[K_S]_m)} \underset{nx1}{\{U_S\}} = \underset{nxn}{[K]_m} \underset{nx1}{\{X_G\}} - \underset{nx1}{\{F\}_P} \quad (3.11)$$

or

$$\underset{nxn}{[K_{SYS}]_m} \underset{nx1}{\{U_S\}} = \underset{nxn}{[K]_m} \underset{nx1}{\{X_G\}} - \underset{nx1}{\{F\}_P} \quad (3.12)$$

where

$$\underset{nxn}{[K_{SYS}]_m} = \underset{nxn}{[K_P]} + \underset{nxn}{[K_J]_m} + \underset{nxn}{[K_S]_m} \quad (3.12a)$$

$$\underset{nxn}{[K_S]_m} = \underset{nxn}{[K_S]} - \underset{nxn}{[K_S]_{Inel}} \quad (3.12b)$$

and

$$\underset{nxn}{[K]_m} = \underset{nxn}{[K_P]} + \underset{nxn}{[K_J]_m} - \underset{nxn}{[K_{BJ}]_m} \quad (3.12c)$$

where $[K_{SYS}]_m$, $[K_S]_m$, $[K_J]_m$, and $[K_{BJ}]_m$ are the modified stiffness matrices for the system, surrounding soil, the intermediate joint and the boundary joint, respectively, and

$\{F\}_p$ is called the inelastic force vector. Note that for elastic case, $[K_{SYS}]_m=[K_{SYS}]$, $[K]_m=[K]$, $[K_{BJ}]_m=[K_{BJ}]$ and $\{F\}_p=\{0\}$, Eq. (3.12) is identical to Eq. (2.33).

Equation (3.12) will be used to solve for inelastic relative soil-pipe responses, $\{U_S\}$, in global coordinates. Then by back substitutions, the responses of pipe, $\{u_P\}$, and joint, $\{u_J\}$, in local coordinates can be obtained.

3.5 Iterative Procedure

Observing Eq. (3.12), one can find that this equation can not be solved for the unknown inelastic responses, $\{U_S\}$, directly. Because once the unknown displacements, u_S and/or u_J, are in the inelastic range, the corresponding stiffness matrices will be changed and so will the inelastic nodal forces, all of which are functions of the unknown displacement responses, u_S and u_J. Therefore, an iterative procedure to solve this inelastic problem is developed as described in the following sections.

3.5.1 Initial Stage of Inelastic Responses of Soil/Joints

As shown in Fig. 3.6 for surrounding soil, there are eight possible yielding conditions along a pipe segment . For each case, the soil stiffness will change and be affected by the extent of inelastic portion. The modified soil stiffness matrix, $[K_S]_m$, and the inelastic nodal force vector, $\{F\}_p$, can be generated by the energy approach as

described before. For an inelastic joint, the secant stiffness is employed. Then, by assembling the modified system stiffness matrix, $[K_{SYS}]_m$, can be obtained. Note that the stiffness of a pipe will remain constant since the behavior of the pipe is assumed to be elastic. The instantaneous inelastic equilibrium equation in a trial calculation can be expressed as:

$$\underset{nxn}{[K_{SYS}]_m^i}\ \underset{nx1}{\{U_S\}^i} = \underset{nxn}{[K]_m^i}\ \underset{nx1}{\{X_G\}} - \underset{nx1}{\{F\}_P^i} \tag{3.13}$$

where

$$\underset{nxn}{[K_{SYS}]_m^i} = \underset{nxn}{[K_P]} + \underset{nxn}{[K_S]_m^i} + \underset{nxn}{[K_J]_m^i} \tag{3.13a}$$

$$\underset{nxn}{[K]_m^i} = \underset{nxn}{[K_P]} + \underset{nxn}{[K_J]_m^i} - \underset{nxn}{[K_{BJ}]_m^i} \tag{3.13b}$$

and $\{F\}_P$ is the nodal force vector contributed by inelastic portion of soil, which can be calculated by Eqs. (3.5c and 3.6c). The superscript, i, indicates the number of iterations. As i=1, the initial trial, $\{U_S\}_1$, is the elastic solution. In this case, $\{F_P\}^1 = \{0\}$ and Eqs. (3.2 and 3.11) are identical. Based on the information of inelastic responses of the soil and the joints, the updated matrices, $[K_{SYS}]^{i+1}$ and $[K]^{i+1}$, and the inelastic force vector, $\{F_P\}^{i+1}$, are generated. Then solving Eq. (3.13), a new set of responses, $\{U_S\}^{i+1}$, are obtained. Following

criterion is applied to check the convergence of new solutions.

$$\left| \{U_S\}^{i+1} - \{U_S\}^{i} \right| \leq \{e\} \qquad (3.14)$$

where e is the prescribed tolerance. If any violation occurred in Eq. (3.14), then the procedure is repeated, recalculating the modified stiffness matrices, $[K_S]_m$, $[K_J]_m$, $[K]_m$ and $[K_{SYS}]_m$, and the inelastic force vector, $\{F_P\}$, to obtain another update responses, $\{U_S\}^{i+1}$, by Eq.(3.13) until Eq. (3.14) is completely satisfied.

3.5.2 Iterative Procedure after the Initiation of Inelastic Responses

After the initial inelastic responses are obtained as described in the previous section, some additional efforts need to be made to obtain the inelastic responses for the remaining time history of ground motions. Since the seismic shaking induced ground displacements are time dependent, the hysteretic characteristics of the soil and joints should be considered.

It is necessary to track the loading status after the initiation of inelastic responses take place due to the hysteretic characteristics of soil and joints springs. Hence an incremental equilibrium equation as following:

$$\underset{nxn}{[K_{SYS}]} \ \underset{nx1}{\{\Delta U_S\}_j} = \underset{nxn}{[K]} \ \underset{nx1}{\{\Delta X_G\}_j} \qquad (3.15)$$

where subscript j represents present time step, and $\{\Delta U_S\}_j$ is the incremental response vector corresponding to the incremental ground displacement vector, $\{\Delta X_G\}_j$, is applied to detect the loading path of inelastic elements and joints. After solving Eq. (3.15) for incremental responses, $\{\Delta U_S\}_j$, the initial trial responses, $\{U_S\}_j$, at time t_j are obtained by:

$$\underset{nx1}{\{u_S\}_j^1} = \underset{nx1}{\{u_S\}_{j-1}} + \underset{nx1}{\{\Delta u_S\}_j} \tag{3.16}$$

Based on the information of the loading path for inelastic elements and joints and Eq. (3.16) which provides possible additional inelastic elements or joints, the update stiffness and inelastic nodal force of the individual element and joint can be developed as described in section 3.4. Then the modified stiffness matrices, Eqs. (3.13a) and (3.13b), and the inelastic force vector, $\{F_P\}$, can be obtained by assembling/modifying the original matrices. The iterative procedure for initiation of inelastic responses described before is again applied to solve the responses, $\{U_S\}_j$. This procedure will be repeated for the rest of time history of seismic shaking.

It should be noted that there are two possible failure modes: (I). Foundation Failure: The surrounding soil is completely plastified. In this case, the pipeline system

becomes unstable. (II). Joint Failure: The relative joint displacement (longitudinal) is greater than the ultimate joint displacement. In this case, the joint is classified as pull-out failure. Hence following two conditions have been checked at each iteration.

$$Det[K_S]_m \;/\; Det[K_S] \geq e^* \qquad (3.17)$$

$$\{u_{JA}\} \leq \{u_{J,u}\} \qquad (3.18)$$

where

$Det[K_S]_m$ = determinant of modified system soil stiffness

$Det[K_S]$ = determinant of elastic system soil stiffness

e^* = tolerance to determine if the surrounding soil is failure

$\{u_{JA}\}$ = the relative longitudinal joint displacement vector

$\{u_{J,u}\}$ = the ultimate (pull-out) relative joint displacement vector.

3.6 Elastic Limit for Load-displacement Relationship of Surrounding Soil and Joint

As mentioned before there are few testing results for buried pipelines available. However in order to study the pipe and joint responses due to the inelastic behavior of surrounding soil and joints, the elastic limits for the surrounding soil, $u_{SA,y}$ in longitudinal direction and $u_{SL,y}$ in lateral direction, and joint, $u_{JA,y}$ in longitudinal

(axial) direction and $u_{JR,y}$ in rotational direction, are the most important factors that will affect the responses. Hence from the available sources the values of elastic limits of surrounding soil and joints were studied.

3.6.1 Elastic Limit of Surrounding Soil

In 1977 Audibert et al. [2] presented testing results for lateral responses of a buried pipeline. In order to utilize these nonlinear curves for the elasto-plastic analysis, the method presented by Thomas [45] is adopted. For a nonlinear load-displacement curve, the elastic limit is obtained by drawing a straight line connecting origin and the point of 70% ultimate load and intersecting another horizontal line passed the peak point of the curve as shown in Fig. 3.7. Applying this method the values of elastic limit for the curves of different burial depths presented in Ref. [2] are calculated and presented in Table 3.1.

Another available source for elastic limit of surrounding soil for buried pipelines was presented in reference [7]. In reference [7] equations for calculating elastic limits for both longitudinal and lateral reactions with two different soil conditions, sand and clay, were given. Because backfill materials used around buried pipelines are usually granular, it was decided only the equations for sand are of interest. The equations for longitudinal and lateral elastic limit of soil-pipe

longitudinal and lateral elastic limit of soil-pipe interaction are given as:

$$u_{SA,y} = 0.1 \text{ to } 0.2 \text{ inches for dense to loose sand} \quad (3.19)$$

$$u_{SL,y} = \begin{cases} 0.03 \text{ to } 0.05(H+D/2) \text{ for medium sand} & (3.20a) \\ 0.02 \text{ to } 0.03(H+D/2) \text{ for dense sand} & (3.20b) \end{cases}$$

where

H = burial depth from soil surface to centerline of the pipeline

D = outer diameter of pipeline.

Using Eqs. (3.20a) and (3.20b), the values of lateral elastic limit, $u_{SL,y}$, for different pipe sizes and burial depths were calculated and presented in Table 3.2.

From Tables 3.1 and 3.2, one can see that the elastic limit of soil in the lateral direction, $u_{SL,y}$, depends on the soil conditions, the pipe size and burial depth, and the values vary from 0.1 inches (OD=1 inch, H/D=2) to 4.2 inches (OD=24 inches, H/D=3). These values and the longitudinal elastic limits shown in Eq. (3.19) are referred later in the parametric study.

3.6.2 Elastic Limit of Joint

From Figs. 1.1 and 1.2 presented by Singhal, 1984 [40], the elastic limits of rubber gasket joint springs in longitudinal, $u_{JA,y}$, and rotational, $u_{JR,y}$, directions are

given in Table 3.3. It is shown in Table 3.3 that for rubber gasket joint springs, the values for $u_{JA,y}$ are in the range of 0.1 to 0.6 inches while $u_{JR,y}$ 0.2 to 0.5 degrees for pipes of 4 to 10 inch diameter. These values will be referred in the parametric study in the following section.

3.7 Solution and Computer Program

A computer program for elasto-plastic analysis has been developed. The computer program is able to solve elastic and inelastic responses of buried pipeline (continuous and segmented) system subjected to any kind of ground motions with various traveling velocities and arbitrary incident angle. The program starts with solving Eq. (3.2) elastically until soil and/or joint response exceeds its elastic limit. Then the iterative procedure described in Sec 3.5 begins. The modified stiffnesses, $[K_S]_m$, $[K_J]_m$ and $[K_{SYS}]_m$, and inelastic force vector, $\{F\}_p$, due to the inelasticity of soil and/or joint are generated automatically at each iteration. A smaller time step, which depends on the elastic limits of soil and joint, might be required in order to achieve convergency of solutions. In general, a time step of 0.001 second will be suitable for all kinds of inelasticity of soil and/or joint. The details of input/output data and listing of the computer program will be given in a separate report [55].

This program is not meant to solve a buried pipeline system with large degrees of freedom. Experiences have shown that most pipeline damages occurred at the junctions or boundary areas where the stiffnesses are suddenly changed. In general, for purposes of design, or checking the safety of a buried pipeline system subjected to ground shaking, only the portions including boundary and junctions are needed to be considered. In other words, this program may be sufficient for real case investigations with limited total degrees (say 250) of freedom. To upgrade the current program to a large comprehensive program, a skyline scheme which can save storage space as well as computational time, or a parallel computing code may be considered in a future study.

3.7.1 Verification of the Developed Program for Elasto-plastic Analysis

It was tried to compare the inelastic pipe responses obtained by the developed program and those presented by Takada, et al. [42]. The comparisons showed that the Takada's results are smaller (about 1.5 to 2 times less) than those obtained by the developed program. Since Takada did not consider the hysteretic characteristics of soil and joints, the smaller inelastic pipe responses are expected. Using the developed program, a series of parametric studies have been done as shown in the following section and the

trends of the inelastic responses of buried pipelines are reasonable.

3.8 Parametric Study

To study the inelastic behavior of a buried pipeline system subjected to ground shaking, the same cross type pipeline as mentioned in Sec. 2.2 is used.

The focus of this study is the effects of the inelastic responses with various elastic limits of soil and/or joint compared to the elastic responses. Therefore, some of the parameters, such as pipe size, wave velocity and incident angle, used in the elastic parametric analysis along with various elastic limits of soil and/or joint are used also for this inelastic parametric study. The referenced and the parametric conditions set for the comparison of results are given in Table 3.4.

3.9 Results and Discussions

Using the developed program as mentioned in Sec. 3.7, the parametric study of inelastic analysis has been done. The results are shown in Figs. 3.8 to 3.14 for continuous pipeline responses while Figs. 3.15 to 3.29 display the segmented pipeline responses.

3.9.1 Responses of Continuous Pipelines

The inelastic responses of continuous pipelines are shown in Figs. 3.8 to 3.11 for two different pipe sizes, OD = 6 and 24 inches; two wave velocities, c_p = 2400 and 12000 in/sec; and two incident angles, ϕ = 0° and 45° with soil elastic limits, $u_{SA,y} = u_{SL,y}$ = 0.05, 0.1, 0.2 and 0.5 inches. The corresponding elastic responses are also presented in each figure for comparison purposes.

Note that the effect of lateral soil elastic limits in the range of 0.05 to 0.5 inches which covers the available data mentioned in Sec. 3.6.1 have been evaluated, and the results showed that the responses in lateral direction will remain in elastic range, i.e., $u_{SL} < u_{SL,y}$. Therefore, the inelastic responses shown in Figs. 3.8 to 3.11 represent only the inelastic behavior of the pipe due to longitudinal soil yielding (slippage).

Figure 3.8 shows the inelastic responses of a continuous pipeline of 6 inch diameter subjected to a ground wave of 2400 in/sec traveling velocity and 0° incident angle. As shown in Fig. 3.8, the inelastic pipe responses decrease as the elastic limit of soil, $u_{SA,y}$, decreases. The smaller the elastic limit of soil, the easier the soil becoming inelastic will be, or the easier the slippage will occur. Therefore, inelastic pipe responses are expected to be smaller than the elastic responses. For given pipeline

conditions, the elastic response becomes the upper bound of the inelastic responses.

The same trend of inelastic behavior due to soil yielding (slippage) for different pipe size, wave velocity, and incident angle can be found in Figs. 3.9 to 3.11. The effects of pipe size, wave velocity and incident angle of ground motion are shown in Figs. 3.12 to 3.14, respectively. In each figure the results of $u_{SA,y}$ = 0.5 and 0.2 inches are plotted for demonstration purposes.

Figure 3.12 shows the effect of pipe size on the inelastic pipe strain responses. One can see that the pipe strain responses decrease as the pipe size increases. The same trend is also found in elastic analysis.

Figures 3.13 and 3.14 show that the pipe strain responses decrease as the wave velocity and incident angle increases except in very small range of k_{SA}. Since higher propagation velocity and larger incident angle will yield smaller ground strain which was shown in elastic analysis, the chance of the soil becoming inelastic for these cases is smaller than that for the lower velocity and smaller incident angle cases. On the contrary, for lower wave velocity and smaller incident angle, the induced ground strain is higher, and therefore more portions of soil might become inelastic than that of higher velocity or larger incident angle. The maximum pipe strain produced by C_p = 2400 in/sec and ϕ = 0° may be in the inelastic stage, while

the maximum pipe strain produced by C_P = 12000 in/sec and ϕ = 45° may be in the elastic stage. Consequently, the maximum strain of the former is less than the latter case.

3.9.2 Responses of Segmented Pipelines

The results of inelastic analysis for segmented pipelines are shown in Figs. 3.15 to 3.29. The elastic limits of the soil spring for the parametric study are set to be ∞ (elastic), 0.5, 0.2, 0.1 and 0.05 inches. The tensile elastic limit and the available compressive contact spaces of the longitudinal joint spring, i.e., $u_{JA,y}$ and u_{Jc}, varied from 0.1 to 0.5 inches; and the elastic limit of the rotational joint spring, $u_{JR,y}$, from 0.1 to 0.5 degrees. The pipe body is assumed to remain elastic and the pipeline itself is assumed to remain functioning, i.e., no pull-out failure of joints, in the study. For comparison purposes, in each figure, the corresponding elastic responses of the continuous and the segmented pipeline are also presented.

Under seismic shaking environments, the rotational joint responses are found to be relatively small and within the elastic limit, i.e., $u_{JR} < u_{JR,y}$. Therefore, the results indicated only the inelastic behavior of longitudinal soil and joint spring responses in the longitudinal direction.

Figures 3.15 to 3.19 show the inelastic pipe strain responses of a 6 inches diameter pipe subjected to a ground

motion with velocity of 2400 in/sec and incident angle of 0°. The variables are the elastic limits of soil spring, $u_{SA,y}$, tensile elastic limit, $u_{JA,y}$, and the available compressive contact space, u_{Jc}, of the longitudinal joint spring, and the elastic limit of the rotational joint spring, $u_{JR,y}$. The corresponding elastic continuous and segmented pipe responses are also shown. One can see that the inelastic pipe responses increase as the available contact space of longitudinal joint spring decreases. The elastic responses of continuous and segmented pipes appear to be the upper and lower bound, respectively, of the inelastic pipe responses. It is interesting to note that as the contact space of joint decreases, the pipe will behave more like continuous pipe regardless of the inelasticity of soils and joints. The effects of soil yielding, $u_{SA,y}$, on the segmented pipeline for the specified joint properties can be seen by comparing Fig. 3.15 to Fig. 3.19. In general, pipe strain decreases as $u_{SA,y}$ decreases. That is to say that the pipe strain is reduced because of soil slippage (yielding).

The effects of the pipe size, wave velocity and the incident angle of ground motion under elastic soil and inelastic joint conditions, $u_{JA,y} = u_{Jc} = 0.1$ and 0.3 inches, are plotted in Figs 3.20 to 22, respectively.

Figure 3.20 shows that the pipe strain response decreases as pipe size increases as discussed in the elastic

analysis. It is also shown in Fig. 3.20 that the larger the $u_{JA,y}$ and u_{Jc} are, the smaller the pipe strain responses will be. This trend also concurs with the conclusion obtained from the elastic analysis since the larger values of $u_{JA,y}$ and u_{Jc} represent a more flexible (ductile) joint.

In Fig. 3.21, the effect of wave velocity on the pipe strain response is presented. One can see from this figure that the larger the wave velocity is, the smaller the pipe strain response is. Also, for C_p = 12000 in/sec, the pipe strain response is not affected by the value of $u_{JA,y}$ and u_{Jc} for k_{SA} > 10 ksi. For k_{SA} < 10 ksi (soft soil), small variations can be seen for different u_{Jc} values. For C_p = 2400 in/sec, the value $u_{JA,y}$ and u_{Jc} will affect the pipe strain response in the entire range of k_{SA}.

From Fig. 3.22, the effect of incident angle of ground motion can be seen. The pipe strain response decreases as the incident angle increases. Again, the trend is also shown in the elastic analysis. For incident angle of 45°, the value of $u_{JA,y}$ and u_{Jc} will affect the pipe strain responses in the range of k_{SA} < 100 ksi.

The corresponding relative joint displacement in longitudinal direction for different wave velocities and incident angles are shown in Figs. 3.23 and 3.24, respectively.

Figure 3.23 shows the effect of wave velocity on the relative joint displacement response. The relative joint

displacement response decreases as the wave velocity increases. It also shows that for lower wave velocity, C_p = 2400 in/sec, the value of $u_{JA,y}$ and u_{Jc} affects the relative joint displacement response almost in the entire range of k_{SA} up to k_{SA} = 1000 ksi, as the same for pipe strain response. For C_p = 12000 in/sec, the value of $u_{JA,y}$ and u_{Jc} affects the relative joint displacement response in the range of k_{SA} < 10 ksi, and the variation is small.

The effect of incident angle of ground motion on the relative joint displacement response is shown in Fig. 3.24 . The response decreases as the incident angle increases and the same trend is also found in elastic analysis. For the incident angle of 45°, the value of $u_{JA,y}$ and u_{Jc} affects the relative joint displacement response in the range of k_{SA} < 100 ksi. Because the pipeline system under study is symmetrical, the behavior for an incident angle greater than 45° can be obtained through the image of that from an incident angle less than 45°.

The inelastic as well as the corresponding elastic relative joint displacement responses of a pipe of 6 inch diameter subjected to a ground motion with wave velocity of 2400 in/sec and incident angle of 0° are presented in Figs. 3.25 to 3.29. The variables are the same as those used to study the inelastic pipe strain responses. These figures show that the longitudinal joint responses increase as the contact space of joint decreases. Since if the available

contact space of a longitudinal joint spring is small, the joint responses switch from compressive to tensile side after the contact. Thus, the joint response, is easier to reach and exceed the tensile elastic limit. From joint response point of view, a smaller contact space of joint will be unfavorable because the joint responses become easier to reach and exceed the pull-out joint limit, $u_{JA,u}$. Also, a small contact space of joint will give higher pipe strains as discussed earlier. These figures also show that the elastic joint response appears to be the lower bound of inelastic joint responses. The effects of soil yielding to relative joint displacement of segmented pipelines can be seen by comparing Fig. 3.25 to Fig. 3.29. In general, soils with smaller elastic limit yield higher joint responses.

From the above observations, one can conclude that for a continuous pipeline, the response of the elastic analysis is conservative, especially for smaller values of the elastic limit, e.g., $u_{SA,y} = u_{SL,y} \leq 0.1$ ksi, and softer soil, $k_{SA} = k_{SL} \leq 10$ ksi of soil spring. For the segmented pipeline, the value of u_{JC} plays an important role in the inelastic behavior of pipes and joints. For a soft soil, say $k_{SA} < 100$ ksi, the inelastic analysis should be considered since both pipe and joint responses of elastic analysis will underestimate the real responses if soil and/or joint becomes inelastic. However, for very high wave velocity, $C_P = 12000$ in/sec, the elastic analysis may be

sufficient for estimation of the responses of pipe as well as joint due to wave propagation. For future aseismic design of buried pipeline, more flexible (ductile) joint should be concerned to accommodate larger relative joint displacement (without pull-out failure). Accordingly the pipe strain can be reduced also.

Table 3.1 Elastic Limit of Soil in Lateral Direction, $u_{SL,y}$, Obtained from Figs. 3.7 and 3.8 as Presented in Ref. [2]

	Elastic Limit $u_{SL,y}$ (in)	Note
Laboratory Testing	0.1 - 0.5	OD=1", 2.45" and 4.5" H/D=2, 3, 6, 12 and 24
In-Situ Testing	0.54	OD=9" H/D=4

Table 3.2 Elastic Limit of Soil in Lateral Direction, $u_{SL,y}$, Obtained from Eqs. (3.20a and 3.20b) as Presented in Ref. [7]

		Elastic Limit, $u_{SL,y}$ (in)	
D(in)	H/D	Medium Sand	Dense Sand
6	2	0.45 - 0.75	0.3 - 0.45
	4	0.81 - 1.35	0.54 - 0.81
	6	1.17 - 1.95	0.78 - 1.17
12	2	0.9 - 1.5	0.6 - 0.9
	3	1.26 - 2.1	0.84 - 1.26
	4	1.62 - 2.7	1.08 - 1.62
24	2	1.8 - 3.0	1.2 - 1.8
	3	2.52 - 4.2	1.68 - 2.52

Table 3.3 Elastic Limits of Joint, $u_{JA,y}$ and $u_{JR,y}$, Obtained from Figs. 1.1 and 1.2 [39, 40]

Elastic Limit $u_{JA,y}$ (in)	Elastic Limit $u_{JR,y}$ (deg)	Note
0.1 - 0.6	0.2 - 0.5	Nominal Pipe Diameter = 4", 6", 8" and 10"

Table 3.4 Referenced and Parametric Conditions

Used in Inelastic Parametric Study

Physical Parameter	Referenced Condition	Parametric Conditions
Pipe Material	Steel E=30,000 ksi	-
Diameter	OD = 6"	24"
Soil Stiffness	$k_{SA} = k_{SL} = 1$ ksi	k_{SA} = 0.1 to 1,000 ksi k_{SL} = 0.1 to 1,000 ksi
Joint Stiffness	Continuous	k_{JA} = 1.0 k/in k_{JR} = 1.0 k-in/deg
Wave Velocity	C_p = 2400 in/sec	C_p = 12,000 in/sec
Incident Angle	ϕ = 0°	ϕ = 45°
Elastic Limit	Elastic (Continuous and Segmented)	$u_{s,y}$ = 0.05, 0.1, 0.2, 0.5 inches $u_{J,y}$ = 0.1, 0.3, 0.5 inches $u_{J,c}$ = 0.1, 0.2 0.3, 0.5 inches

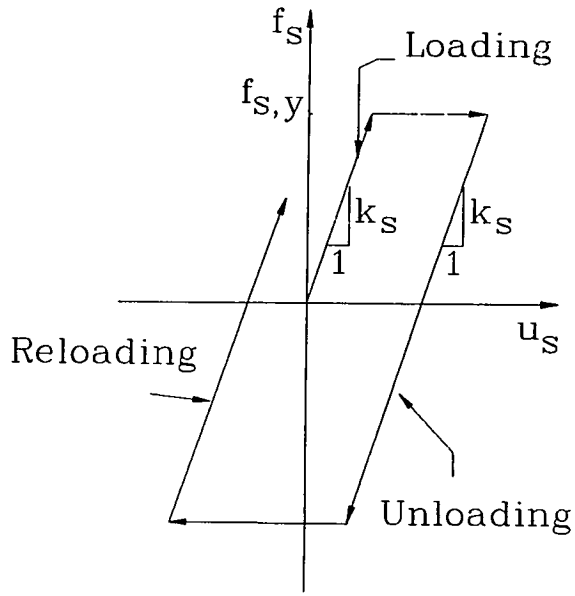

Fig. 3.1 Hysteretic Characteristic of Soil

Fig. 3.2a Axial Hysteretic Characterestic of Joint

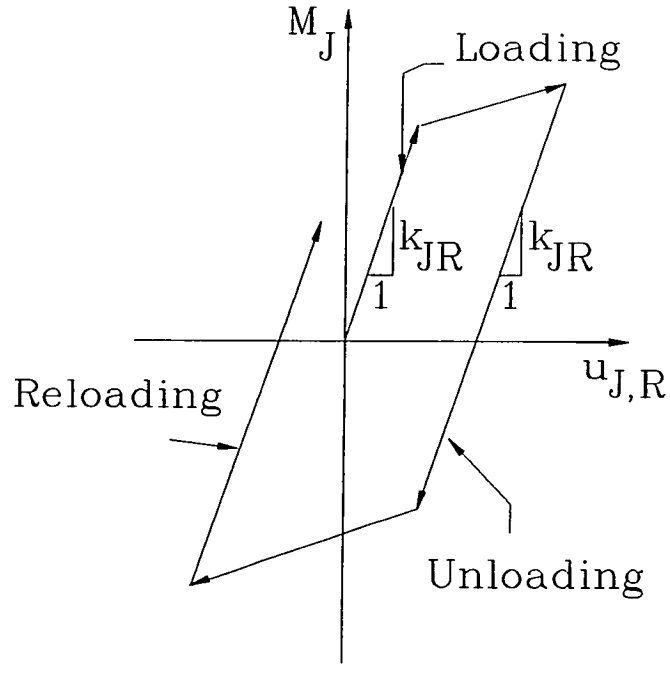

Fig. 3.2b Rotational Hysteretic Characteristic of Joint

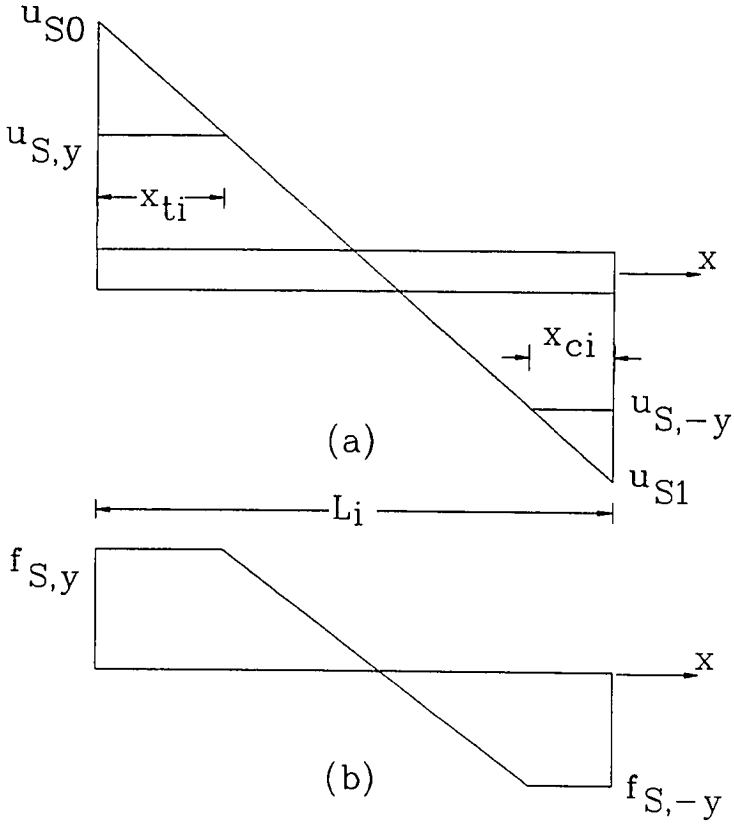

Fig. 3.3 General Case for (a) Inelastic Soil–pipe Response and (b) Corresponding Resistant Force

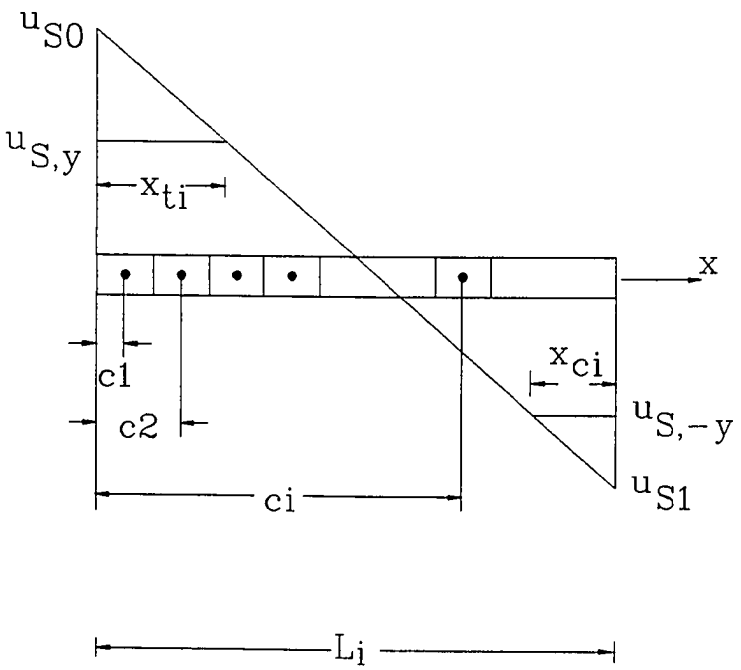

Fig. 3.4 Simplified Approach for Calculating Modified Soil Stiffness and Inelastic Nodal Force

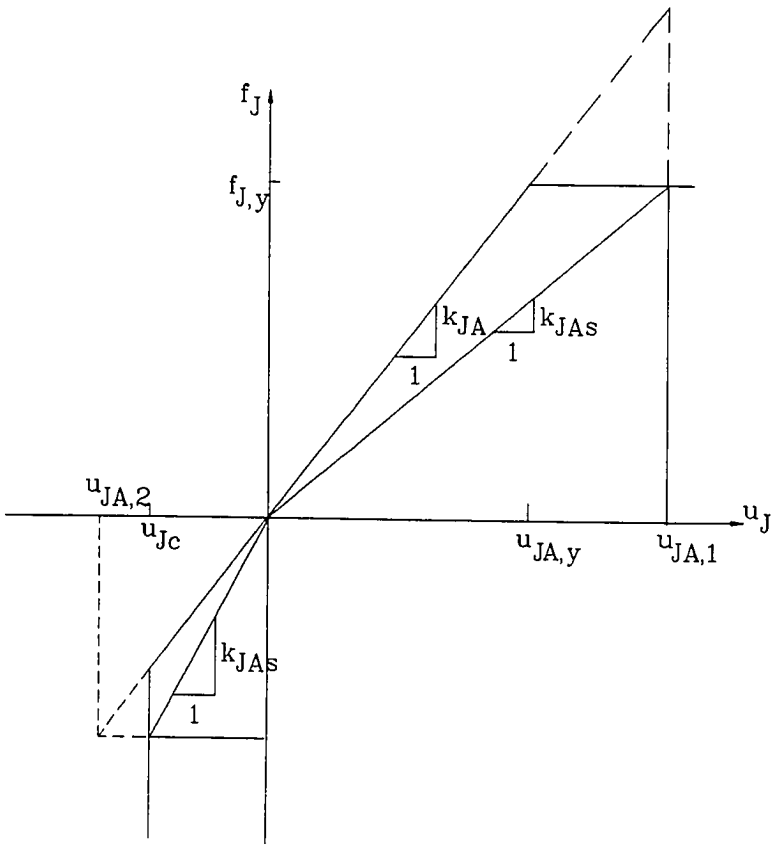

Fig. 3.5a Longitudinal Secant Modulus of Joint

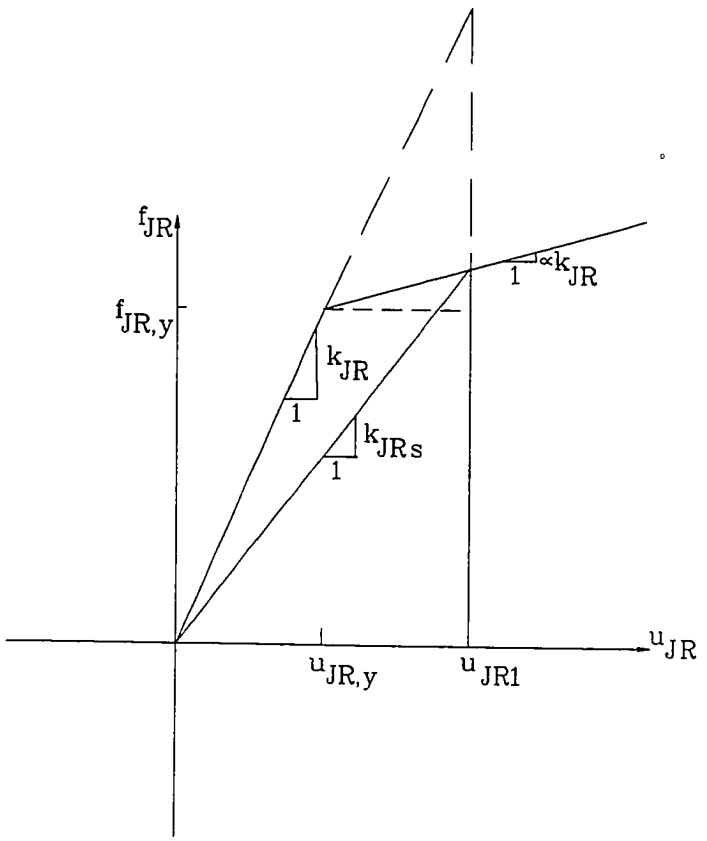

Fig. 3.5b Rotational Secant Modulus of Joint

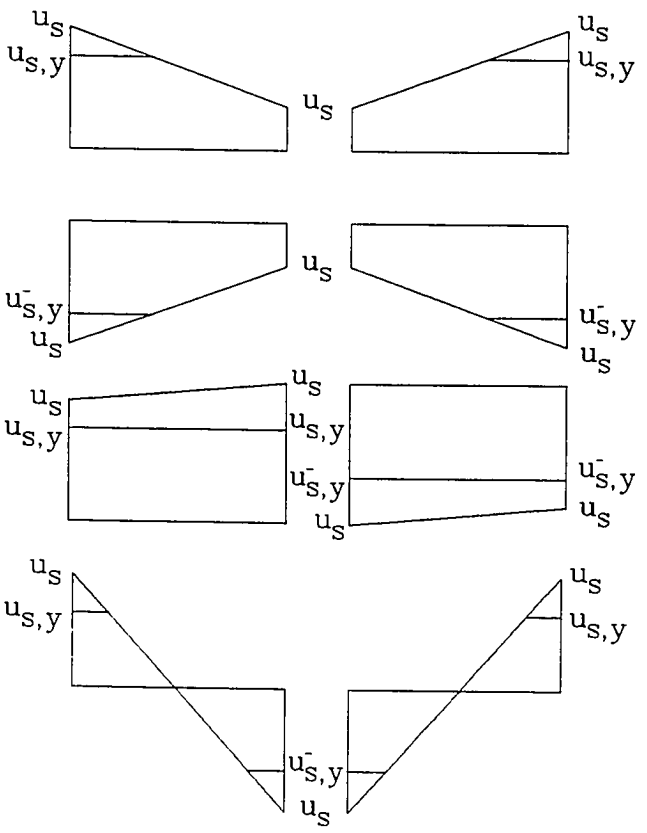

Fig. 3.6 Cases of Soil Frictional Force Partially Plastified

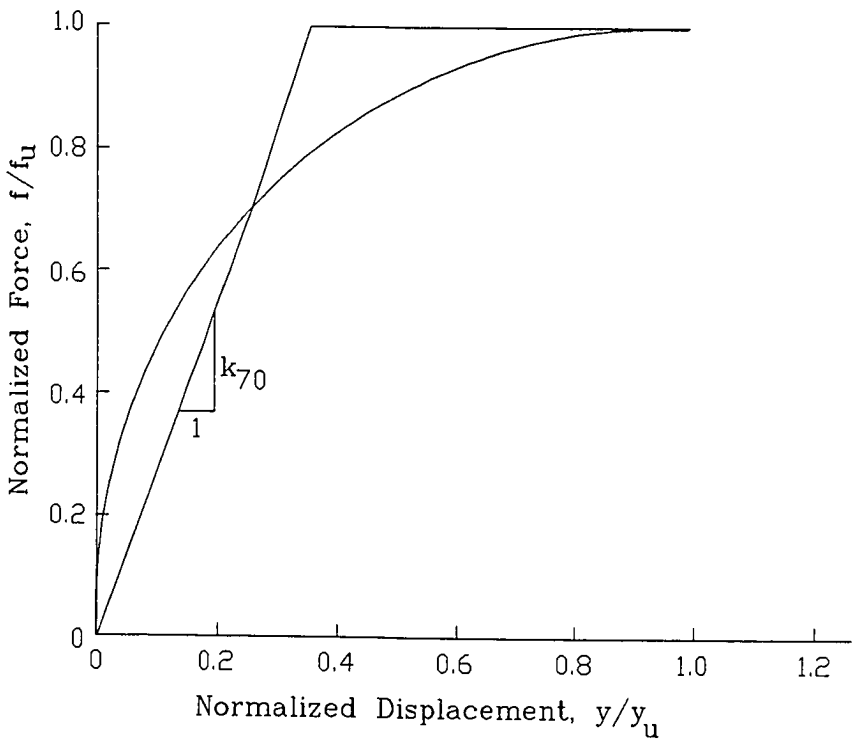

Fig. 3.7 Application of Bilinear Model to Force – Displacement Relationship of Soil

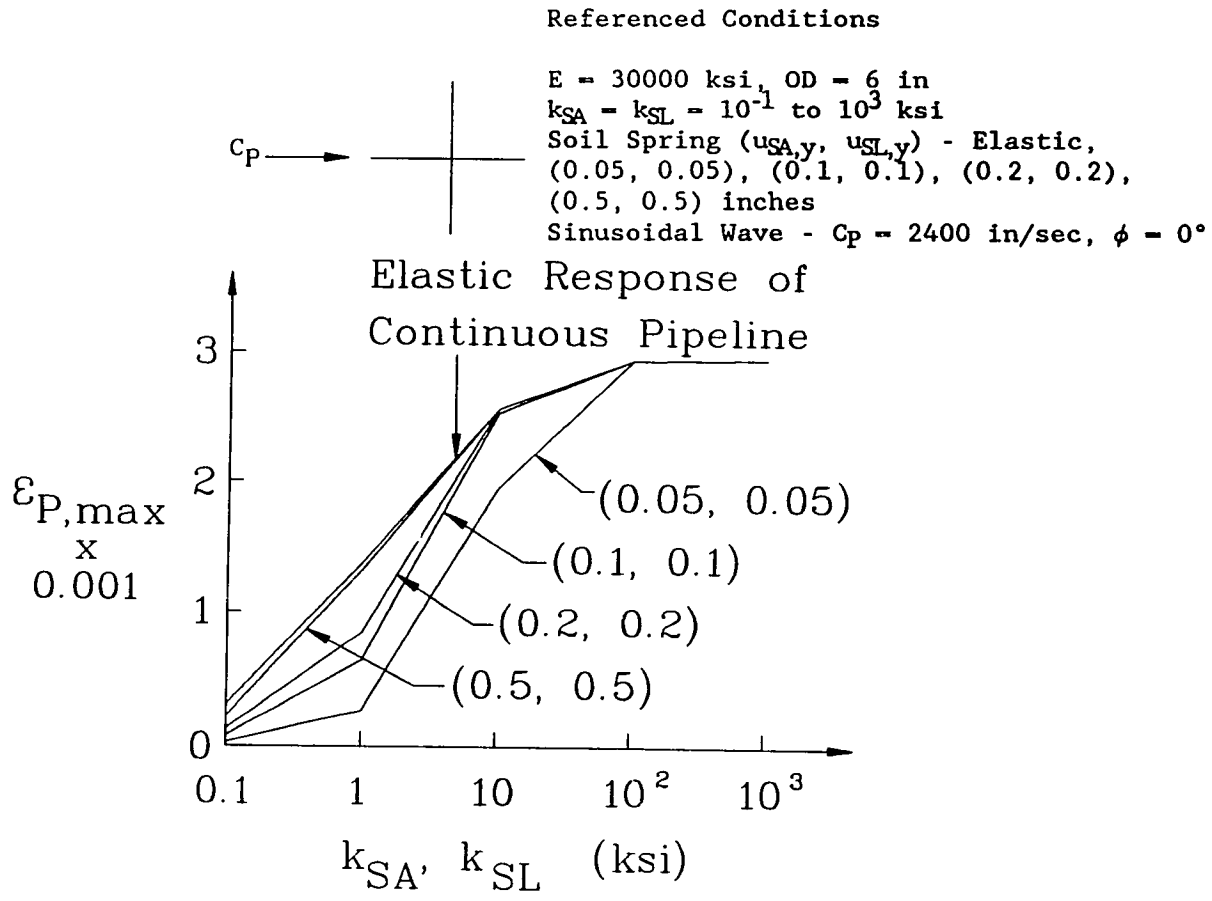

Fig. 3.8 Comparison of Elastic and Inelastic Pipe Strain Responses

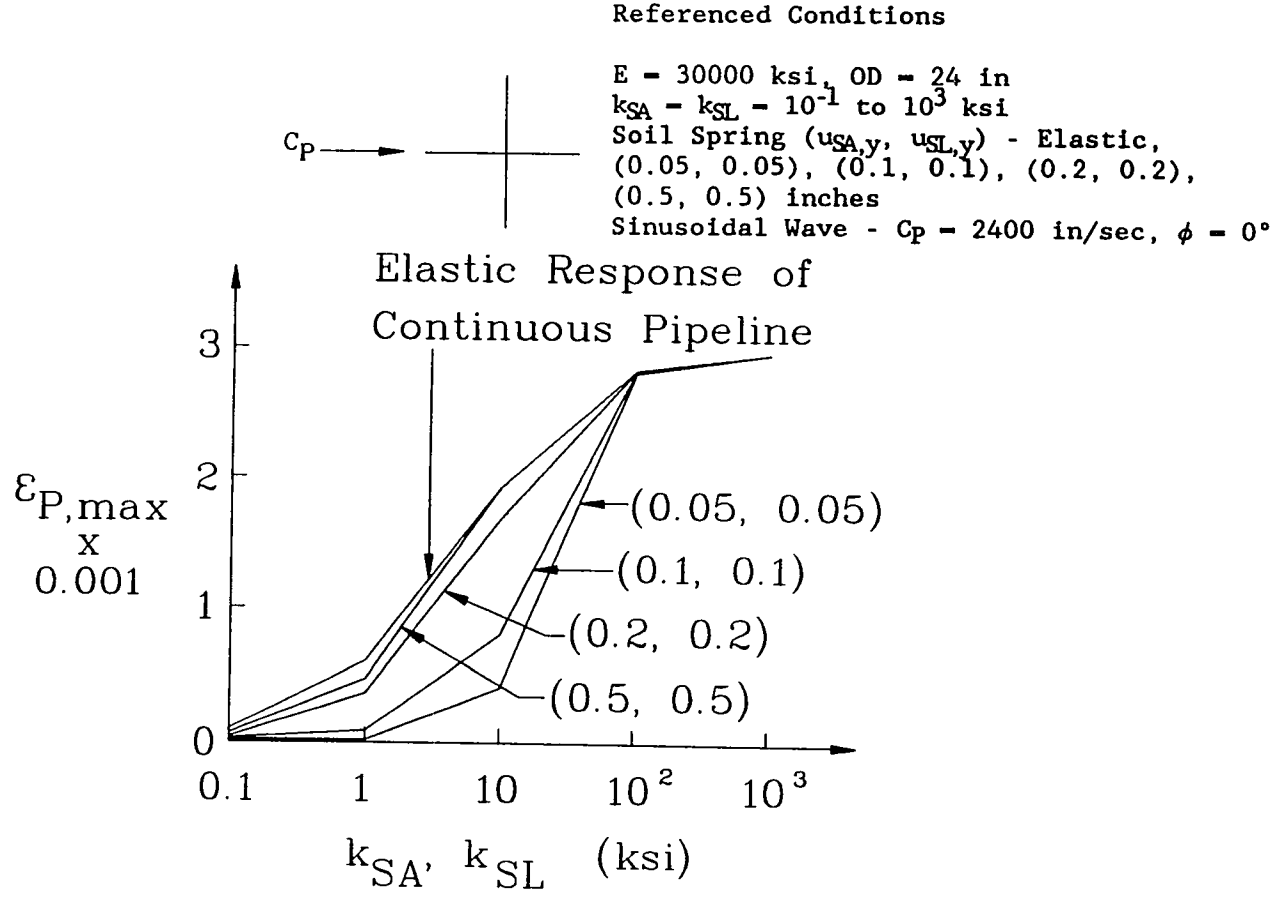

Fig. 3.9 Comparison of Elastic and Inelastic Pipe Strain Response

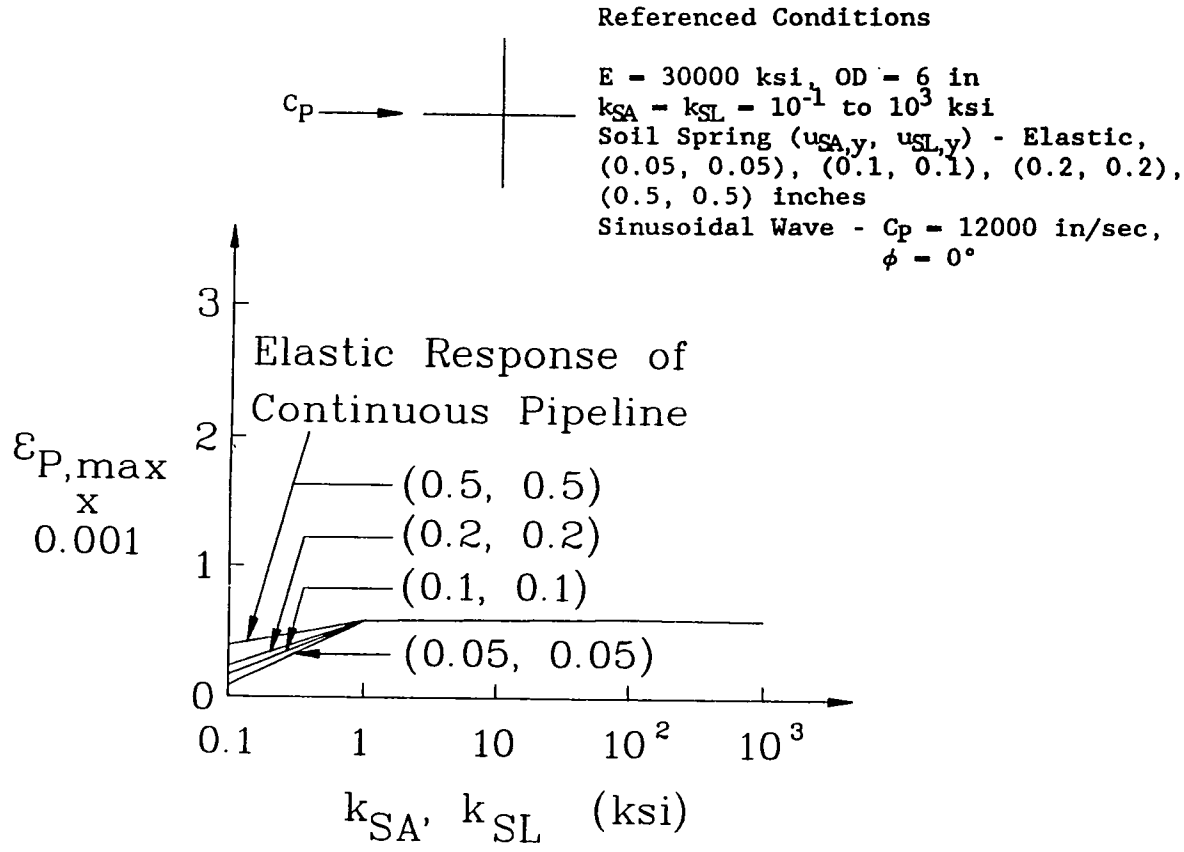

Fig. 3.10 Comparison of Elastic and Inelastic Pipe Strain Response

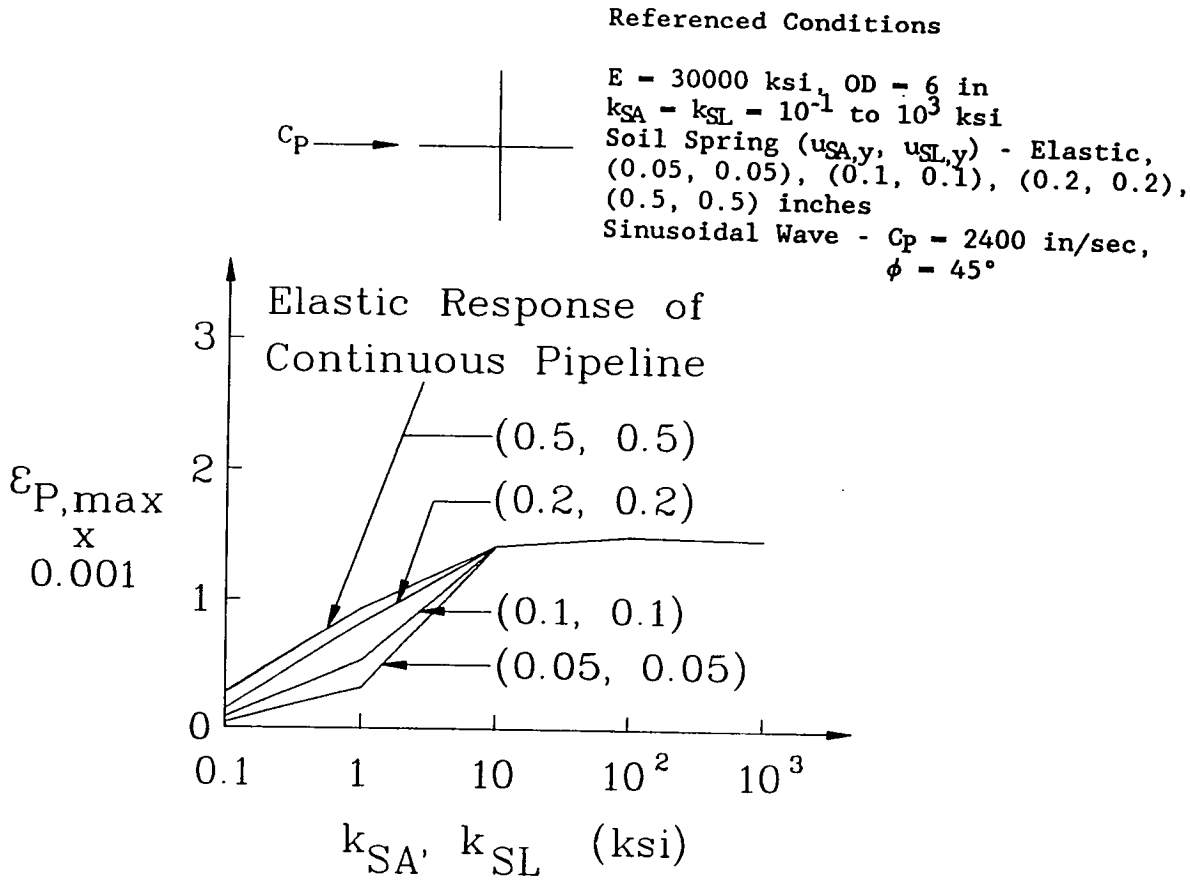

Fig. 3.11 Comparison of Elastic and Inelastic Pipe Strain Response

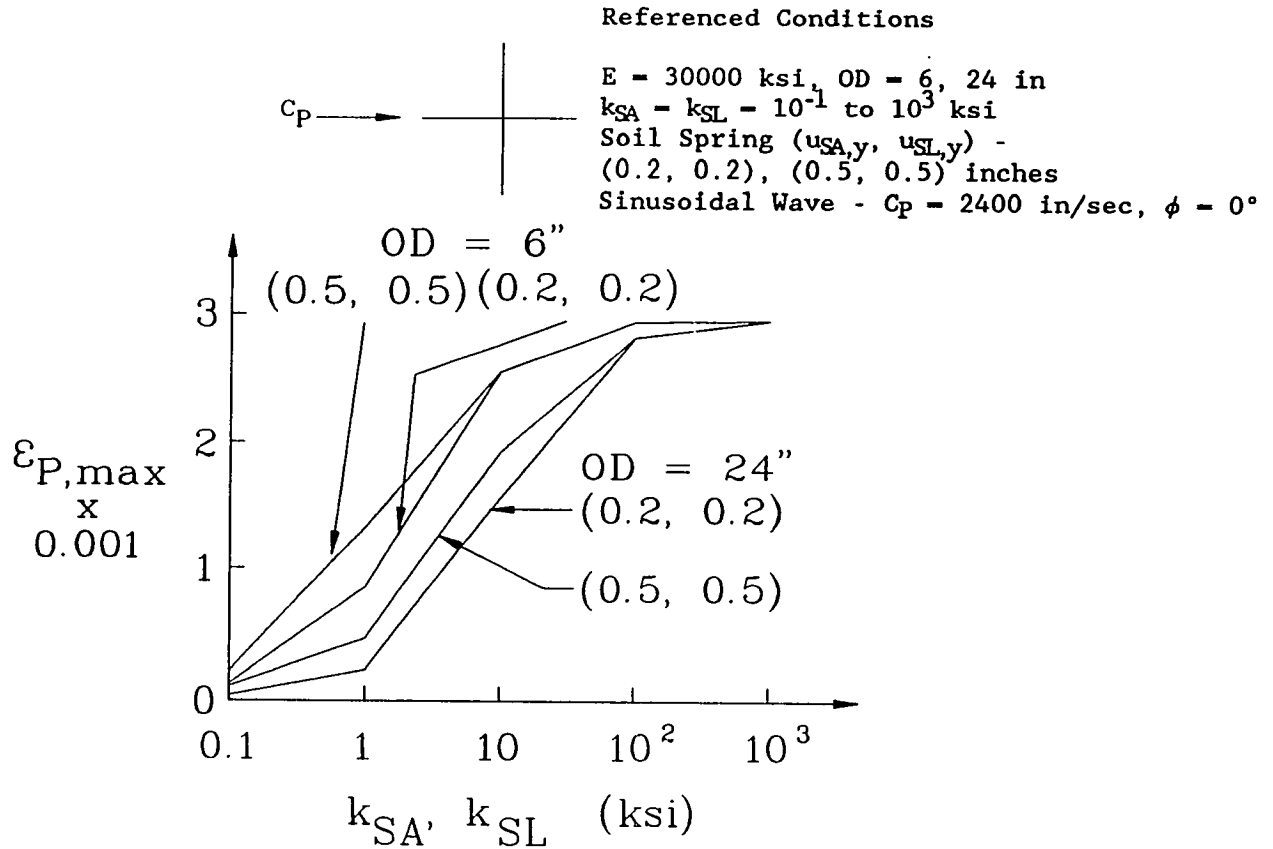

Fig. 3.12 Effect of Pipe Size on Pipe Strain Response

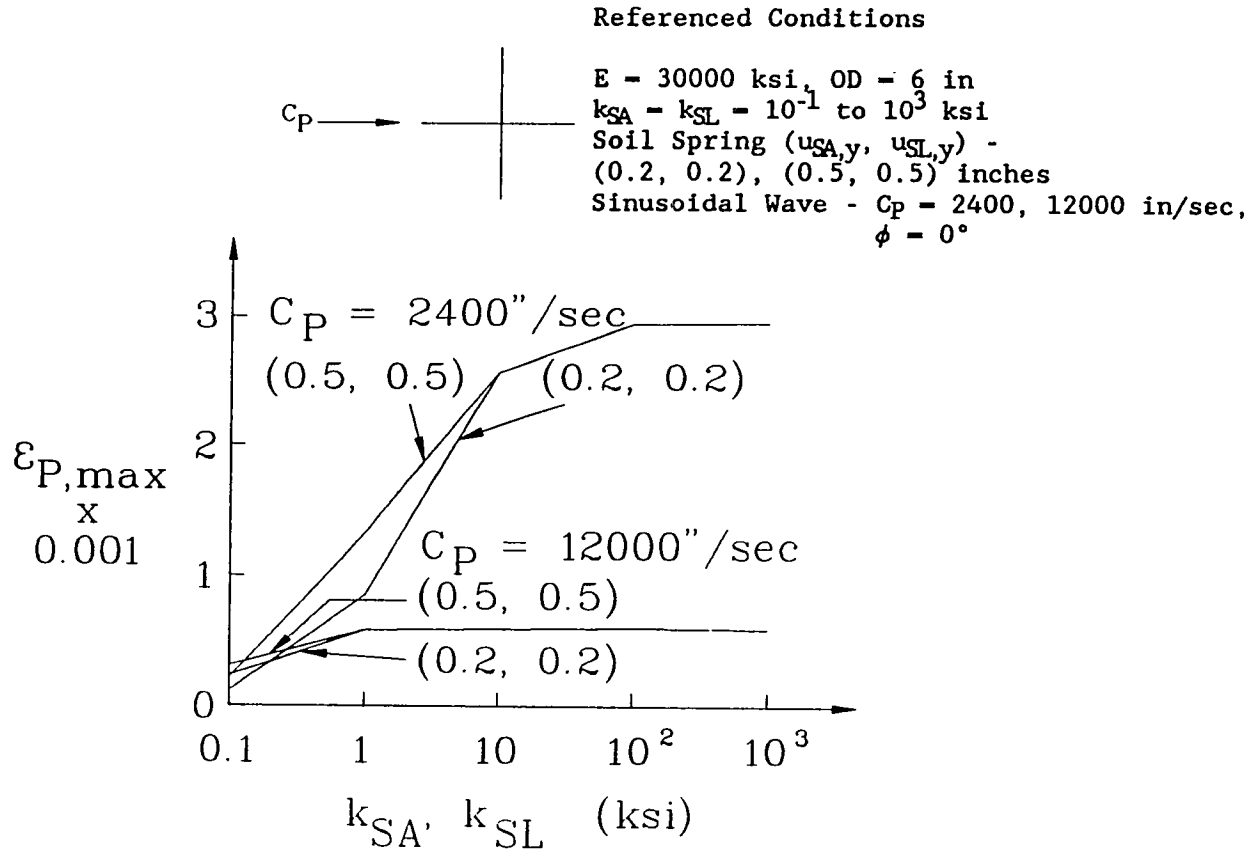

Fig. 3.13 Effect of Wave Velocity on Pipe Strain Response

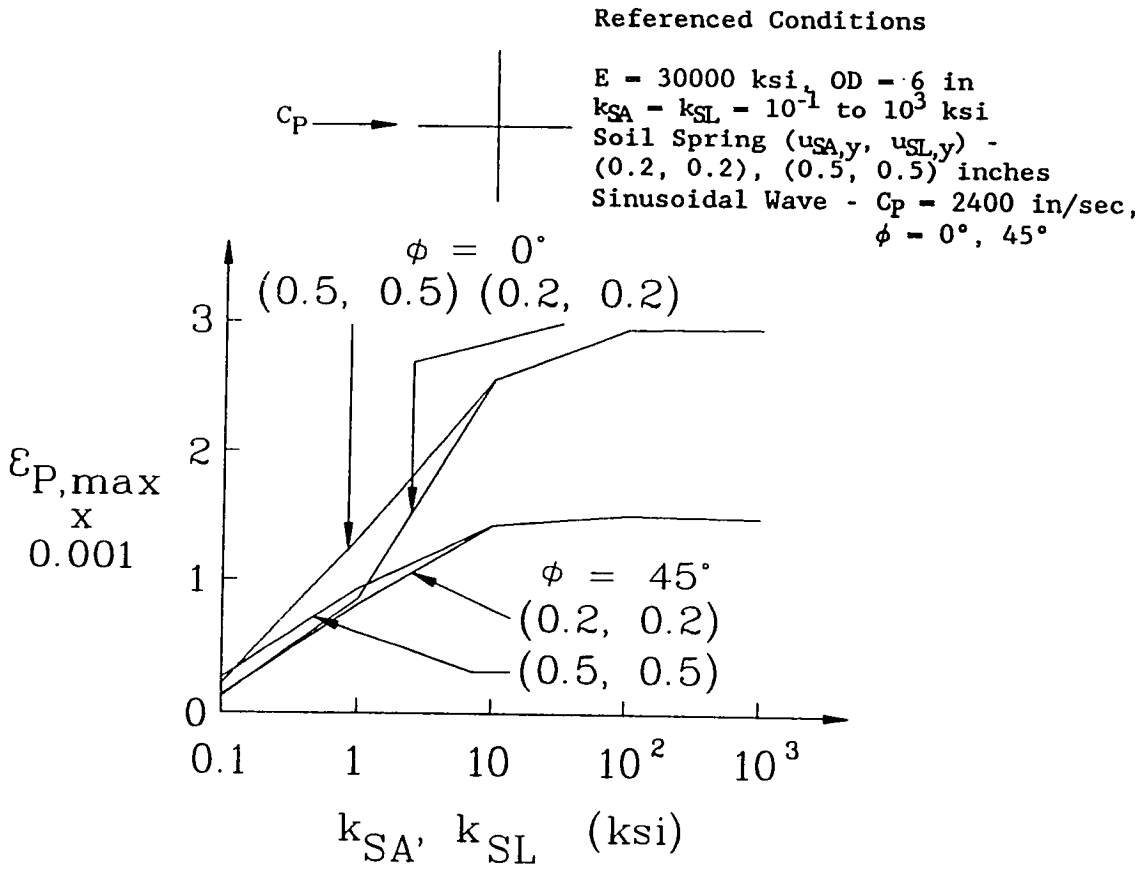

Fig. 3.14 Effect of Incident Angle on Pipe Strain Response

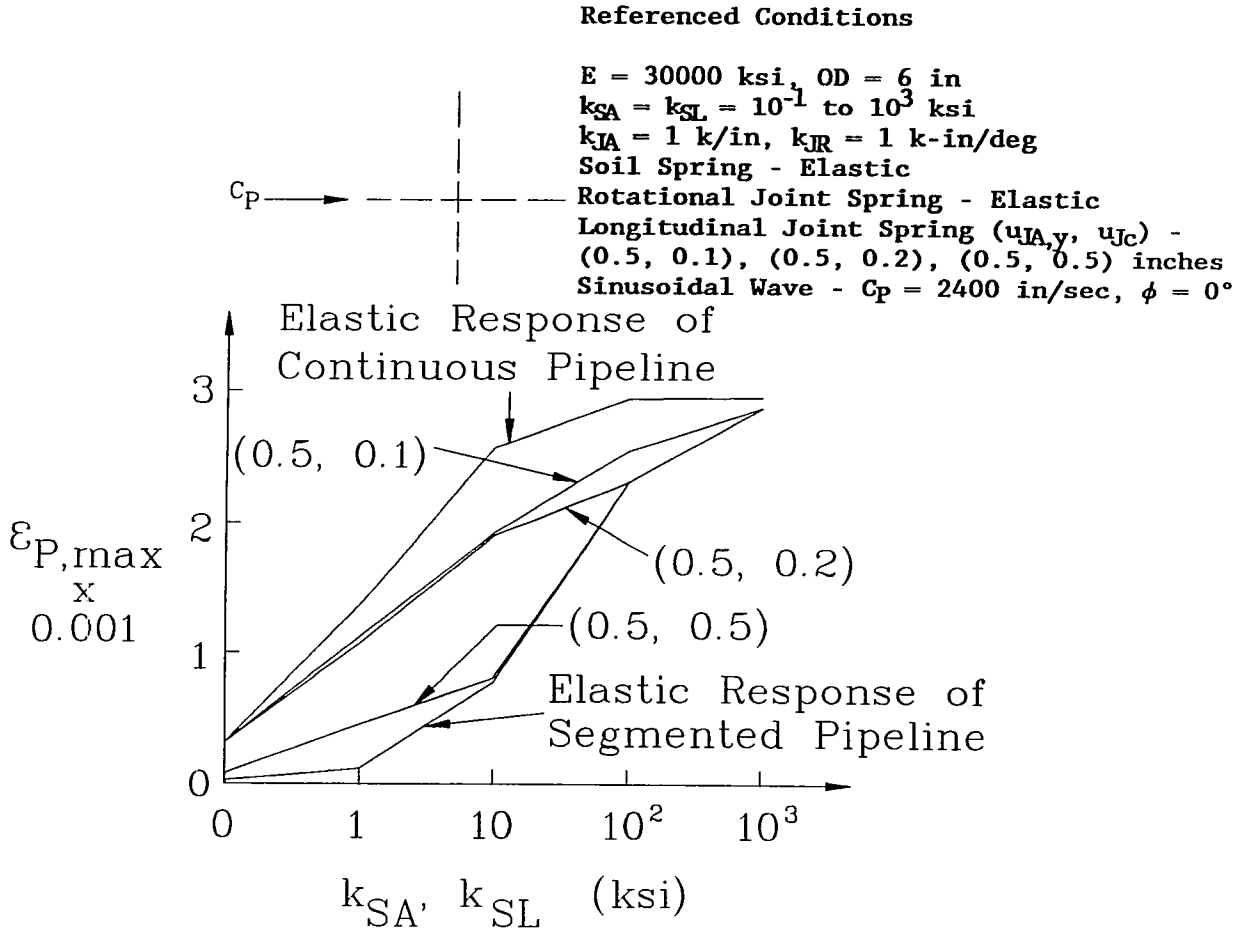

Fig. 3.15 Comparison of Elastic and Inelastic Pipe Strain Responses

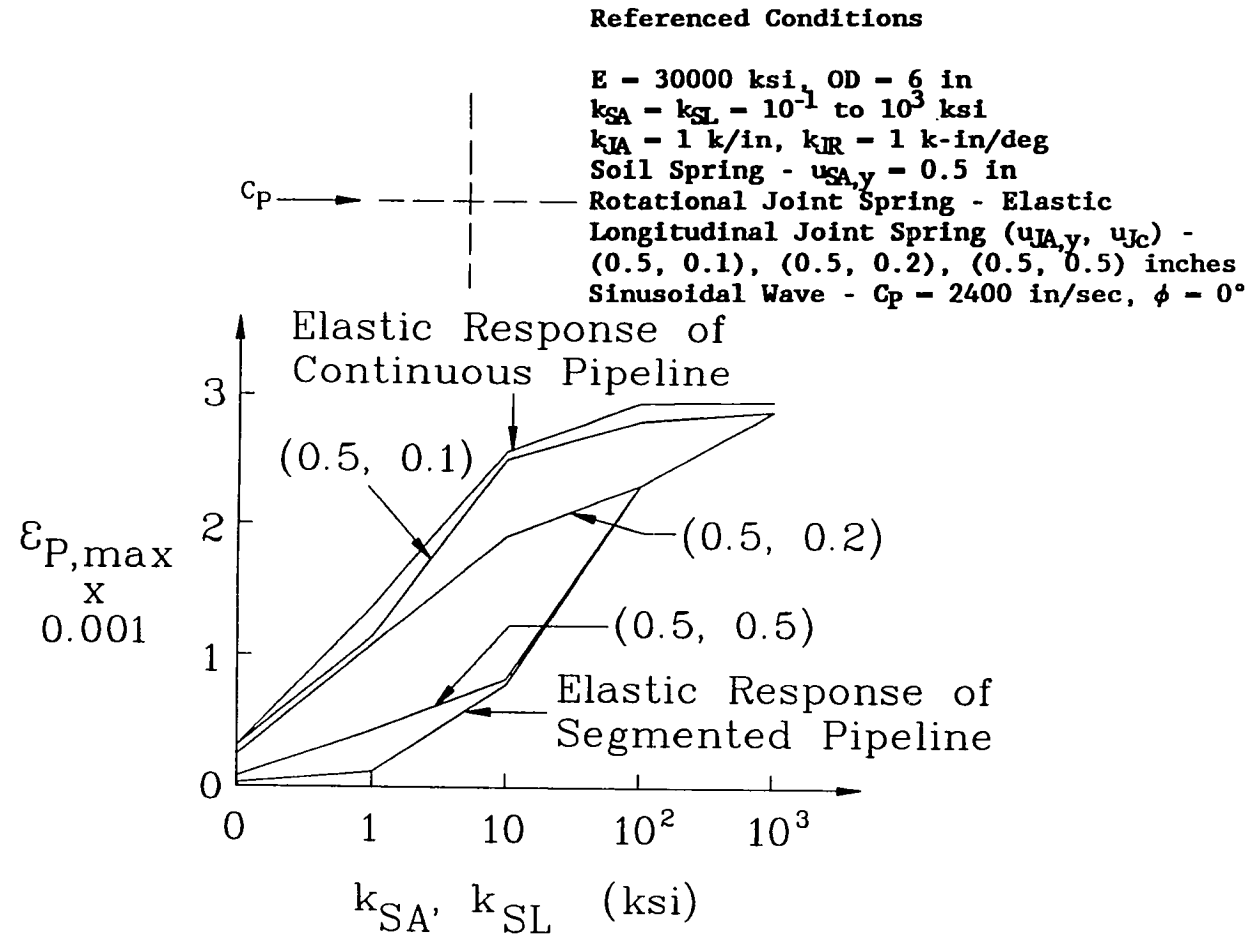

Fig. 3.16 Comparison of Elastic and Inelastic Pipe Strain Responses

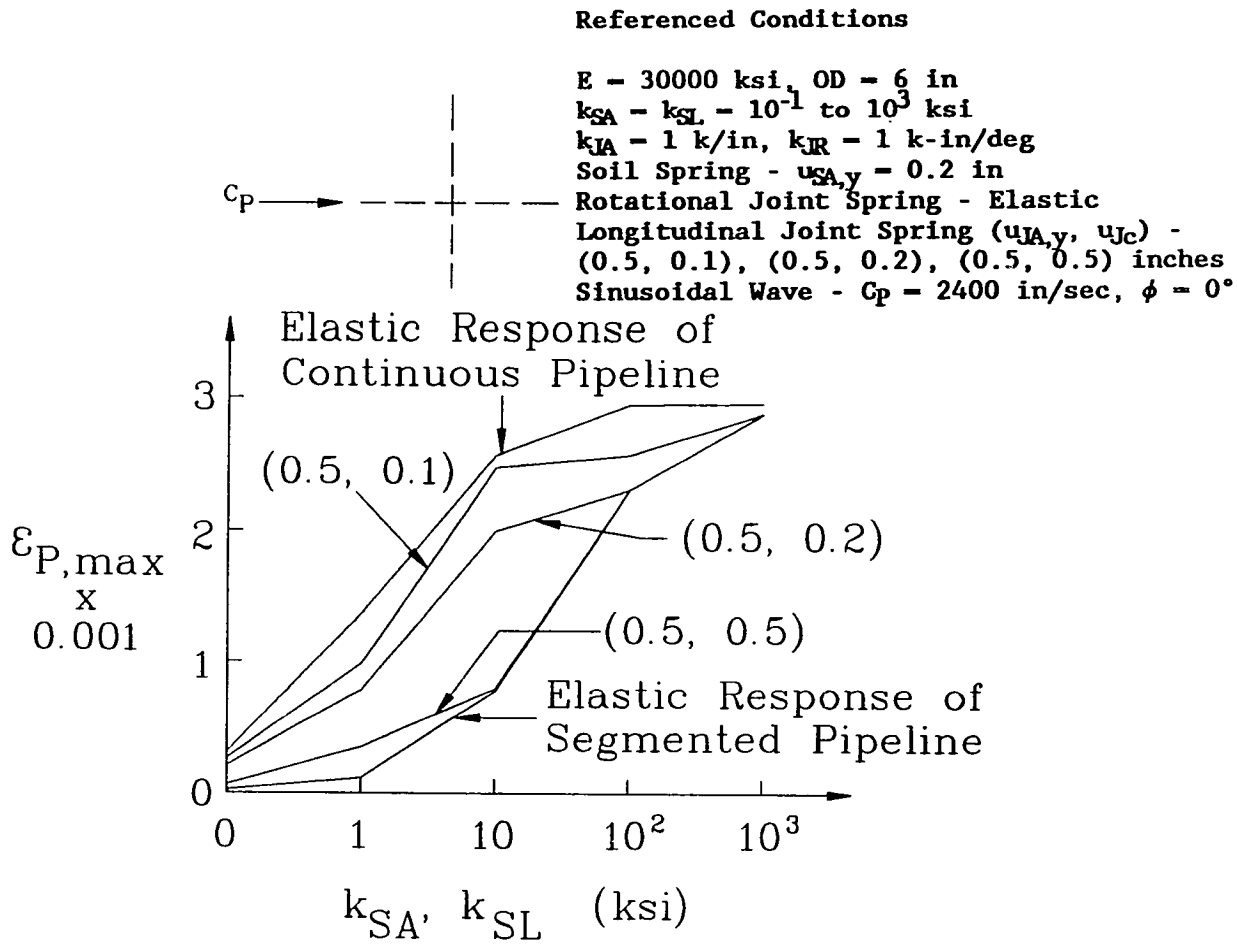

Fig. 3.17 Comparison of Elastic and Inelastic Pipe Strain Responses

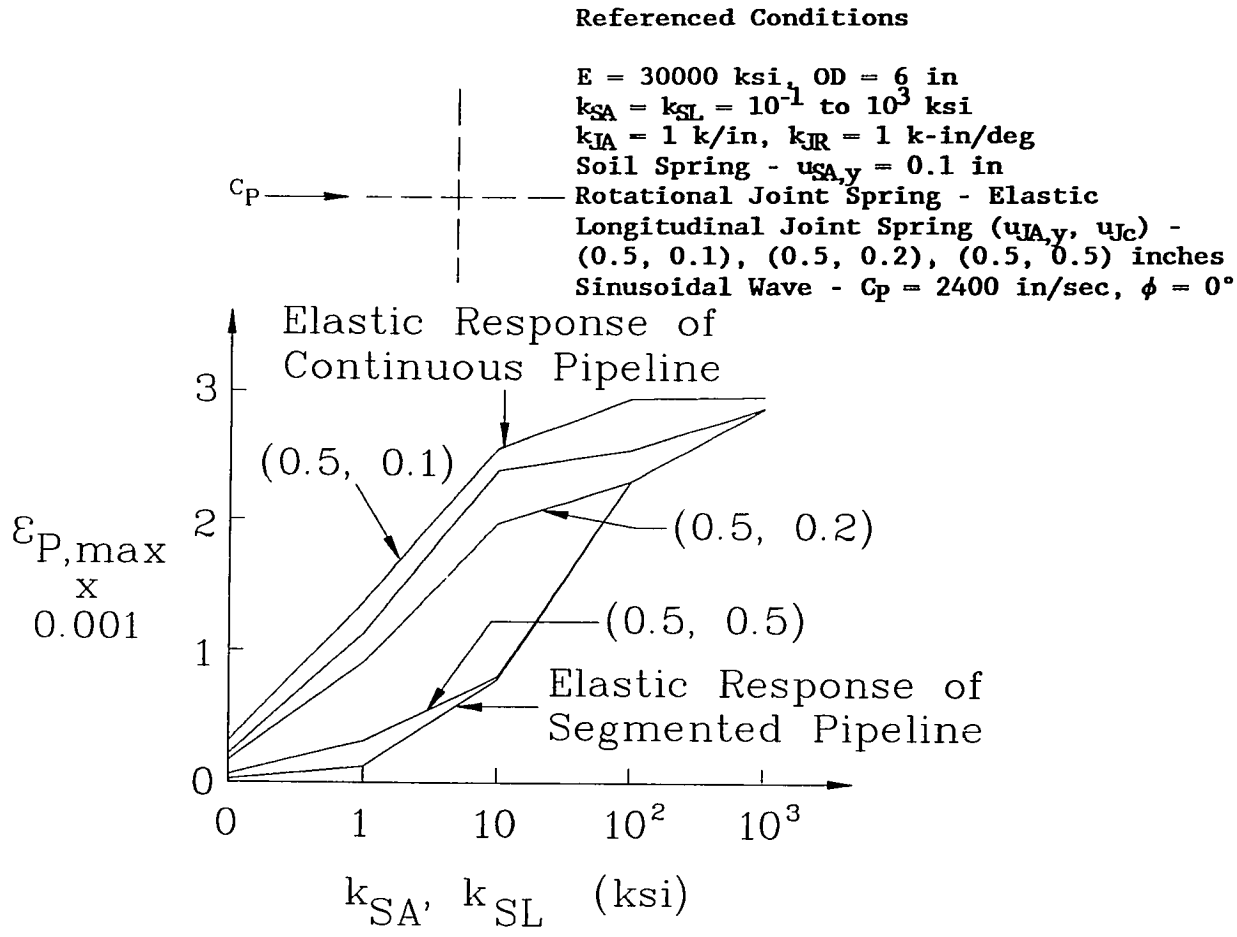

Fig. 3.18 Comparison of Elastic and Inelastic Pipe Strain Responses

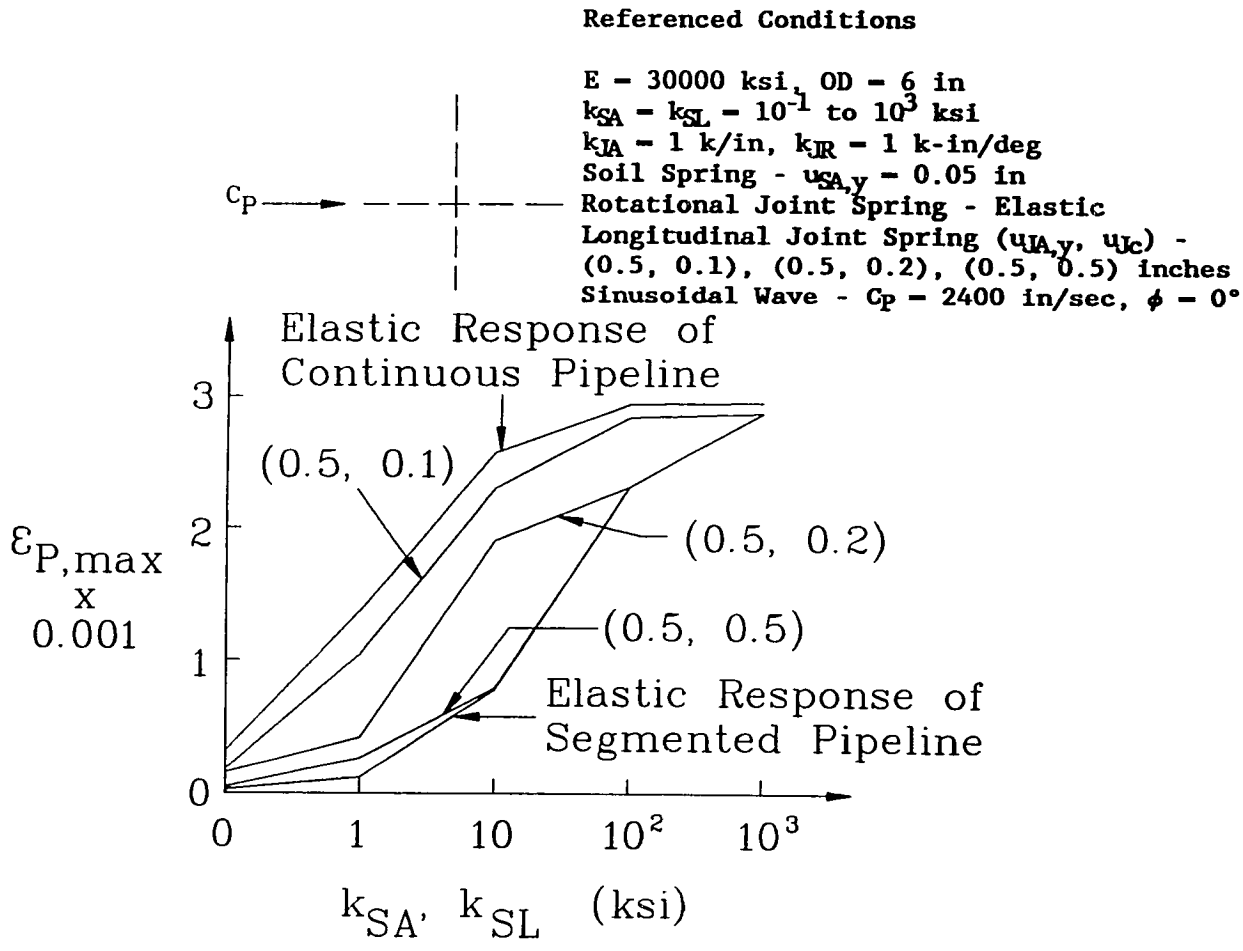

Fig. 3.19 Comparison of Elastic and Inelastic Pipe Strain Responses

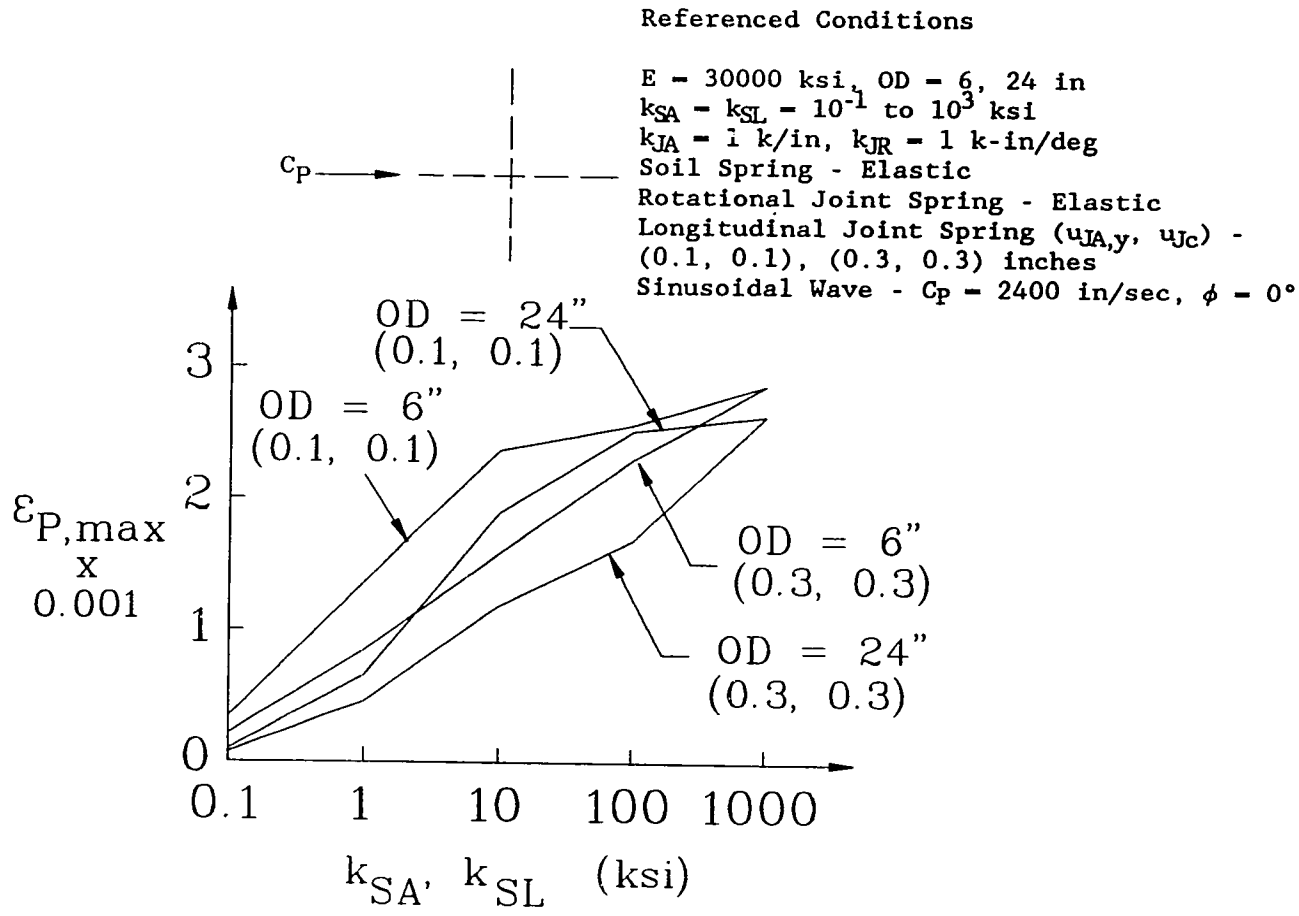

Fig. 3.20 Effect of Pipe Size on Pipe Strain Responses

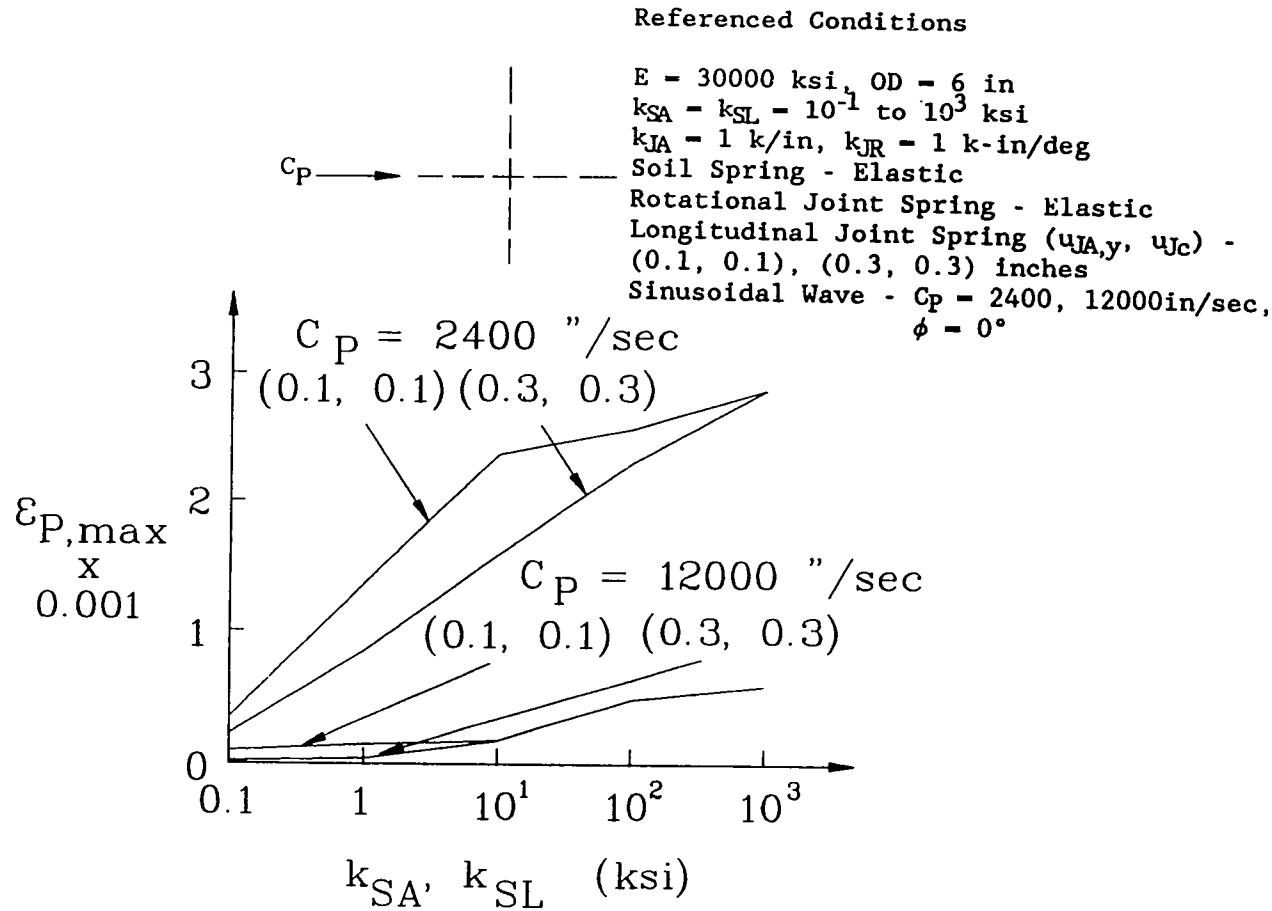

Fig. 3.21 Effect of Wave Velocity on Pipe Strain Responses

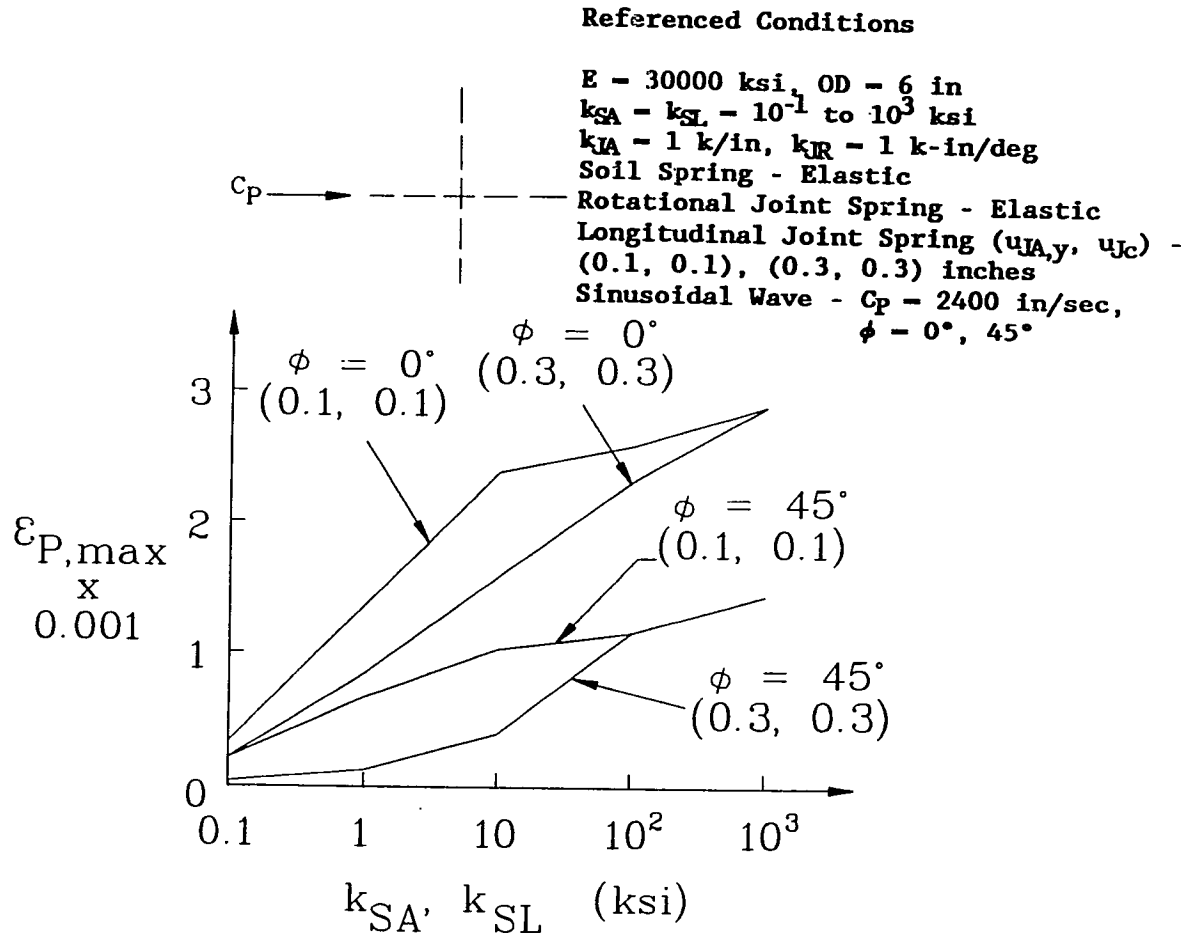

Fig. 3.22 Effect of Incident Angle on Pipe Strain Responses

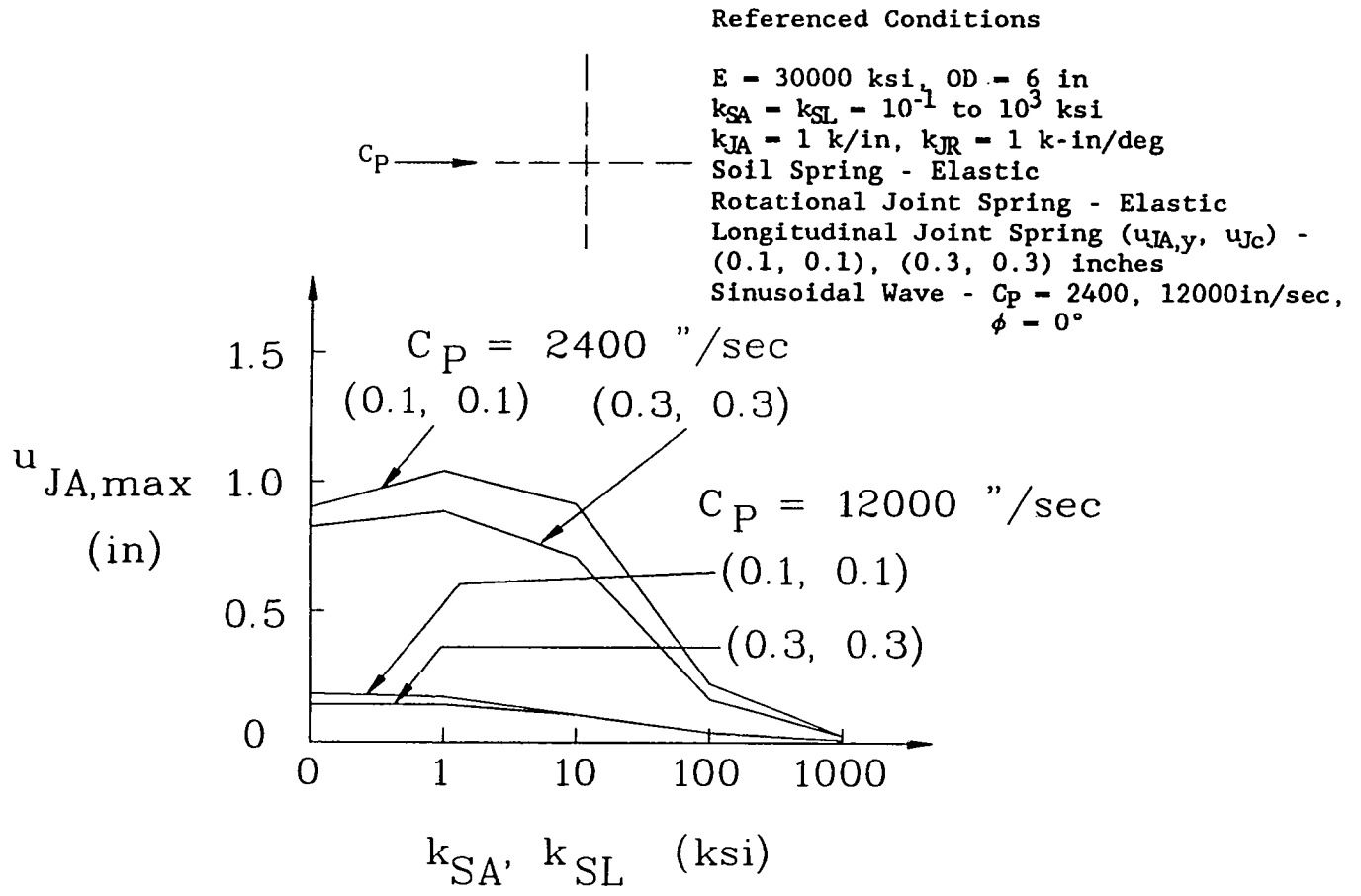

Fig. 3.23 Effect of Wave Velocity on Relative Joint Displacement

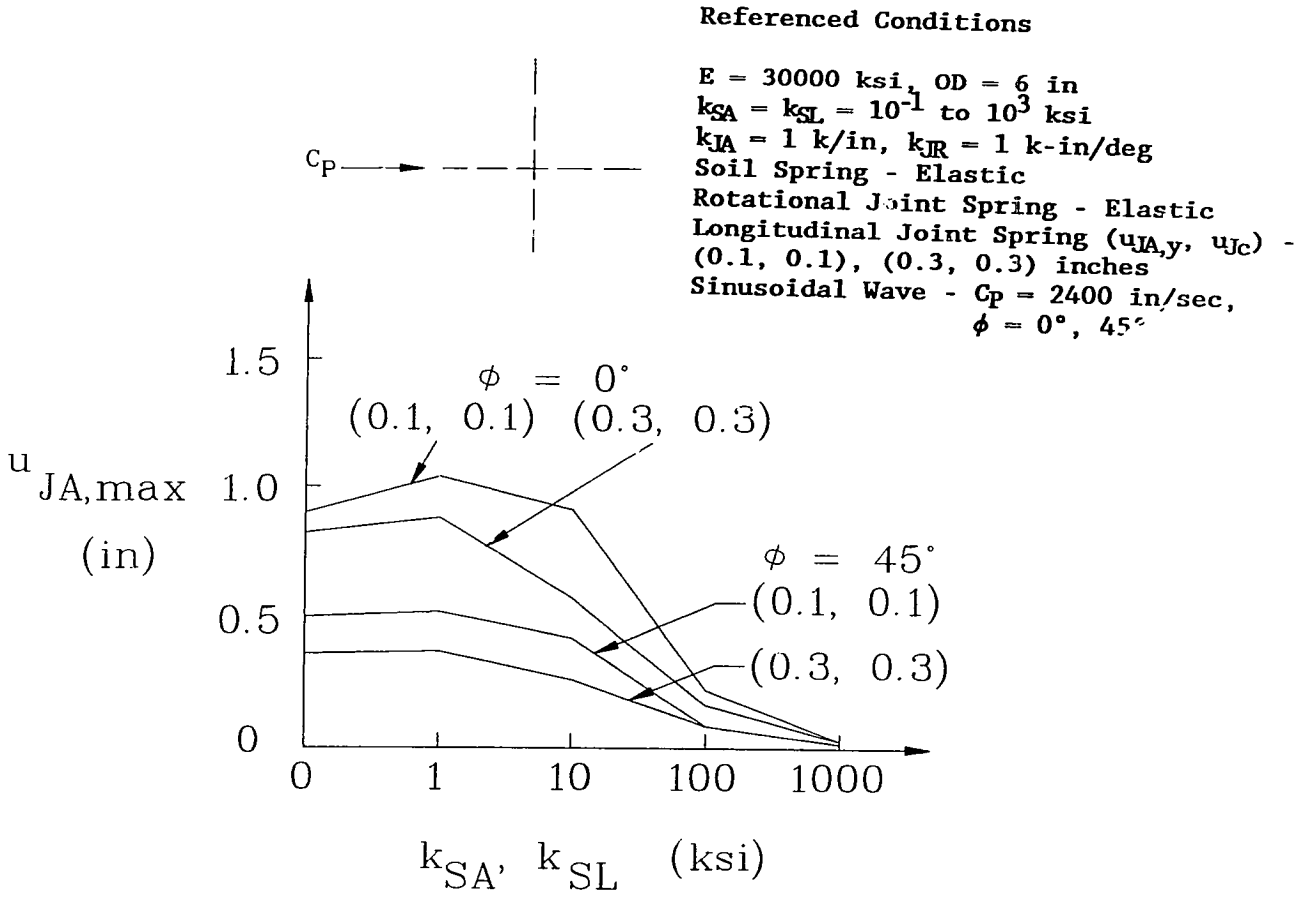

Fig. 3.24 Effect of Incident Angle on Relative Joint Displacement Responses

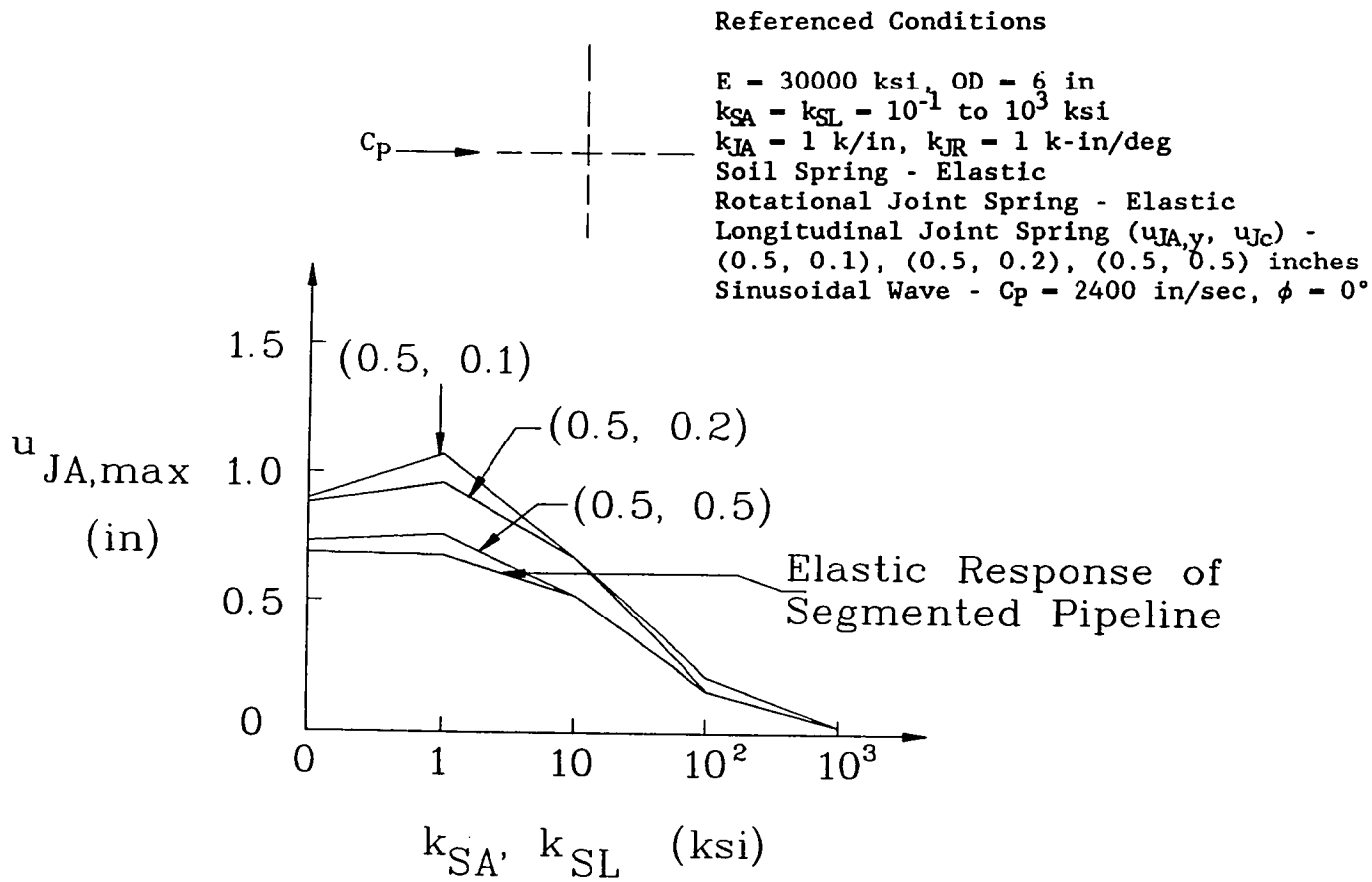

Fig. 3.25 Comparison of Elastic and Inelastic Relative Joint Displacement Responses

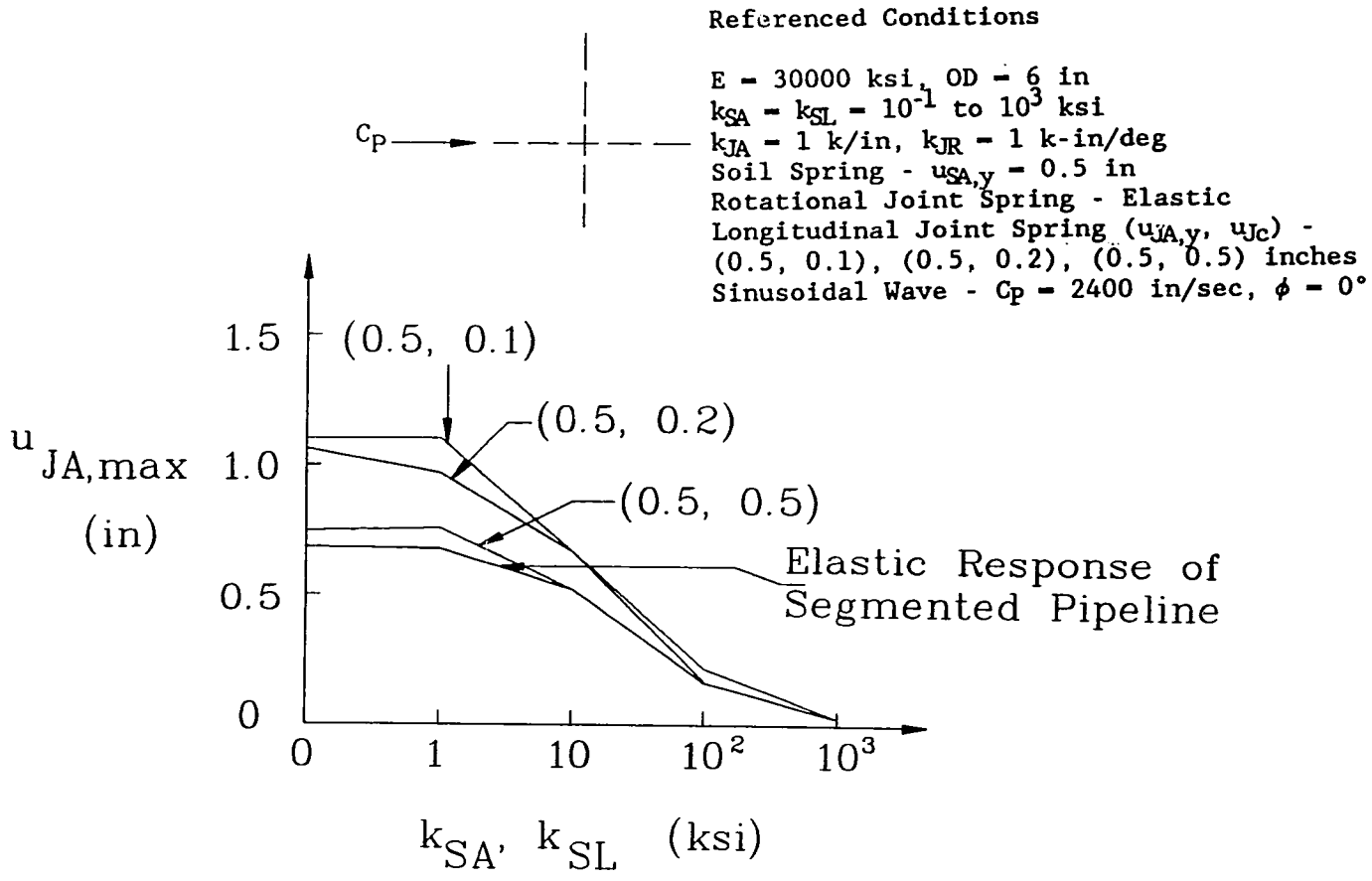

Fig. 3.26 Comparison of Elastic and Inelastic Relative Joint Displacement Responses

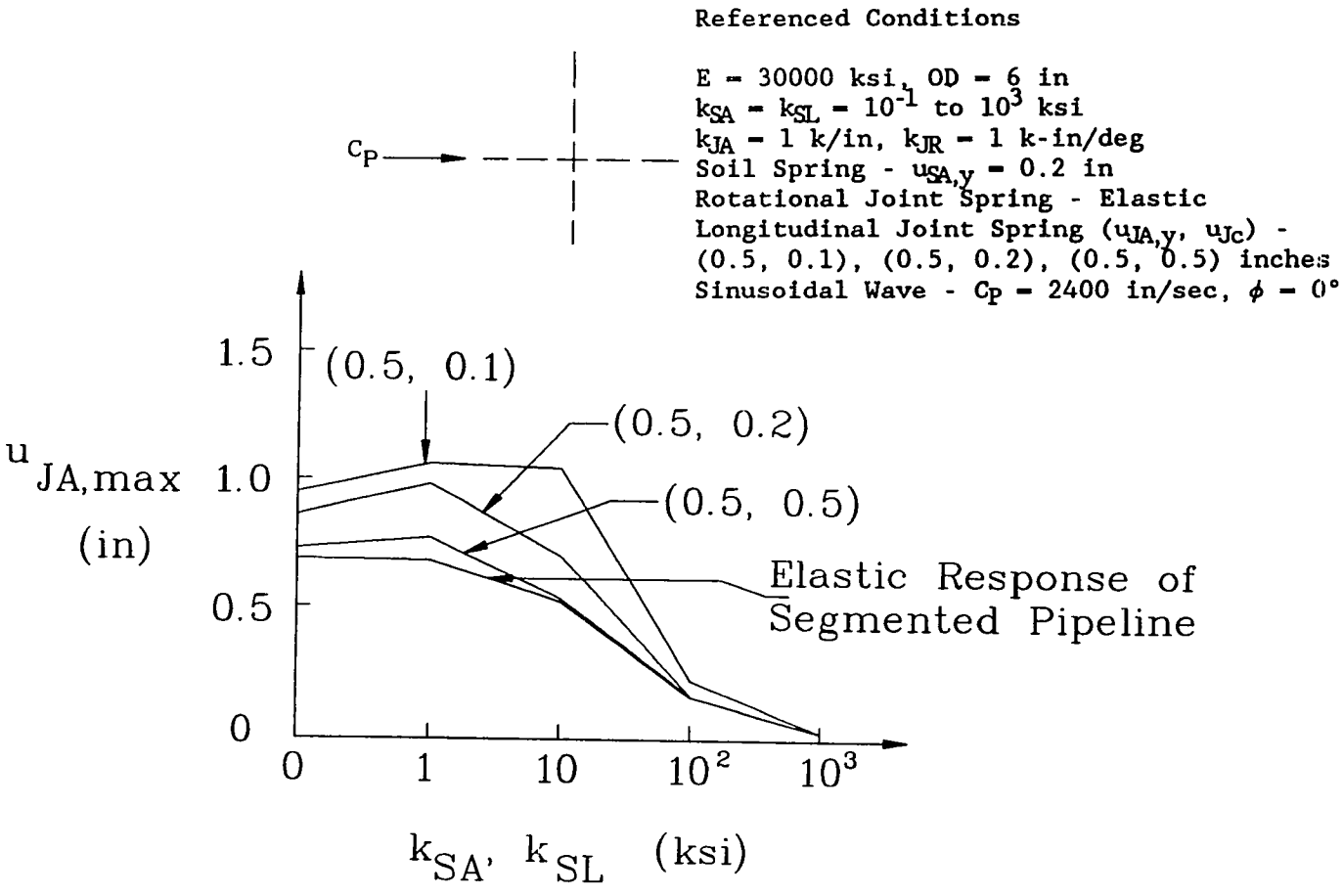

Fig. 3.27 Comparison of Elastic and Inelastic Relative Joint Displacement Responses

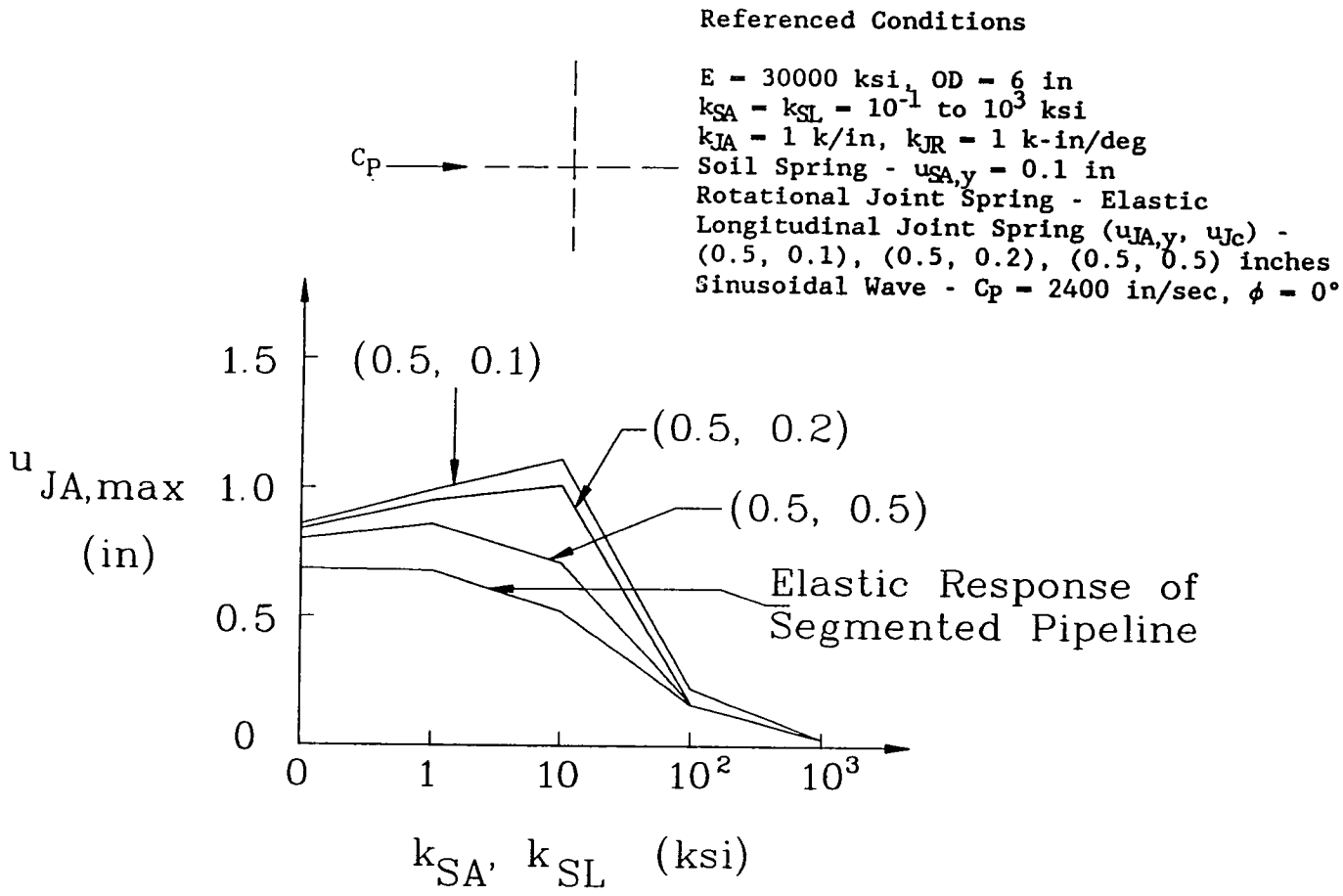

Fig. 3.28 Comparison of Elastic and Inelastic Relative Joint Displacement Response

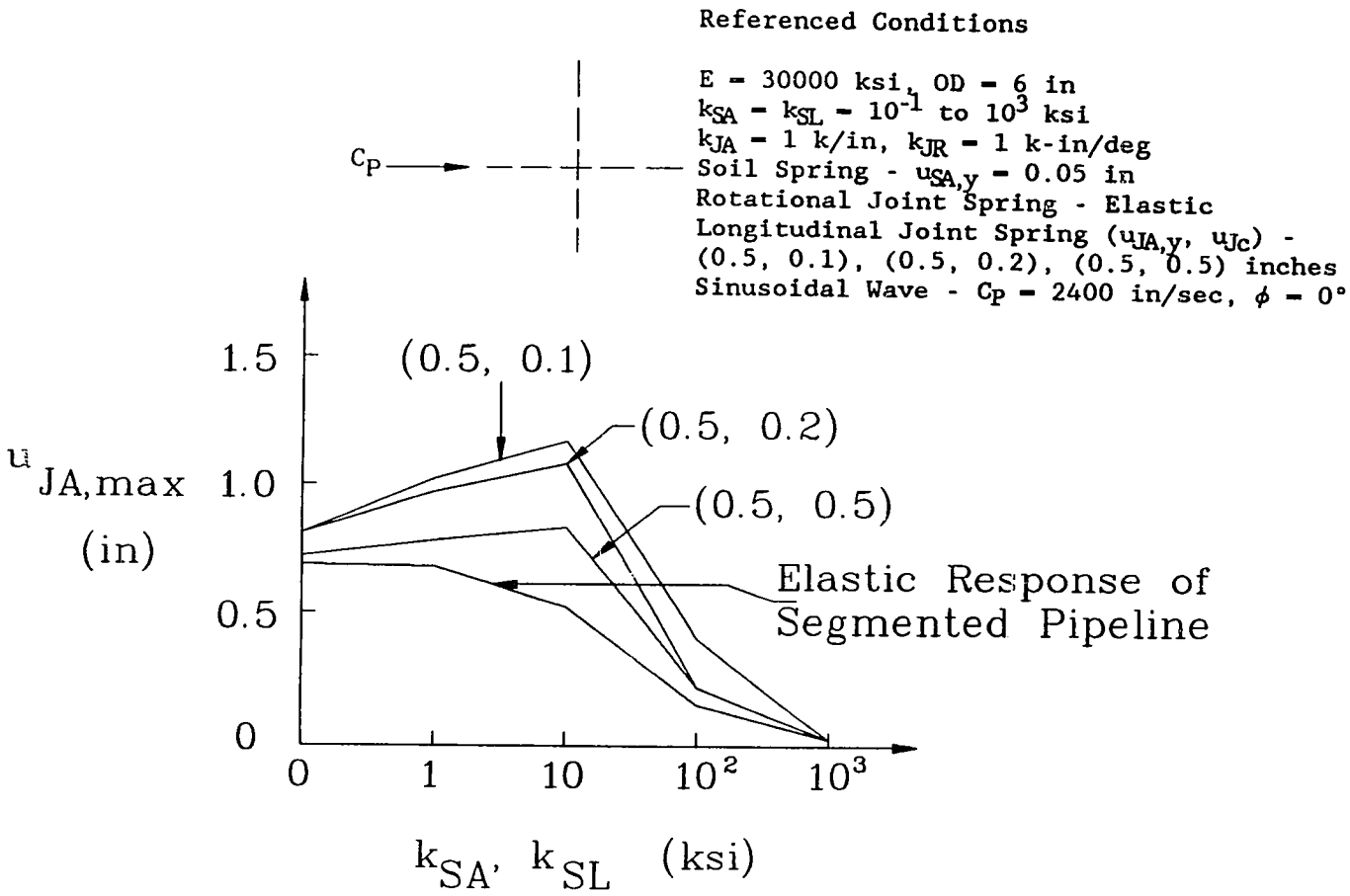

Fig. 3.29 Comparison of Elastic and Inelastic Relative Joint Displacement Responses

Chapter 4

SUMMARY AND CONCLUSIONS

The behavior of buried pipeline systems under ground shaking has been studied. The quasi-static equilibrium equations for both elastic and inelastic analyses have been derived. A rigorous iterative procedure considering the hysteretic characteristics of soil and joint has been developed. A computer program which is capable of solving both the elastic and inelastic responses of buried pipeline system has been developed. Using the developed program, the parametric studies for both elastic and inelastic analyses were done. From the results, some conclusions can be made as follows:

1. The smaller the pipe size, the larger the pipe responses will be.
2. The faster the ground wave velocity, the smaller the pipe responses will be.
3. The longitudinal (axial) pipe responses dominate the behavior of buried pipelines.

4. The pipe which is parallel to the direction of ground motion (incident angle = 0°) will experience higher responses.
5. The more flexible (ductile) the joint, the smaller pipe strain responses will be.
6. The elastic pipe strain responses of continuous pipelines are upper bounds compared to the inelastic pipe strain responses of both continuous and segmented pipes.
7. The elastic pipe strain and the relative joint displacement responses of segmented pipelines appear to be the lower bound of inelastic pipe strain and relative joint displacement responses.
8. The available contact space of joint, $u_{J,c}$, plays the major role in the inelastic behavior of segmented pipes. The smaller the contact space, the larger the pipe strain as well as the relative joint displacement responses will be.
9. The softer (lower stiffness) the surrounding soil, the smaller the pipe strain responses will be. However, the larger joint response will be expected.
10. For very fast ground wave velocities, e.g., $C_p \geq$ 12000 in/sec, the elastic responses of pipe and joint are sufficient for estimating inelastic

responses of pipe and joint, especially for stiffer soil, say k_{SA} > 10 ksi.

To verify the results, laboratory and in-situ experiments of buried pipeline subjected to ground waves are needed. Accordingly, a more realistic model for the hysteretic characteristic of soil and joint can be developed. To aid future designs, the operating pressure of water supply pipelines and circumferential distortion of pipes should be included.

REFERENCES

1. Abe, T. and Ang, A. H-S, "Seismic Response of Structures Buried Partially in a Multi-Layered Soil Medium," Proc. of 5th World Conference (1973) on Earthquake Engineering, Rome, 1974, pp. 1840-1850.

2. Audibert, J. M. E., and Nyman, K. J., "Soil Restraint against Horizontal Motion of Pipes," Journal of the Geotechnical Engineering Division, ASCE, Vol. 103, No. GT10, Oct. 1977, pp. 1119-1142.

3. Audibert, J. M. E. and Nyman, K. J., "Coefficients of Subgrade Reaction for the Design of Buried Piping," ASCE, Special Conference on Structural Design of Nuclear Plant Facilities, New Orleans, LA, Dec. 1975, pp. 109-141.

4. Berger, E. and Mahin, S. A., "Simplified Method for Evaluating Soil-Pile-Structure Interaction Effects," Proc. of 9th Annual Offshore Technology Conference, Houston, Texas, May 1977, pp. 589-598.

5. Brumund, W. and Leonards, G., "Experimental Study of Static and Dynamic Friction between Sand and Typical Construction Materials,"Journal of Testing and Evaluation, JTEVA, Vol. 1, No. 2, 1973, pp. 162-165.

6. Colton, J., Chang, p., Lindberg, H. and Abrahanson, G., "Measurement of Dynamic Soil-Pipe Axial Interaction for Full-Scale Buried Pipelines under Field Laying Conditions," SRI International, Menlo Park, Calif., Nov. 1981.

7. Committee on Gas and Liquid Fuel Lifelines, "Guidelines for the Seismic Design of Oil and Gas Pipeline Systems," ASCE, New York, NY, 1984.

8. Duke, C. M. and Moran, D. F., "Guidelines for Evolution of Lifeline Earthquake Engineering," Proceedings of the U.S. National Conference on Earthquake Engineering, Ann Arbor, MI., 1975, pp. 367-376.

9. Goodling, E. C., "Buried Piping-An Analysis Procedure Update," Proceedings of the International Symposium on Lifeline Earthquake Engineering, Portland, Oregon, ASME, 1983, pp. 225-237.

10. Hakuno, M., "Evaluation of Dynamic Properties of Pile Foundation Based on Wave Dissipation Theory," Proc. of 5th World Conference (1973) on Earthquake Engineering, IAEE, Rome, 1974, pp. 2628-2637.

11. Hall, W. J. and Newmark, M. N., "Seismic Design Criteria for Pipelines and Facilities," Journal of the Technical Councils of ASCE, Vol. 104, No. TC1, Nov. 1978, pp. 91-107.

12. Hardin, B. O. and Dernvich, V. P., "Shear Modulus and Damping in Soils: Measurement and Parameter Effects," Journal of Soil Mechanics and Foundations, ASCE, June 1972, pp. 603-624.

13. Ieda, R. and Tsuchiyama, S., "Effect of Earthquake Motion on the Dynamic Behavior of Underground Transmission Lines," Developments in Geotechnical Engineering 45 - Structures and Stochastic Methods, Edited by A. Cakmak, Elsevier, Amsterdam, 1987.

14. Igbal, M. and Goodling, E., "Seismic Design of Buried Piping," ASCE, Special Conference on Structural Design of Nuclear Plant Facilities, New Orleans, 1975.

15. Isenberg, J. and Wright, J. P., "Survey of Existing Underground Water Pipelines with Emphasis on Their Seismic Resistance," Report No. IR-1, Weidlinger Associates, New York, NY, July 1977.

16. Isenberg, J., Weidlinger, P., et al., "Underground Pipelines in a Seismic Environment," Proceedings of Technical Council on Lifeline Earthquake Engineering, ASCE, Special Conference, Los Angeles, CA, Aug. 1977, pp. 267-281.

17. Ishibashi, I., Wang, L. R. L., and Kennedy, H. Jr., "Energy Dissipation and Resistant Characteristics of a Flexible Pipe Joint," Earthquake Behavior of Buried Pipelines, Storage, Telecommunication, Transportation Facilities, ASME Pressure Vessels and Piping Conference, PVP-Vol. 162, Honolulu, Hawaii, July 1989, pp. 111-120.

18. Iwamoto, T., Wakai, N., Yamaji, T. and Nagao, S., "Observation of Dynamic Behavior of Buried Ductile Iron Pipelines During Earthquakes," Earthquake Behavior and Safety of Oil and Gas Storage Facilities, Buried

Pipelines and Equipment, PVP-Vol. 77, Portland Oregon, June 1983, pp. 285-293.

19. Jennings, P. C., "Earthquake Problems of Networks and Systems," Proceedings of the U.S.-Japan Seminar on Earthquake Engineering Research with Emphasis on Lifeline Systems, Nov. 1976, pp. 5-14.

20. Katayama, T., Kubo, K. and Sato, N., "Earthquake Damage to Water and Gas Distribution Systems," Proceedings of the U.S. National Conference on Earthquake Engineering, EERI, Ann Arbor, Mich., 1975, pp. 396-405.

21. Koike, T., "Structural Strains of the Buried Pipeline under Seismic Risk," Proceedings of the Trilateral Seminar-workshop on Lifeline Earthquake Engineering, Taipei, Taiwan, Nov. 1985.

22. Kubo, K., "Behavior of Underground Waterpipes During an Earthquake," Proceedings of the Fifth World Conference on Earthquake Engineering, Vol. 1, Rome, 1974, pp. 607 -643.

23. McClure, G. M., Atterbury, T. J. and Frazier, N. A., "Analysis of Blast Effects on Pipelines," Journal of Pipeline Division, Vol. 90, No. PL2, ASCE, Nov. 1964, pp. 25-47.

24. Newmark, N. M., "Problems in Wave Propagation in Soil and Rock," Proceedings of International Symposium on Wave Propagation and Dynamic Properties of Earth Materials, Albuquerque, New Mexico, 1967, pp. 7-26.

25. Newmark, N. M., and Hall, W. J., "Pipeline Design to Resist Large Fault Displacement," Proceedings of U.S. National Conference on Earthquake Engineering, Ann Arbor, MI, 1975, pp. 416-425.

26. Novak, M., Nogami, T. and Aboul-Ella, F., "Dynamic Soil Reaction for Plane Strain Case," Journal of the Engineering Mechanics Division, ASCE, Vol. 104, No. EM4, pp. 953-959.

27. O'Leary, P., and Datta, S., "Dynamics of Buried Pipelines," Int. Journal of Soil Dynamics and Earthquake Engineering, Vol. 4, No. 3, pp. 151-159.

28. O'Rourke M. and Wang, L. R. L., "Earthquake Response of Buried Pipeline," Proceedings on the Specialty Conference on Earthquake Engineering and Soil Dynamics, ASCE, Pasadena, CA., June 1978, pp. 720-731.

29. O'Rourke, M., Castro, G. and Hossain, I., "Horizontal Soil Strain Due to Seismic Waves," Journal of Geotechnical Engineering and Soil Dynamics, Pasadena, Calif., June, 1978.

30. O'Rourke, M. J., Pikul, R. R. and Wang, L. R. L., "Transverse Seismic Waves at Pipeline Junctions," Journal of Technical Councils, ASCE, Vol. 108, No. TC1, May 1982, pp. 173-177.

31. O'Rourke, M., Bloom, M. and Dobry, R., " Apparent Propagation Velocity of Body Waves," Int. Journal Earthquake Engineering Structural Dynamics, Vol. 10, 1982.

32. Potyondy, J. G., "Skin Friction between Various Soils and Construction Materials," Geotechnique International Journal of Soil Mechanics, Vol. 11, No. 4, 1961, pp. 339-353.

33. Saito, K., Nishio, N. and Katayama, T., "Recommended Practice for Earthquake Resistant Design of Medium and Low Pressure Gas Pipe Lines," Earthquake Behavior and Safety of Oil and Gas Storage Facilities, Buried Pipelines and Equipment, PVP-Vol. 77, Portland, Oregon, June 1983, pp. 340-348.

34. Sakurai, A. and Takahashi, T., "Dynamic Stresses of Underground Pipelines during Earthquakes," Proceedings, 4th World Conference on Earthquake Engineering, Santiago, Chile, 1969, pp. 150-162.

35. Shah, H. H., and Chu, S. L., "Seismic Analysis of Underground Structural Elements," Journal of the Power Division 100, No. P01, American Society of Civil Engineers, July 1974, pp. 53-62.

36. Shibata, H., "Fundamental Concept of Aseismic Design Code of Equipment in Lifeline Systems," U.S. Japan Seminar, 1976.

37. Shinozuka, M. and Kawakami, H., "Underground Pipe Damages and Ground Characteristics," Proceedings of Technical Council on Lifeline Earthquake Engineering, ASCE, Special Conference, Los Angeles, CA, Aug. 1977, pp. 293-307.

38. Shinozuka, M., and Koike, T., "Estimation of Structural Strains in Underground Lifeline Pipes," ASME Publication PVP-34, Lifeline Earthquake Engineering-Buried Pipelines, Seismic Risk and Jointed Pipelines," Journal

of Transportation Engineering, ASCE, Vol. 109, No. 3, May 1983.

39. Singhal, A. C., and Benavides, J. C., "Pull Out and Bending Experiments in Buried Pipes," Earthquake Behavior and Safety of Oil and Gas Storage Facilities, Buried Pipelines and Equipment, PVP-Vol. 77, ASME, New York, NY, 1983, pp. 294-303.

40. Singhal, A. C., "Nonlinear Behavior of Ductile Iron Pipeline Joints," Journal of Technical Topics in Civil Engineering 110, No. 1, ASCE, May 1984, pp. 29-37.

41. Takada, S., "Seismic Response Analysis of Buried PVP and Ductile Iron Pipelines," PVP Conference, San Francisco, CA., Aug. 1980, pp. 23-32.

42. Takada, S., Tanabe, K. and Horinouchi, N., "Seismic Response Analyses of Buried Pipelines with Many Branch Pipes," Developments in Geotechnical Engineering 45 - Structures and Stochastic methods, 1987, pp. 39-49.

43. Tamura, C. and Okamoto, S., "On Earthquake Resistant Design of a Submerged Tunnel," Proc. of International Symposium on Earthquake Structural Engineering, Univ. Missouri, Aug. 1976, pp. 809-822.

44. Tamura, C., "Design of Underground Structures by Considering Ground Displacement during Earthquakes," Engineering Research with Emphasis on Lifeline Systems, Tokyo, Nov. 1976, pp. 417-433.

45. Thomas, H. G., discussion of "Soil Restraint Against Horizontal Motion of Pipes," by J. M. E. Audibert and K. J. Nyman, Journal of the Geotechnical Engineering Division, ASCE, Vol. 104, No. GT9, Sep. 1978, pp. 1214-1216.

46. Toki, K., Fukumori, Y., Sako, M. and Tsubakimoto, T., "Recommended Practice for Earthquake Resistant Design of High Pressure Gas Pipe Lines," Earthquake Behavior and Safety of Oil and Gas Storage Facilities, Buried Pipelines and Equipment, PVP-Vol. 77, Portland, Oregon, June 1983, pp. 349-356.

47. Trautmann, C. H. and O'Rourke, T. D., "Behavior of Pipe in Dry Sand under Lateral and Uplift Loading," Geotechnical Engineering Report 83-7, Cornell University, NY, May 1983.

48. Trautmann, C. H., and O'Rourke, T. D., "Lateral Force-Displacement Response of Buried Pipe," Journal of

Geotechnical Engineering, ASCE, Vol. 111, No. 9, Sept. 1985, pp. 1061-1076.

49. Wang, L. R. L., and O'Rourke, M. J., "Overview of Buried Pipelines Under Seismic Loading," Journal of Technical Councils, ASCE, Vol. 104, No. TC1, 1978, pp.121-130.

50. Wang, L. R. L., O'Rourke, M. J. and Pikul, R. P., "Seismic Vulnerability Behavior and Design of Buried Pipelines," Technical Report No. 9, Department of Civil Engineering, Rensselaer Polytechnical Institute, Troy, NY, Mar. 1979.

51. Wang, L. R. L., "Some Aspects of Seismic Resistant Design of Buried Pipelines," Proceedings of ASME 3rd U.S. National Conference of Pressure Vessels and Piping, San Francisco, CA. June, 1979, PVP-34, pp. 117-131.

52. Wang, L. R. L., and Olabimtan, A., "General Quasi-static Seismic Analysis of Buried Straight Piping Systems," Tech. Report LEE-006, School of Civil Engineering and Environmental Science, University of Oklahoma, Sept. 1983.

53. Wang, L. R. L., "Role and Development of Soil Parameters for Seismic Responses of Buried Pipelines," Earthquake Behavior and Safety of Oil and Gas Storage Facilities, Buried Pipelines and Equipment, PVP-Vol. 77, ASME, New York, NY, 1983, pp. 312-323.

54. Wang, L. R. L., "Performance of Water Pipeline Systems from 1987 Whittier Narrows, California Earthquake," Technical Report No. ODU LEE-05, in Lifeline Earthquake Engineering Research Series, Department of Civil Engineering, Old Dominion University, Norfolk, VA., (in progress).

55. Wang, L. R. L. and Lau, J. Y. C., "User's Manual for Computer Program on Elasto-plastic Responses of Buried Pipeline Systems under Wave Propagation," (in progress).

56. Weaver, W. Jr., and Johnston, P.R., "Finite Element for Structural Analysis," Prentice-Hall, NJ, 1984, pp. 9-42.

APPENDIX

STIFFNESS MATRICES OF DIFFERENT TYPES OF JOINT

This appendix presents the stiffness matrices of four different types of joint, i.e., (i) elbow, (ii) T, (iii) Y and (iv) cross, as following:

Stiffness Matrix of Elbow Type of Joint

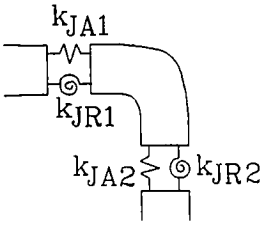

$$[k_J]_{7x7} = \begin{bmatrix} k_{JA1} & 0 & 0 & -k_{JA1} & 0 & 0 & 0 \\ & k_{JA2} & 0 & 0 & 0 & -k_{JA2} & 0 \\ & & k_{JR1}+k_{JR2} & 0 & -k_{JR1} & 0 & -k_{JR2} \\ & & & k_{JA1} & 0 & 0 & 0 \\ & \text{Symmetric} & & & k_{JR1} & 0 & 0 \\ & & & & & k_{JA2} & 0 \\ & & & & & & k_{JR2} \end{bmatrix}$$

Stiffness Matrix of T Type of Joint

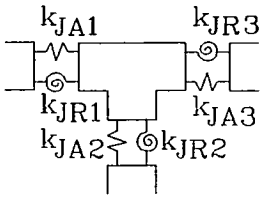

$$[k_J]_{9x9} = \begin{bmatrix} k_{JA1}+k_{JA3} & 0 & 0 & -k_{JA1} & 0 & 0 & 0 & -k_{JA3} & 0 \\ & k_{JA2} & 0 & 0 & 0 & -k_{JA2} & 0 & 0 & 0 \\ & & k_{JR1}+k_{JR2}+k_{JR3} & 0 & -k_{JR1} & 0 & -k_{JR2} & 0 & -k_{JR3} \\ & & & k_{JA1} & 0 & 0 & 0 & 0 & 0 \\ & & & & k_{JR1} & 0 & 0 & 0 & 0 \\ & & \text{Symmetric} & & & k_{JA2} & 0 & 0 & 0 \\ & & & & & & k_{JR2} & 0 & 0 \\ & & & & & & & k_{JA3} & 0 \\ & & & & & & & & k_{JR3} \end{bmatrix}$$

Stiffness Matrix of Y Type of Joint

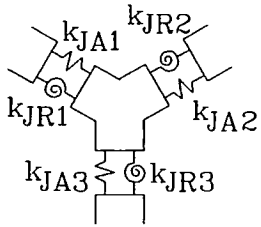

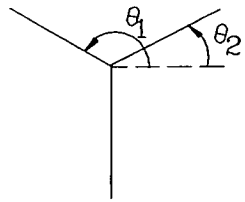

$c_1 = \cos\theta_1 \quad s_1 = \sin\theta_1$

$c_2 = \cos\theta_2 \quad s_2 = \sin\theta_2$

$$
\begin{bmatrix}
k_{JA1}c_1^2 + k_{JA2}c_2^2 & k_{JA1}c_1s_1 + k_{JA2}c_2s_2 & 0 & -k_{JA1}c_1^2 & -k_{JA1}c_1s_1 & 0 & -k_{JA2}c_2^2 & -k_{JA2}c_2s_2 & 0 & 0 & 0 \\
 & k_{JA1}s_1^2 + k_{JA2}s_2^2 + k_{JA3} & 0 & -k_{JA1}c_1s_1 & -k_{JA1}s_1^2 & 0 & -k_{JA2}c_2s_2 & -k_{JA2}s_2^2 & 0 & -k_{JA3} & 0 \\
 & & k_{JR1} + k_{JR2} + k_{JR3} & 0 & 0 & -k_{JR1} & 0 & 0 & -k_{JR2} & 0 & -k_{JR3} \\
 & & & k_{JA1}c_1^2 & k_{JA1}c_1s_1 & 0 & 0 & 0 & 0 & 0 & 0 \\
 & & & & k_{JA1}s_1^2 & 0 & 0 & 0 & 0 & 0 & 0 \\
 & & & & & k_{JR1} & 0 & 0 & 0 & 0 & 0 \\
 & & \text{Symmetric} & & & & k_{JA2}c_2^2 & k_{JA2}c_2s_2 & 0 & 0 & 0 \\
 & & & & & & & k_{JA2}s_2^2 & 0 & 0 & 0 \\
 & & & & & & & & k_{JR2} & 0 & 0 \\
 & & & & & & & & & k_{JA3} & 0 \\
 & & & & & & & & & & k_{JR3}
\end{bmatrix}
$$

Stiffness Matrix of Cross Type of Joint

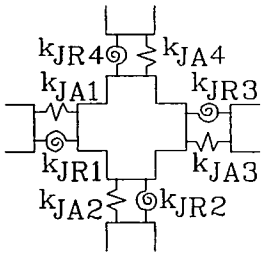

$$[k_J]_{11x11} = \begin{bmatrix}
k_{JA1}+k_{JA3} & 0 & 0 & -k_{JA1} & 0 & 0 & 0 & -k_{JA3} & 0 & 0 & 0 \\
 & k_{JA2}+k_{JA4} & 0 & 0 & 0 & -k_{JA2} & 0 & 0 & 0 & -k_{JA4} & 0 \\
 & & k_{JR1}+k_{JR2}+k_{JR3}+k_{JR4} & 0 & -k_{JR1} & 0 & -k_{JR2} & 0 & -k_{JR3} & 0 & -k_{JR4} \\
 & & & k_{JA1} & 0 & 0 & 0 & 0 & 0 & 0 & 0 \\
 & & & & k_{JR1} & 0 & 0 & 0 & 0 & 0 & 0 \\
 & & \text{Symmetric} & & & k_{JA2} & 0 & 0 & 0 & 0 & 0 \\
 & & & & & & k_{JR2} & 0 & 0 & 0 & 0 \\
 & & & & & & & k_{JA3} & 0 & 0 & 0 \\
 & & & & & & & & k_{JR3} & 0 & 0 \\
 & & & & & & & & & k_{JA4} & 0 \\
 & & & & & & & & & & k_{JR4}
\end{bmatrix}$$